UC San Diego

UC San Diego Electronic Theses and Dissertations

Title

Biological Alteration of Basaltic Glass : Laboratory and Field Studies on Basalt Hosted Microbial Ecosystems

Permalink

https://escholarship.org/uc/item/93g926vr

Author

Bailey, Brad E.

Publication Date

2014

Peer reviewed|Thesis/dissertation

UNIVERSITY OF CALIFORNIA, SAN DIEGO

Biological Alteration of Basaltic Glass: Laboratory and Field Studies on Basalt Hosted
Microbial Ecosystems

A dissertation submitted in partial satisfaction of the
requirements for the degree Doctor of Philosophy

in

Earth Sciences

by

Brad E. Bailey

Committee in charge:

    Hubert Staudigel, Chair
    Bradley Tebo, Co-Chair
    Lihini Aluwihare
    Joris Gieskes
    Alexis Templeton
    Mark Thiemens

2014

The Dissertation of Brad E. Bailey is approved, and it is acceptable in quality and form for publication on microfilm and electronically:

_____

_____

_____

_____

_____

Co-Chair

_____

Chair

University of California, San Diego

2014

DEDICATION

For my Mom,

Who always reminded me to

"Feed my 'Friends'"

EPIGRAPH

The most exciting phrase to hear in science, the one that heralds the most discoveries, is not "Eureka!" (I found it!) but "That's funny..."

Isaac Asimov

A geobiologist talks geology to the biologists and biology to the geologists. Then he meets another geobiologist and they just talk about sports.

Author unknown

TABLE OF CONTENTS

LIST OF FIGURES

LIST OF TABLES

ACKNOWLEDGEMENTS

hard times seem not so hard after all. I thank all of my coauthors for their hard work and insightful contributions. I would also like to thank my committee for taking the time to work with me. A BIG thank you goes out to the crew of the K.O.K. and all the Pisces pilots and support crews, without whom this thesis would not have come about. I have always thoroughly enjoyed my time at sea with this cast of characters. And to my NASA family who has always supported me and gently (and not so gently) pushed me to complete this thesis: Yvonne, Greg, David, Joe, Brian… may the laughter continue forever.

Finally, none of this would have ever been possible without the love and encouragement from my family. For my Mom, who has always been there to support me through everything and my sisters who are always there to keep me humble and laugh with me; for my Aunt Jan who will always be my best friend and for my Grandma who has always taken care of me and made me feel loved. And my sisters who both tried to keep me humble (a never-ending job!). None of this would have been possible without all of these people active in my life and they will have my eternal gratitude.

Chapter 4 is a formatted version of the published work: Bailey B., Templeton A. S., Staudigel H., Tebo B. M. (2009). Utilization of substrate components during basaltic glass colonization by Pseudomonas and Shewanella isolates. Geomicrobiol. J. 26, 648–656. doi: 10.1080/01490450903263376. The dissertation author was the primary investigator and author of this paper.

Chapter 5, in full, is a formatted version of the published work: Orcutt B., Bailey B.E., Staudigel H., Tebo B., Edwards KJ. (2009) An interlaboratory comparison of 16S rRNA gene-based terminal restriction fragment length polymorphism and sequencing methods for assessing microbial diversity of seafloor basalts. Environmental Microbiology, 11(7), 1728-1735. DOI: 10.1111/j.1462-2920.2009.01899.x. The dissertation author was the second author of this paper and completed work for this paper including sample collection and processing, t-RFLP on genomic DNA, and power spectrum density calculations for statistical analysis.

Chapter 6 is a formatted version of a paper to be submitted for publication: Bailey B., Moyer C.M., Templeton A.S., Staudigel H., Tebo B.M. Basalt-Hosted Bacterial Community Structure at Loihi Seamount. (in prep). The dissertation author was the primary investigator and author of this paper.

1998 B.S., Rose-Hulman Inst. Of Technology, Terre Haute, IN
     Major: Physics Minors: Applied Optics, Chemistry, Japanese

2000 M.S., New Mexico Inst. Of Mining and Tech., Socorro, NM
     Major: Physics, Specialty in Astrophysics

2001 Project engineer for International Space Station, Lockheed Martin/NASA
     Ames Research Center, Moffett Field, CA

2001-2008 Research Assistant, Scripps Institute of Oceanography, La Jolla, CA

2008-2013 Staff Scientist, NASA Lunar Science Institute, NASA Ames Research Center

2013-2014 Staff Scientist, NASA Solar System Exploration Research Virtual Institute,
     NASA Ames Research Center

2014 Ph.D., UC San Diego, Scripps Institution of Oceanography, La Jolla, CA
     Specialty: Earth Science

PUBLICATIONS

Bailey B., Moyer C.M., Templeton A.S., Staudigel H., Tebo B.M. Basalt-Hosted Bacterial Community Structure at Loihi Seamount. In preparation to be submitted to *Geomicrobiology Journal.*

Bailey B., Templeton A. S., Staudigel H., Tebo B. M. (2009). Utilization of substrate components during basaltic glass colonization by Pseudomonas and Shewanella isolates. *Geomicrobiology. Journal.* 26, 648–656. doi: 10.1080/01490450903263376

Orcutt B., Bailey B.E., Staudigel H., Tebo B., Edwards KJ. (2009) An interlaboratory comparison of 16S rRNA gene-based terminal restriction fragment length polymorphism and sequencing methods for assessing microbial diversity of seafloor basalts. Environmental Microbiology, **11**(7):1728-1735. DOI: 10.1111/j.1462-2920.2009.01899.x

Templeton A. S., Knowles E. J., Eldridge D. L., Arey B. W., Dohnalkova A. C., Webb S. M., Bailey B. E.., Tebo B. M., Staudigel H. (2009). A seafloor microbial biome hosted within incipient ferromanganese crusts. *Nature Geoscience* **2**:872–876. doi: 10.1038/ngeo696

C. Schröder, B. Bailey, G. Klingelhöfer and H. Staudigel. (2006) Fe Mössbauer spectroscopy as a tool in astrobiology. *Planetary and Space Science*. 54(15):1622-1634

Staudigel H., S.R. Hart, A. Pile, B.E. Bailey, E.T. Baker, S. Brooke, D.P. Connelly, L. Haucke, C.R. German, I. Hudson, D. Jones, A.A. Koppers, J. Konter, R. Lee, T.W. Pietsch, B.M. Tebo, A.S. Templeton, R. Zierenberg, C.M. Young. 2006. Vailulu'u Seamount, Samoa: Life and death on an active submarine volcano. *Proceedings of the National Academy of Sciences*. 103(17):6448

C. Schröder, G. Klingelhöfer, B. Bailey, and H. Staudigel. (2005) Mössbauer spectroscopy as a tool in astrobiology. *Hyperfine Interactions*. 166:567-571

ABSTRACT OF THE DISSERTATION

Biological Alteration of Basaltic Glass: Laboratory and Field Studies on Basalt Hosted
Microbial Ecosystems

by

Brad E. Bailey

Doctor of Philosophy in Earth Sciences

University of California, San Diego, 2014

Hubert Staudigel, Chair

Bradley Tebo, Co-Chair

Only in the last 30 years of science have we discovered that not all life on Earth is based upon photosynthesis. The deep biosphere has emerged as an incredibly diverse ecosystem with life thriving in environmental conditions ranging from sub-zero to 120°C+ temperatures, hyper saline brine pools to low pH environments. This body of work contributes to several key questions about life in the deep biosphere: 1) Which microbes are present in the deep biosphere, 2) what are their sources of energy, 3) how do they attain required nutrients for metabolic function and growth and 4) what is the effect of substrate composition on each of the above questions.

In order to address these first order questions, we focused our efforts on Loihi Seamount, off the SE coast of the Big Island of Hawai'i, which provides us with raw materials and microbes for laboratory experiments as well as an in-situ deep-sea laboratory so that we can study effects of microbiology on basalt weathering. Due to the high iron content (~10-12%), basalts are an attractive source of reduced iron as an energy source for chemolithoautotrophic growth. We explored microbial diversity associated with basaltic glass substrates across a range of different environments in and around Loihi using t-RFLP, clone library data, and culturing/isolation techniques. Results show that γ- and α-Proteobacteria tend to dominate these surfaces and one of our Fe(II)-oxidizing isolates, a *Pseudomonas* sp. LOB-7, is represented as one of the most dominant members of the microbial communities on several basalts indicating that perhaps Fe(II)-oxidizing microbes are important players in the microbially mediated dissolution and alteration of basaltic glass.

Investigations into substrate specificity by microbes under energy- and nutrient-limiting conditions reveal that *Pseudomonas* and *Shewanella* isolates are able to obtain Fe and/or phosphorus directly from a basaltic glass silicate matrix. This finding provides a direct relationship between substrate composition and the activity of particular microbes, which will allow us to provide insights into how substrate composition can control microbial diversity and consequently chemical fluxes between seawater and the basaltic ocean crust.

Chapter 1

Introduction

1.1 Preface

Through recent studies over the past 25 years, it has become increasingly apparent that microbial processes can significantly contribute to water-rock interactions in the deep oceanic basins. These interactions control geochemical fluxes into and out of both seawater and the host ocean crust which ultimately points to microbial activity as being a controlling factor in global ocean chemical composition. Therefore, if we are to understand the geochemical interactions affecting ocean chemistry, we must look to the biology controlling these reactions. Several questions must be asked and investigated in order to help elucidate this biogeochemical mystery: 1) Which microbes are present in the deep biosphere? 2) Which microbes are responsible for basaltic dissolution and what is their role in the overall microbial community? 3) What are their sources of energy? 4) How do they attain required nutrients for metabolic function and growth? And 5) what is the effect of substrate composition on each of the above questions? Several studies have been focused on each individual question listed, however, no definitive answers have been given and much remains unknown. This introduction will detail and expand on what is currently known of the above topics from scientific literature and outline each chapter of this dissertation as to how we contributed to the overall scientific knowledge base on this intriguing topic.

1.2 Biological Alteration of Basalt

Basalts are the dominant rock type (~70%) on the earth's surface, comprising most of the upper oceanic crust as well as several continental formations (e.g. Columbia River Flood Basalts) (Francis, 2001) and thus are the main constituent in water-rock interactions at the earth's surface. Staudigel and Hart (1983) predicted that ~20% of the upper oceanic crust is basaltic glass and can vary up or down depending upon presence of hyaloclastites and pillow lavas vs large scale sheet flows. Basaltic glass is very important to the overall reaction rates in the basaltic crust as its relative thermodynamic instability results in higher reaction rates than mineral assemblages (Stroncik and Schmincke, 2002).

Hydrous alteration of basaltic glass can fall into one of two catergories: abiotic alteration and biotic alteration. Abiotic alteration typically is the result of a process called palagonitization, in which the basaltic glass oxidizes, hydrates and swells resulting in the first stable mineral of mafic glass alteration (See Stroncik and Schmincke (2002) for a comprehensive review on palagonite formation). Palagonitization fronts extend normally from the glass-water interface into the glass at a constant rate in the early phases of alteration, but slow down as authigenic minerals collect on the glass-water bondary and increase the travel distance for water to interact with the glass (Furnes, 1974). This authigenic mineral formation will eventually fill the interstitial spaces within the basalt (cracks, vesicles) and ultimately halt all reactions, leaving an unaltered basalt glass core surrounded by palagonite rinds.

Biotic alteration, on the other hand, is almost purely textural, resulting in "granular" and "tubular" features which are etched into the basalt surface, most

commonly along preexisting cracks in the glass surface (Furnes et al. 2001a). These features have been estimated to increase the water-rock contact area by to up to 200 fold (Staudigel and Furnes, 2004) which can greatly enhance the water-rock interactions and subsequent authigenic mineral formation. No microbes have been specifically identified as being the target organisms responsible for this biotic alteration; however, a number of lines of evidence indicate that microbial activity is indeed the cause of these alteration/dissolution features. First, the granular features in the glass are typically 1-3 microns wide and the tubular features are ~1-3 microns wide and can extend back into the glass >70 microns (Furnes and Staudigel, 1999). The dimensions associated with these features are congruent with typical bacterial cell size and diameter. Current thoughts on the tubular features suggest that these tubes are created by a single bacterium (or a string of bacteria) boring into the glass. Other studies suggest these tubular features are the result of fungal hyphae extending back into the glass (Gadd, 1999). Additionally, nucleic acid staining (Thorseth et al., 1995; Furnes et al, 1996; Giovannoni et al., 1996, Torsvik et al., 1998) and X-ray element mapping of these basalts reveal increased levels of C, N, P, as well as carbon isotopic measurements (Furnes et al., 2001b) located within the tubular alteration features suggesting that microbial life was at least present in, if not the source of, these textural features. (For a complete review of biotic alteration, see Staudigel et al., 2004). Now that we're aware of microbial abilities to alter basaltic glass, let's look at the deep oceanic biosphere to see how far this biotic alteration extends and how it affects the biogeochemical element cycling at depth.

1.3 The Deep Oceanic Biosphere

Microbial alteration features have been witnessed in nearly every type of submarine basalt structures from seamounts (e.g. Fisk et al. 1998) to very young (< 50 ka) crust (Thorseth et al. 2001) to very old (> 110 Ma) crust (Furnes et al., 2001a; Staudigel and Furnes, 2004; Staudigel et al., 2004) to ancient ophiolites (Staudigel et al. 2006a). The deep oceanic biosphere (DOB) has been shown to extend well beyond sediments into the volcanic basement with biotic alteration of the basalt (and therefore microbial activity) present up to 500m (Furnes and Staudigel, 1999; Furnes et al., 2001). Biotic alteration was reported to represent up to 90% of the total glass alteration in the upper 250m of basaltic crust; however, this number starts to fall dramatically to less than 10% at a depth of 500m into the basaltic basement (Furnes and Staudigel, 1999). Additionally, Furnes et al. (2001a) show that alteration textures are present in oceanic basalts of all ages (6 Ma through > 70 Ma), but that the alteration likely was produced within the first 6 Ma of the crust's history. Upon initial extrusion and cooling at mid-ocean ridges, massive quantities of seawater gets cycled and filtered through the newly formed basalt crust (Stein et al. 1995), which could sow the "seeds" of biotic dissolution by entraining microbes into the crust. The entrained microbial populations in these environments can initially increase reaction rates and aid in the dissolution of the basaltic substrates which further increases the surface contact area between rock and seawater, further enhancing dissolution. However, this resultant dissolution produces a large amount of secondary authigenic minerals which can collect on the water-rock boundary and effectively seal off the ocean crust from further reactions at an accelerated rate when compared to abiotic alteration (Staudigel et al., 2004). This boundary can be initiated in

the form of microbial communities which form biofilms and sequester these alteration products, essentially acting as a sink for several seawater elements and oxides. Staudigel et al. (2008) provide a comprehensive review of basaltic glass bioalteration in both the laboratory and over 3.5 Ga of glass formation.

This biotically controlled basalt alteration may have a significant impact on Fe, Mn, S and C biogeochemical cycling between seawater and the oceanic crust. Bach and Edwards (2003) hypothesize that up to ~5 x10^{11} g C/year can be fixed through biomass production associated with iron and sulfur oxidation in the upper ocean crust. Laboratory studies completed by Maurice et al. (2001) show enhanced rates of Al and Si release in biologically enhanced mineral dissolution and Daughney et al. (2004) showed enhanced release of Fe and Mn when basalt was exposed to bacterial communities. Further studies all corroborate enhanced silicate weathering by biological processes (e.g. Ullman et al., 1996; Liermann et al., 2000) with some bacterial weathering processes specifically targeting nutrients in nutrient-limiting environments (Rogers et al., 1998; Bennett et al., 2001) . Interestingly, Welch and Banfield (2002) found a reduced rate of mineral dissolution upon reaction with an acidophyllic bacterium; however, they attributed this effect to surface adsorption of added Fe^{3+} reacting with the olivine surface, forming an impenetrable barrier.

Basalt and reactions of basalt with seawater provide several potential energy sources which may represent the primary form of energy for microbial ecosystems in the oceanic crust. Mid-ocean ridge basalts contain ~10-12 wt% of Fe, of which, 90% of that Fe is in the reduced Fe(II) form. Other redox available elements are present in basalts, including Mn, U, S, Ti, Ni, etc, which could be used as electron donors or acceptors.

Chemical reactions with basalts and ultramafic rocks in these environments could produce other energy sources for utilization by the microbial communities. Hydrogen is an electron donor for anaerobic chemolithoautotrophic bacteria and is produced in the oxidation of Fe by serpentinization of peridotites in the basalts:

$$3 \ Fe_2SiO_4 + 2 \ H_2O \rightarrow 2 \ Fe_3O_4 + 3 \ SiO_2 + 2 \ H_2$$
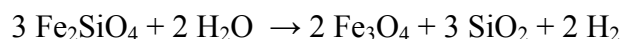
Methane may also be produced in a similar serpentinization reaction

$$(Fe, Mg)_2SiO_4 + nH_2O + CO_2 \quad Mg_3Si_2O_5(OH)_4 + Fe_3O_4 + CH_4$$

and used as a electron donor for methanotrophs. Low temperature (<100°C) serpentinite formation has been suggested (Stevens and McKinley, 1995) to produce enough H_2 to support a subsurface microbial population.

1.4 Iron Biogeochemistry and Related Microorganisms

This dissertation primarily focuses on iron as the major energy source found in the DOB. Its abundance in basalt and reduced form (Fe(II)) make it an attractive target for chemolithoautotrophic growth. The amount of energy gained from the reaction

$$Fe^{2+} + 0.25O_2(aq) + H^+ = Fe^{3+} + 0.5H_2O$$
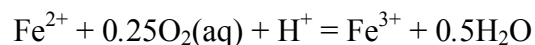
is reported as $\Delta G^R = -82 \ kJ/mol$ Fe (Edwards et al., 2004) within the given constraints of environments found on Loihi Seamount. The overall bioavailability of iron within basaltic glass is unknown; however, several studies have shown enhanced microbial growth on basaltic glass of obligate Fe(II)-oxidizing bacteria resulting in the highest growth rates and cell yields (Edwards et al., 2003). The mechanisms by which microbes are able to utilize the reduced iron held within the silicate matrix are currently not known. Recent studies suggest that the production of organic acids and metal chelaters/ligands,

which break down the silicate matrix, could be responsible for the alteration/dissolution (e.g. Duff *et.al.* 1963; Thorseth et al. 1992; Stillings et.al. 1996; Rogers and Bennett 2004).

Microorganisms which are able to oxidize Fe(II) and reduce Fe(III) are widespread in the environment. While fungi have been reported to oxidize Fe(II) (e.g. de la Torre and Gomez-Alarcon, 1994) and reduce Fe(III) (e.g. Ottow and von Klopotek, 1969), we primarily focus on bacteria as our model organisms for iron-cycling within the DOB. Iron-cycling microorganisms are phylogenetically diverse, represented in nearly every major bacterial phyla, with the most abundant representation within the *Proteobacteria* phyla, but also commonly present in *Acidobacteria, Firmicutes* and *Nitrospirales*. The energetics associated with Fe(II) oxidation are fairly low and thus require large amounts of iron "fixing" to produce a relatively small amount of biomass (Madigan et al., 2000). This is the likely explanation for low relative biomass calculations from iron-(hydr)oxide microbial mats found on the central volcanic cone, Nafanua, on Vailulu'u Seamount (Staudigel et al., 2006).

Perhaps the most "famous" marine Fe(II)-oxidizing bacteria is *Gallionella ferruginea*, which converts Fe(II) to Fe(III) and leaves behind a "twisted stalk" composed of biogenic iron oxide precipitate (Ridgeway, Means, and Olson, 1981). Halbach, Koschinsky, and Halbach (2001) found *G. ferruginea* at an active marine hydrothermal vent field and . As mentioned before, Edwards et al. (2003) describe several microbial species which are obligate iron-oxidizing lithoautotrophs and are closely related phylogenetically to *Marinobacter aquaeolei* and *Hyphomonas jannaschiana*. *M. aquaeolei* and *H. jannaschiana* are both heterotrophic organisms, so it is important to

remember that phylogeny does not necessarily equate to function. Several Fe(II)-oxidizing and Fe(III)-reducing bacterial species have been isolated from basalts and microbial mats on Loihi Seamount including *Mariprofundus ferrooxydans PV-1* (Emerson and Moyer, 2002), *Shewanella loihica PV-4* (Gao et al., 2006), *Pseudomonas* sp. LOB-7 (Templeton, unpublished data). It is important to note that while manganese is not as abundant in basalts (~0.2 wt%) as iron, it does represent another biogeochemically important redox element in these environments. Templeton et al. (2005) describe 26 unique Mn(II)-oxidizing heterotrophic bacterial species isolated from basaltic surfaces in and around Loihi Seamount.

1.5 Phylogenetic Characterization of Microbial Communities on Loihi and in the Basaltic Deep Biosphere

Since the discovery of the DOB, efforts have undergone to discover the microbial diversity associated with these basalt surfaces. However, only within the past 10 years have we been able to reliably begin phylogenetically identifying bacterial species due to improved laboratory methodology, lower cost, and high throughput gene sequencing. Even now, there are only a handful of studies characterizing bacterial communities on marine basalt surfaces.

Thorseth et al. (2001) performed polymerase chain reaction (PCR) denaturing gradient gel electrophoresis (DGGE) on samples from Knipovich Ridge and compared the basalt community to background seawater. They sequenced strong bands from the DGGE analysis which were determined to be present only on the basalt surface and found

most of their bacterial sequences belonging to the γ- Proteobacteria class with a few other sequences from the ε-Proteobacteria and CFB groups. Lysnes et al. (2004a, 2004b) performed similar PCR-DGGE studies on the arctic and southeastern Indian spreading ridges and found γ-, β, and α-Proteobacteria, CFBs and Actinobacteria sequences to be the dominant taxonomic groups present on these basalts, again with γ-proteobacteria returning the most sequences. Several studies also looked at Archaeal populations on basalt surfaces and found marine Group-1 Crenarchaeota to dominate each basalt surface (Thorseth et al., 2001; Fisk et al., 2003; Mason et al., 2007).

Two studies incorporated multiple research sites into their data sets to try and elucidate overall trends in microbial diversity on basaltic substrates. Mason et al. (2007) profiled each of the above studies, combined those results with additional data from Brown Bear Seamount and found γ- and α-Proteobacteria to be by far the most abundant phylotypes associated with basalt surfaces (Figure 1.1).
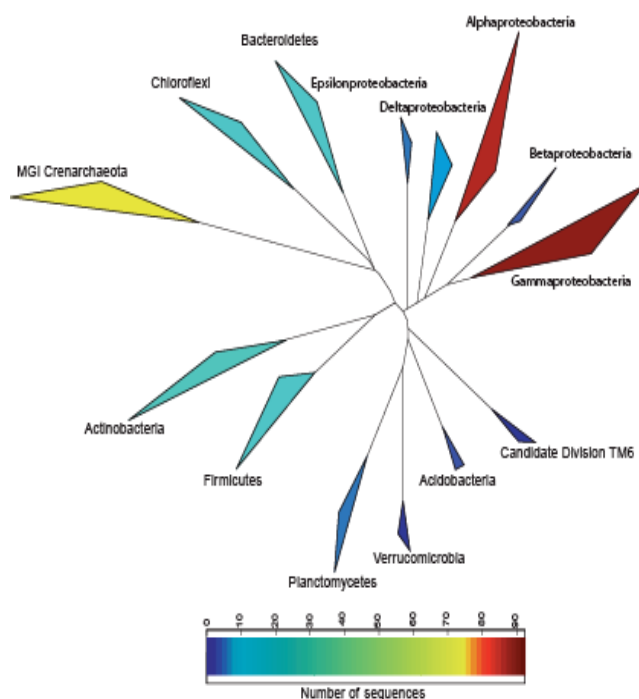
Figure 1.1. Bacterial and Archaeal phylogenetic diversity associated with marine basalts. Number of detected sequences are color coded. Figure modified from Mason et al. (2007).

Santelli et al. (2008) extracted DNA from East Pacific Rise (EPR) basalts as well as basalts from two locations on Loihi Seamount and generated clone libraries from each sample. They then used rarefaction curves to determine species richness (diversity) in each sample. Results indicated that the bacterial communities on marine basalts are incredibly diverse with > 400 predicted unique taxa. Major clades on these basalts are also dominated by g-Proteobacteria, with all subclasses of Proteobacteria representing > 60% of all detected OTUs on both EPR and Loihi basalts. Phylogenetic analysis was also completed on OTUs from EPR deep seawater to compare against basalt hosted microbial communities. Results show that EPR deep water has low diversity with only 6 OTUs

overlapping with basalt OTUs. This result indicates that basalts host a unique microbial community

Each of these studies indicates that basaltic substrates are extremely important to the deep biosphere either as a source of energy, potential nutrients, or a place for surface attachment.

1.6 Outline of the Thesis.

The work presented in this dissertation was directed at contributing to the growing body of evidence which scientific questions addressed in the preface: 1) Which microbes are present in the deep biosphere? 2) Which microbes are responsible for basaltic dissolution and what is their role in the overall microbial community? 3) What are their sources of energy? 4) How do they attain required nutrients for metabolic function and growth? And 5) what is the effect of substrate composition on each of the above questions? We used a combination of laboratory studies and an in-situ "natural" laboratory, Loihi Seamount, to explore the nature of microbial colonization and population of basaltic glass substrates. Chapter 2 describes a new laboratory protocol devised to deal with common problems associated with DNA extraction from natural environments characterized by high metal content, low biomass, and spore forming bacterial cells. Chapter 3 demonstrates how specific species of Fe(II)-oxidizing and Fe(III)-reducing bacteria can obtain needed energy sources and/or nutrients from basaltic glasses and how substrate chemical composition can affect microbial community development on the surface. Chapter 4 uses a combination of t-RFLP and clone libraries to characterize microbial diversity on a suite of basalt samples from off-shore Hawai'i

and Loihi Seamount. Chapter 5 is a methodology comparison paper between t-RFLP and clone library analysis of basalt-hosted microbial diversity. Chapter 6 demonstrates how Mössbauer spectroscopy can be used to analyze iron oxidation states in fine-grained samples after years of deployment/reaction on Loihi Seamount.

1.7 References

Bach, W. and K.J. Edwards (2003) Iron and sulphide oxidation within the basaltic ocean crust: Implications for chemolithoautotrophic microbial biomass production. *Geochimica et Cosmochimica Acta.* **67**:3871–3887.

Bennett, P.C., J.R. Rogers and W.J. Choi. (2001) Silicates, Silicate Weathering and Microbial Ecology. *Geomicrobiology Journal.* **18**:3-19

Daughney, C.J., J-P. Rioux, D. Fortin and T. Pichler. (2004) Laboratory Investigation of the Role of Bacteria in the Weathering of Basalt near Deep Sea Hydrothermal Vents. *Geomicrobiology Journal.* **21**:21-31

De la Torre, M.A. and G. Gomez-Alarcon. (1994) Manganese and iron oxidation by fungi isolated from building stone. *Microbial Ecology.* **27**(2):177-188

Duff, R. B., D. M. Webley, and R. 0. Scott. (1963) Solubilization of minerals and related materials by 2-ketogluconic acid-producing bacteria. *Soil Science.* **95**:105-114.

Edwards, K.J., D.R. Rogers, C.O. Wirsen, and T.M. McCollom. (2003) Isolation and Characterization of Novel Psychrophilic, Neutrophilic, Fe-Oxidizing, Chemolithoautotrophic a- and g-*Proteobacteria* from the Deep Sea. *Applied and Environmental Microbiology.* **69**(5):2906-2913

Edwards, K.J., W. Bach, T.M. McCollom and D.R. Rogers. (2004) Nertrophilic Iron-Oxidizing Bacteria in the Ocean: Their Habitats, Diversity, and Roles in Mineral Deposition, Rock Alteration and Biomass Production in the Deep-Sea. *Geomicrobiology Journal.* **21**:393-404

Emerson D, Moyer CL. 2002. Neutrophilic Fe-oxidizing bacteria are abundant at the Loihi seamount hydrothermal vents and play a major role in Fe oxide deposition. *Appl Environ Microbiol* 68:3085–3093.

Fisk, M.R., S.J. Giovannoni and I.H. Thorseth, Alteration of oceanic volcanic glass: textural evidence of microbial activity. *Science* **281** (1998), pp. 978–979

Fisk, M.R., M.C. Storrie-Lombardi, S. Douglas, R. Popa, G. McDonald, and C.A. Di Meo-Savoie. (2003) Evidence of biological activity in Hawaiian subsurface basalts. *Geochemistry Geophysics Geosystems.* **4**:10.1029/2002GC000387

Francis, P. (2000) Volcanoes: a planetary perspective. Oxford University Press, Oxford, United Kingdom.

Furnes, H. (1974) Volume Relations between Palagonite and Authigenic Minerals in Hyaloclastites, and Its Bearing on the Rate of Palagonitization. *Bulletin of Volcanology.* **38:**173–186

Furnes, H., I.H. Thorseth, O. Tumyr, T. Torsvik and M.R. Fisk, Microbial activity in the alteration of glass from pillow lavas from Hole 896A, in: J.C. Alt, H. Kinoshita, L.B. Stokking, P. Michael (Eds.). *Proc. Ocean Drill. Prog., Sci. Results* **148** (1996), pp. 191–206

Furnes, H. and H. Staudigel. (1999) Biological mediation in ocean crust alteration: how deep is the deep biosphere? *Earth and Planetary Science Letters.* **166**:97–103

Furnes, H., Staudigel, H., Thorseth, I.H., Torsvik, T., Muehlenbach, K., Yumyr, O., (2001a) Bioalteration of basaltic glass in the oceanic crust. *Geochemistry Geophysics Geosystems* **2**(8) Paper number 2000GC000150

Furnes, H., K. Muehlenbachs, T. Torsvik, I.H. Thorseth, O. Tumyr. (2001b) Microbial fractionation of carbon isotopes in altered basaltic glass from the Atlantic Ocean, Lau Basin and Costa Rica Rift. *Chemical Geology* **173**:313–330

Gadd, G.M. (1999) Fungal production of citric and oxalic acid: importance in metal speciation, physiology and biogeochemical processes. *Advances in Microbial Physiology.* **41**:47-92

Gao, H., A. Obraztova, N. Stewart, R. Popa, J.K. Fredrickson, J.M. Tiedje, K.H. Nealson and J. Zhou. (2006) *Shewanella Loihica* sp. nov., isolated from iron-rich microbial mats in the Pacific Ocean. *Int. J. Syst. Evol. Microbiol.* **56**:1911-1916

Giovanoni, S.J. M.R. Fisk, T.D. Mullins and H. Furnes, Genetic evidence for endolithic microbial life colonizing basaltic glasses/seawater interfaces, in: J.C. Alt, H. Kinoshita, L.B. Stokking, P. Michael (Eds.). *Proc. Ocean Drill. Prog., Sci. Results* **148** (1996), pp. 207–214.

Halbach, M., A. Koschinsky, and P. Halbach. 2001. "Report on the discovery of *Gallionella ferruginea* from an active hydrothermal field in the deep sea." *InterRidge News*. **10**(1):18-20

Laura J. Liermann, A.S. Barnes, B.E. Kalinowski, X. Zhou and S.L. Brantley. (2000) Microenvironments of pH in biofilms grown on dissolving silicate surfaces. *Chemical Geology*. **171**(1-2):1-16

Lysnes, K., I.H. Thorseth, B.O. Steinsbu, L. Øvreas, T. Torsvik, and R.B. Pedersen. (2004a) Microbial community diversity in seafloor basalt from the Arctic spreading ridges. *FEMS Microbiol Ecol* **50:**213–230

Lysnes, K., T. Torsvik, I.H. Thorseth and R.B. Pedersen. (2004b) Microbial populations in ocean floor basalt: results from ODP Leg 187. *Proc ODP, Sci Res* **187:**1–27 [http://www-odp.tamu.edu/publications/187_SR/VOLUME/CHAPTERS/203.PDF]

Madigan, M. T., J. M. Martinko, and J. Parker. 2000. *Brock Biology of Microorganisms*, 9th ed. Prentice-Hall, Inc., Upper Saddle River, N.J.

Mason, O.U., U. Stingl, L.J. Wilhelm, M.M. Moeseneder, C.A. Di Meo-Savoie, M.R. Fisk and S.J. Giovannoni. (2007) The phylogeny of endolithic microbes associated with marine basalts. *Environmental Microbiology.* **9**:2539-2550

Maurice, P.A., M.A. Vierkorn, L.E. Hersman, J.E. Fulghum and A. Ferryman. (2001a) Enhancement of kaolinite dissolution by an aerobic Pseudomonas mendocina bacterium. *Geomicrobiology Journal*. **18**:21-35.

Ottow, J. C. G., and A. von Klopotek. 1969. Enzymatic reduction of iron oxide by fungi. *Appl. Microbiol*. **18**:41-43.

Ridgeway, H.F., E.G. Means and B.H. Olson. (1981) Iron Bacteria in Drinking-Water Distribution Systems: Elemental Analysis of Gallionella Stalks, Using X-Ray Energy-Dispersive Microanalysis. *Applied and Environmental Microbiology.* **41**(1):288-297

Rogers, J.R., P.C. Bennett, W.J. Choi. (1998) Feldspars as a source of nutrients for microorganisms. *American Mineralogy* **83**:1532–1540.

Rogers, J.R. and P.C. Bennett. (2004) Mineral stimulation of subsurface microorganisms: release of limiting nutrients from silicates. *Chemical Geology*. **203**: 91-108

Santelli, C., B. Orcutt, E. Banning, C. Moyer, W. Bach, H. Staudigel, K. Edwards. (2008) Abundance and diversity of microbial life in the ocean crust. *Nature.* **453**: 653-656.

Staudigel, H. and S. Hart. (1983) Alteration of basaltic glass: Mechanisms and significance for the oceanic crust-seawater budget. *Geochimica et Cosmochimica Acta*. **47**:337-350.

Staudigel, H., and H. Furnes, (2004) Microbial mediation of oceanic crust alteration. In: Davis, E., Elderfield, H. (Eds.), *Hydrology of the Oceanic Lithosphere.* Cambridge University Press, 608–626

Staudigel, H., H. Furnes, K. Kelley, T. Plank, K. Muehlenbachs, B. Tebo, A. Yayanos. (2004) The oceanic crust as a bioreactor. AGU Monograph. *Deep Subsurface Biosphere at Mid-Ocean Ridges,* **144**:325–341.

Staudigel, H., Furnes, H., Banerjee, N.R., Dilek, Y., Muehlenbachs, K., 2006a. Microbes and volcanoes: a tale fromthe oceans, ophiolites and greenstone belts. *GSA Today* **16**(10). doi:10.1130/GSAT01610A.1.

Staudigel, H., S. R. Hart, A. Pile, B. E. Bailey, E. T. Baker, S. Brooke, D. P. Connelly, L. Haucke, C. R. German, I. Hudson, D. Jones, A. A. P. Koppers, J. Konter, R. Lee, T. W. Pietsch, B. M. Tebo, A. S. Templeton, R. Zierenberg, and C. M. Young. 2006. Vailulu'u Seamount, Samoa: life and death on an active submarine volcano. *Proceedings of the National Academy of Sciences USA*. **103**:6448–6453

Staudigel, H., H. Furnes, N. McLoughlin, N.R. Banerjee, L.B. Connell and A. Templeton. (2008) 3.5 billion years of glass bioalteration: Volcanic rocks as a basis for microbial life? *Earth-Science Reviews*. **89**:156-176

Stein C. A., Stein S., and Pelayo A. (1995) Heat flow and hydrothermal circulation. In *Seafloor Hydrothermal Processes* (eds. S. E. Humphris, R. A. Zierenberg, L. S. Mullineaux, and R. E. Thomson), pp. 425–445. American Geophysical Union

Stevens, T. O., and J. P. McKinley. (1995) Lithoautotrophic microbial ecosystems in deep basalt aquifers. *Science* **270:**450-454

Stillings, L.L., J.I. Drever, S.L. Brantley, Y. Sun and R. Oxburg. (1996) Rates of feldspar dissolution at pH 3-7 with 0-8 mM oxalic acid. *Chemical Geology*. **132**(1-4):79-89

Stroncik, N.A., and Schmincke, H.-U., 2002, Palagonite - A review: International Journal of Earth Sciences. **91**:680–697. doi: 10.1007/s00531-001-0238-7

Templeton, A., H. Staudigel and B. Tebo. (2005) Diverse Mn(II)-oxidizing bacteria isolated from submarine basalts at Loihi Seamount. *Geomicrobiology Journal* **22:** 127–139

Thorseth, I.H., H. Furnes and M. Heldahl. (1992) The importance of microbiological activity in the alteration zone of natural basaltic glass. *Geochimica et Cosmochimica Acta* **55**:731–749.

Thorseth, I.H., T. Torsvik, H. Furnes and K. Muehlenbachs, Microbes play an important role in the alteration of oceanic crust. *Chem. Geol.* **126** (1995), pp. 137–146.

Thorseth, I., T. Torsvik, V. Torsvik, F. Daae, R. Pedersen, and K.-S. Party. (2001) Diversity of life in ocean floor basalt. *Earth Planet. Sci. Lett.* **194:**31–37.

Torsvik, T., H. Furnes, K. Muehlenbachs, I.H. Thorseth and O. Tumyr, Evidence for microbial activity at the glass-alteration interface in oceanic basalts. *Earth Planet. Sci. Lett.* **162** (1998), pp. 165–176.

Ullman W.J., D.L. Kirchman, S.A. Welch, and P. Vandevivere. (1996) Laboratory evidence for microbially mediated silicate mineral dissolution in nature. *Chemical Geology.* **132**(1–4):11–17.

Welch S. A. and J.F. Banfield. (2002) Modification of olivine surface morphology and reactivity by microbial activity during chemical weathering. *Geochimica et Cosmochimica Acta.* **66**:213–221.

Chapter 2

A New Laboratory DNA Extraction Protocol for Spores and Metal-Rich Low Biomass Samples.

Abstract

This study compares two commercially available environmental DNA extraction kits to an in-house protocol in order to determine effective DNA yields from each method. Our goal was to produce a simple, inexpensive extraction protocol using existing laboratory equipment, reagents and techniques to reliably produce high-quality, high molecular weight, amplifiable DNA from environmental samples with a high metal oxide abundances. Each protocol was tested using a Manganese oxide forming spore laboratory culture and two different environmental samples (spore forming *Bacillus* sp., iron-oxide dominated microbial mat and rock/mineral surfaces). All samples have historically proven difficult to either lyse the cells for their DNA contents or else the DNA adsorbs onto remaining material in the extraction process. Our in-house method makes use of both chemical and physical disruption methods in order to maximize cell lysis and a DNA stabilizer, which acts as a DNase inhibitor. Results show that in all sample types, our in-house method produces 2.5-7 times total DNA yields over the conventional extraction kits. The resultant DNA is of sufficient purity to be easily amplified with no further cleanup or desalting processes necessary. Additionally, our method approximately halves the cost per extraction relative to the other kits tested in this study.

2.1 Introduction

Effective and unbiased DNA extraction is arguably the most critical step in molecular biological characterization of environmental samples. Unfortunately, most current extraction protocols result in biased extraction (Frostegarde et al, 1999) of easily extracted DNA or low DNA yields due to low biomass or insufficient lysis. At best, these problems result in biased results, and in the worst case, insufficient DNA yields prohibit any meaningful molecular characterization. Over the past few decades, several methods for extracting DNA from cells have been conceived (e.g. sodium dodecyl sulfate (SDS), lysozyme, bead beating, proteinase K, phenol/chloroform, freeze-thaw, freeze-boil, mortar grinding, achromopeptidase, EDTA, etc) (Miller et.al., 1999) such that it is now almost a trivial exercise to perform DNA extractions in the lab.

Unfortunately, most DNA extraction protocols remain biased and rarely possess the capability to extract DNA from every cell type found in environmental samples. Gram-positive and spore forming bacteria are historically difficult to retrieve DNA from due to tough cell walls and high peptidoglycan content (Fisher et al, 1995). Other methods result in a high degree of DNA shearing due to prolonged mechanical shearing stress from bead beating (e.g. Krsek and Wellington, 1999; Miller et.al. 1999).

The goal of this study was to develop a method using existing techniques and common laboratory supplies for extracting DNA from difficult environmental samples containing high metal content with high recovery rates and large DNA fragments with minimal shearing. The unique characteristics of these environmental samples require a new, more effective protocol to retrieve as much DNA for molecular work as possible. To this end, we decided on a mixture of previously defined protocols which involve a

careful balance between mechanical and chemical stress for cell lysis and a DNA clean up step embedded in the protocol to produce high quality amplifiable DNA. The result is a method that provides up to three times amplifiable DNA over commercial soil DNA extraction kits using three traditionally difficult sample types at a fraction of the cost and is readily adapted to the specific needs of most laboratories.

2.2 Materials and Methods

Our protocol (CMF) is a combination of chemical and mechanical stress for cell lysis, coupled to a filtration step to produce high yield, clean DNA. Three different environmental samples and a pure laboratory culture were chosen for this study as the three environmental samples are historically difficult to extract DNA from and the pure culture possessed high levels of metal oxides.

2.2.1 Samples

Samples: 1. The first sample came from *Bacillus* sp. SG-1 spore preps, which are known manganese oxidizers (Francis and Tebo, 2002) and had abundant Mn-oxides present.   2. The second sample of iron-oxide encrusted microbial floc collected on Vailulu'u Seamount via submersible suction sampler was used as our high iron content sample (described in Staudigel et.al., 2006). Organic carbon content was determined to be relatively small compared to the overall iron content (Staudigel et.al., 2006). 3. The third sample was a basaltic glass sampled on the southern flank of Loihi Seamount

(Hawai'i). Nucleic acid stains reveal a relatively low biomass associated with the glass surfaces and in most places only a monolayer biofilm was present.

2.2.2 Sample Preparation

The *Bacillis* sp. SG-1 spores were prepared after Dick et.al. (2006). The iron oxide floc was homogenized using a vortexer and 1.5 ml was aliquoted into 2 ml tubes and centrifuged to concentrate cells and oxides. The pellet was then transferred to each kit for extraction. The basaltic rock had the outer glass rind chipped away and the glass was then ground into a powder using a mortar and pestle and a 300mg aliquot was used in each of our extraction experiments.

2.2.3 Extraction Protocols

We tested our chemical-mechanical filtration (CMF) extraction protocol against two popular, commercially available environmental extraction kits: QBioGene FASTDNA SPIN kit for Soil (http://www.QBioGene.com , Catalog #6560-200) (referred to hereafter as Kit Q) and MoBio Ultraclean Soil DNA Kit (http://www.mobio.com, Cat. #11-114) (Kit M). For Kit Q and Kit M, we followed the manufacturer's recommended protocol; however for Kit M, we replaced the Inhibitor Removal Solution (IRS) with distilled deionized water in the iron floc samples. All final elutions were done with 100μl of 18.3 MΩ DDI autoclaved water.

CMF: The following protocol was used for the CMF tests. 2.0 ml screw cap tubes with o rings were prepared by filling with 200mg each of acid washed 0.1, 0.5, 2.0

mm zirconium glass beads and then autoclaved. 300 mg of sample was then added to each tube. We then added 580 ul lysis solution (300mM EDTA, 300 mM NaCl, 300 mM Tris buffer, pH 7.5) to the tubes along with 70 µl 15% Sodium Dodecyl Sulfate (SDS), 15ul of Polyadenylic Acid (PolyA, 10mg/ml, Roche Diagnostics Cat. #108626) and 35 µl Dithiothreitol (DTT) (1M DTT in 0.01 M Acetate, Acros Organics Cat. #327190100). The tubes were then homogenized using a vortexer and incubated at 70°C for 30 mins. After cooling to < 40°C, 14 ul lysozyme (5%) was added. The tubes were again vortexed and incubated at 37°C for 20 mins. The tubes were then placed in the FastPrep FP120A instrument (BioGene, Cat# 6001-120) and beat for two cycles at speed 5.5 for 30 secs in order to lyse the cells. The tubes were placed on ice for 2-4 mins between FastPrep treatments. We then added 150 ul KCl (1M), vortexed and place on ice for 5 mins. The samples were centrifuged for 5 mins at 14k x g. Up to 400 ul of clear supernatant was transferred to a Microcon Centrifugal Filter Device (http://www.millipore.com, Cat# 42416) and centrifuged at 1000 x g for 15 mins and the filtrate was discarded. We repeated the process until all supernatant has been through the filter. On the last run, we added enough TE buffer (10mM Tris pH 7.5, 1mM EDTA) to have a total volume of 400 ul. To rinse the DNA, we added 400 ul TE buffer to the filter unit and centrifuged at 1000 x g for 15 mins and discard filtrate. Invert filter into a clean tube and add 100 ul TE buffer to the filter, centrifuge for 15 mins and discard filter. The DNA was stored at -20°C for later use. DNA yields were quantified via the Picogreen Assay (Invitrogen, Carlsbad, CA, USA, SKU# P11495) and a Perkin Elmer/Tecon HTS 7000 Bio Assay Plate Reader.

2.3 Results and Discussion

The CMF method is a combination of chemical stress to disrupt cell wall structure and mechanical stress to lyse the cells and extract the DNA. Chemical disruption was carried out through the use of Sodium Dodecyl Sulfate (SDS), a known protein denaturant, Dithiothreitol (DTT) which disrupts protein disulfide bonds and can act as a chemical reductant, and lysozyme which attacks the peptidoglycan structure of cell walls and renders the cell permeable. Mechanical stress was completed on a bead beater in combination with three different size zirconium beads designed to achieve different goals: small beads to break open individual cells, and large beads to disrupt cell aggregates and ensure homogenization throughout the process. Tests ran with longer bead beating periods resulted in significant DNA shearing and reduced fragment sizes as the time increased. KCl was added to the tube and placed on ice to precipitate out potassium-SDS-protein complexes (Trask, et.al., 1984). The DNA purification steps involved filtration through a Montage filter unit which served to collect, desalt and purify the DNA while keeping the DNA in solution. Each extraction protocol was run in triplicate to determine error and reproducibility.

We compared DNA yields from the CMF, Kit Q and Kit M for all three samples. In all cases, the CMF method outperformed the commercial extraction kits, and in one case up to seven times the final DNA yield. Figure 2.1 shows the results of our DNA extraction protocol versus Kit Q and Kit M for the three environmental samples. The *Bacillus* spore extractions yielded a 140% increase in recovered DNA with the CMF method over Kit M and ~70% increase over Kit Q.   The iron floc results mirrored the bacillus results where the CMF method outperformed Kits M and Q by ~700% and 300%

respectively. Extractions performed on the iron floc samples with Kit M using the manufacturer protocol resulted in a low density polymer forming after addition of the salt solution. This polymer served to absorb the DNA, and subsequently clog up the silica filter unit, rendering the DNA yield from this method below detection limits. The MoBio tech support recommended replacing the Inhibitor Removal Solution with DDI water as they suspected a reaction with the high levels of iron present in the sample. This substitution removed the low density polymer and allowed subsequent DNA recovery on this sample. The relative low biomass on the rock surfaces makes it difficult to resolve any major differences in the DNA yields between the kits, but the CMF method resulted in a slightly higher total yield of 0.22 ug versus 0.12 and 0.09 ug or a 180% and 240% increase overkits Q and M respectively (Figure 2.1).

DNA Yields from Different DNA Extraction Protocols for Environmental Samples
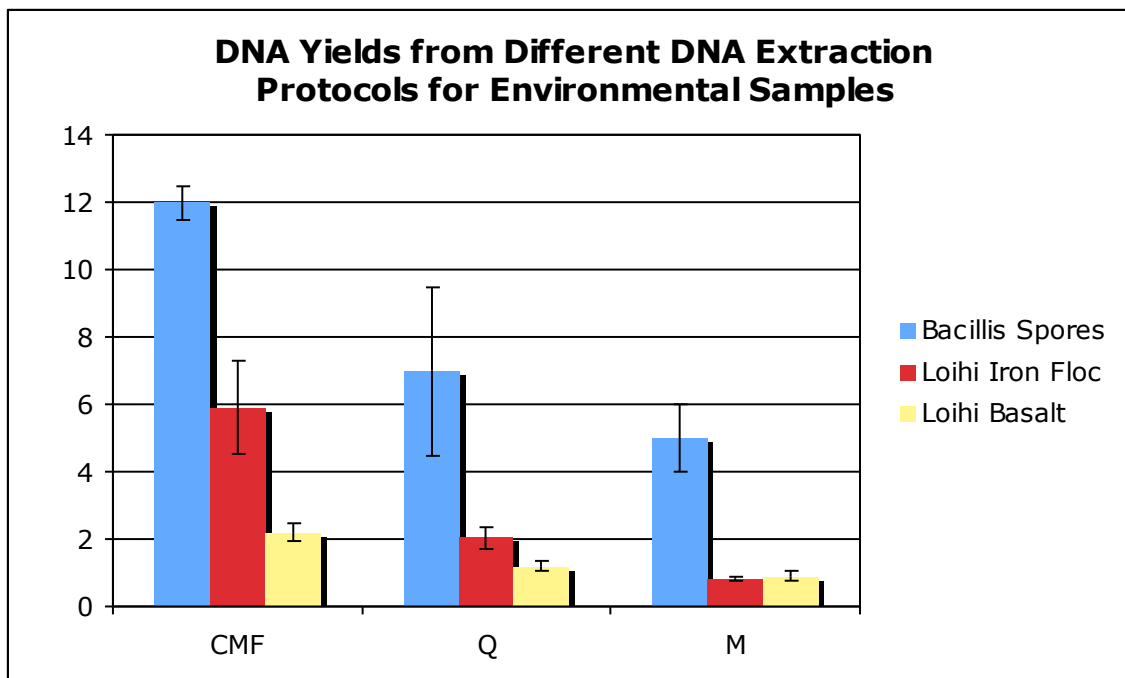
Figure 2.1. DNA yields in ng/ul from Bacillus spores (blue), Iron oxides from Loihi (red) and basaltic glass from Loihi (yellow) for the CMF protocol, Kit Q and Kit M. Error bars represent one standard deviation.

While the specific chemistry and reagents are not published for either Kit Q or Kit M, it is possible to draw some comparisons to the CMF method through observation. All three methods use a detergent as a protein denaturant which precipitates out proteins via similar methods to the CMF KCl precipitation as well as beads and a bead beater for mechanical stress. However, Kit M only uses a single bead size fraction for bead beating, which might limit its capabilities in lysing cells of differing sizes. Also, neither Kit Q nor Kit M utilizes any chemical reductants or enzymes which require specific temperature incubation periods, which could reduce their effectiveness in lysing spores or cells in a metal oxide rich sample. Both kits seem to use a similar DNA purification protocol through addition of a salt solution and adsorption to a silica filter or silica gel matrix.

The Montage filter unit used by the CMF method leaves the DNA in solution throughout the process which may allow for greater recovery efficiency.

All three extraction methods produced amplifiable DNA of sufficient purity from the Bacillus and iron oxide floc samples (data not shown). However in the basalt samples where biomass is the limiting factor, only the CMF protocol produced enough DNA to reliably amplify using PCR (Figure 2.2). The CMF method has shown to be more successful at lysing spores and cells in the presence of normal inhibitors (high metal content). It is likely that the larger yields are attributed to an enhanced chemical treatment coupled to variable bead sizes aimed at disrupting cell aggregates and lysing individual cells. The relative cost of the CMF method also turned out to be approximately $3 per sample vs $5 per prep for Kits Q and M. The high yields from the CMF method coupled to the high purity of the resultant DNA serves to lessen some of the bias normally associated with conventional environmental DNA extraction protocols.
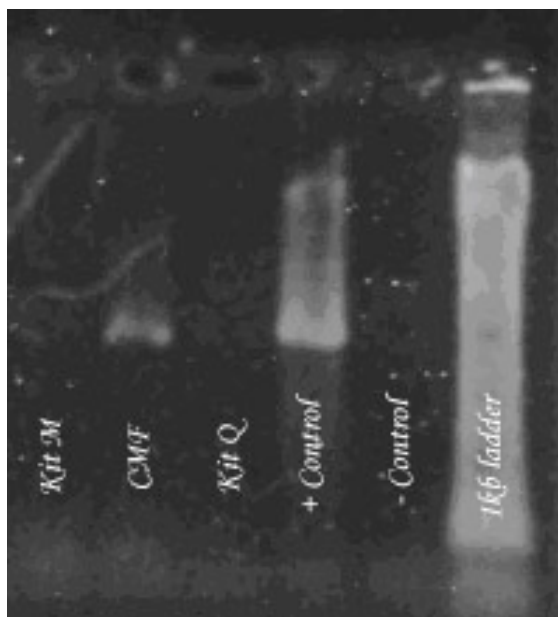
Figure 2.2. Gel electrophoresis of PCR results from Loihi Basalt extractions using Kits Q&M and the CMF protocol. Primers used were 68F and 1510R. Kit Q and Kit M did not produce amplified DNA while CMF resulted in amplified DNA and was used for further molecular analysis (data not shown).

2.4 Acknowledgments

2.5 References

Dick, G.J., Y.E. Lee and B.M. Tebo. (2006) Manganese(II)-Oxidizing *Bacillus* Spores in Guaymas Basin Hydrothermal Sediments and Plumes. Applied and Enivronmental Microbiology. 62: 3184-3190

Fischer K, D. Hahn, W. Hönerlage, F. Schönholzer, J. Zeyer (1995). In situ detection of spores and vegetative cells of *Bacillus megaterium* in soil by whole-cell hybridization. *Systematic and Applied Microbiology.* 18:265–273

Francis CA and B.M. Tebo. (2002) Enzymatic manganese(II) oxidation by metabolicallydormant spores of diverse *Bacillus* species. *Applied and Environmental Microbiology.* 68:874–80

Frostegard, A., S. Courtois, V. Ramisse, S. Clerc, D. Bernillon, F. LeGall, P. Jeannin, X. Nesme, and P. Simonet. (1999) Quantification of bias related to the extraction of DNA directly from soils. *Applied and Environmental Microbiology*. 65:5409–5420.

Jung, W. K., and R. Schweisfurth. (1979) Manganese oxidation by an intracellular protein of a P*seudomonas* species. *Z. Allg. Microbiol*. 19:107–115.

Krsek, M and EMH Wellington. (1999) Comparison of different methods for the isolation and purification of total community DNA from soil. Journal of Microbiological Methods. 39:1-16

Miller, D. N., J.E. Bryant, E.L. Madsen, and W.C. Ghiorse. (1999). Evaluation and optimization of DNA extraction and purification procedures for soil and sediment samples. Applied and Environmental Microbiology, 65:4715–4724

Rosson, R. A., and K.H. Nealson. (1982) Manganese binding and oxidation by spores of a marine *Bacillus*. *Journal of Bacteriology*. 151:1027–1034.

Staudigel H., S.R. Hart, A. Pile, B.E. Bailey, E.T. Baker, S. Brooke, D.P. Connelly, L. Haucke, C.R. German, I. Hudson, D. Jones, A.A. Koppers, J. Konter, R. Lee, T.W. Pietsch, B.M. Tebo, A.S. Templeton, R. Zierenberg, C.M. Young. 2006. Vailulu'u Seamount, Samoa: Life and death on an active submarine volcano. *Proceedings of the National Academy of Sciences*. 103(17):6448

Templeton, A. S., H. Staudigel, and B. M. Tebo. (2005) Diverse Mn(II)-oxidizing bacteria isolated from submarine basalts at Loihi Seamount. *Geomicrobiology Journal*. 22:127-139.

Trask D.K., J.A. Didonato, and M.T. Muller. (1984) Rapid Detection and Isolation of Covalent DNA Protein Complexes – Application to Topoisomerase-I and Topoisomerase-II. *EMBO Journal.* 3(3):671-676.

Chapter 3

Fe Moessbauer Spectroscopy as a Tool in Astrobiology

Christian Schröder[a], Brad Bailey[b], Göstar Klingelhöfer[a], Hubert Staudigel[b]

[a]Institut fur Anorganische und Analytische Chemie, Johannes Gutenburg-Universitat, Staudinger Weg 9, D-55128 Mainz, Germany
[b]Institute of Geophysics and Planetary Physics, Scripps Institution of Oceanography, Univ. of CA, San Diego, La Jolla, CA 92093-0225, USA

Abstract

The element Fe and Fe-bearing minerals occur ubiquitously throughout the field of astrobiology. Cycling between the various oxidation states of Fe provides a source of energy available for life. Banded iron formations may record the rise of oxygenic photosynthesis. The distribution of Fe between Fe-bearing minerals and its oxidation states can help to characterize and understand ancient environments with respect to the suitability for life by constraining the primary rock type and the redox conditions under which it crystallized, the extent of alteration and weathering, the type of alteration and weathering products, and the processes and environmental conditions for alteration and weathering. Fe Moessbauer spectroscopy is a powerful tool to investigate Fe-bearing compounds. It can identify Fe-bearing minerals, determine Fe oxidation states with high accuracy, quantify the distribution of Fe between mineralogical phases, and provide clues about crystallinity and particle sizes. Two miniaturized Moessbauer spectrometers are on board of the NASA Mars Exploration Rovers Spirit and Opportunity. The Fe-bearing minerals goethite, an iron oxide-hydroxide, and jarosite, an iron hydroxide sulfate, were

identified by Moessbauer spectroscopy in Gusev Crater and at Meridiani Planum, respectively, providing in situ proof of an aqueous history of the two landing sites and constraints on their habitability. Hematite identified by Moessbauer spectroscopy at both landing sites adds further evidence for an aqueous history. On Earth, Moessbauer spectroscopy was used to monitor possibly microbially-induced changes of Fe-oxidation states in basaltic glass samples exposed at the Loihi Seamount, a deep sea hydrothermal vent system, which might be analogous to possible extraterrestrial habitats on ancient Mars or the Jovian moon Europa today.

3.1 Introduction

The field of astrobiology includes the study of the origin, evolution and distribution of life in the universe (e.g., Des Marais and Walter, 1999). Hot spots of research in the Solar System comprise above all the planet Mars, followed by Europa and Titan, moons of Jupiter and Saturn, respectively. On Earth much of the research concentrates on the study of so-called extreme environments that can serve as analogues for possible habitats on the planets and moons mentioned above, and on extremophiles—mostly microbial life-forms that thrive in these environments (e.g., Rothschild and Mancinelli, 2001).

The element Fe and Fe-bearing minerals occur ubiquitously throughout the field of astrobiology. The formation of pyrite at hydrothermal vents, for example, may have played a crucial role at the origin of life, providing energy for the fixation of carbon as well as mineral binding surfaces for organic constituents (Waechtershaeuser, 1988, 1992). Banded iron formations (BIFs) are among the oldest rocks on Earth. Layers of

ferric iron in BIFs may record the evolution of oxygenic photosynthesis (Walker, 1979). Fe-rich carbonate globules and magnetite particles, resembling those found in terrestrial magnetotactic bacteria, in the Martian meteorite ALH84001 were interpreted as evidence for possible relic biogenic activity by McKay et al. (1996) and helped to re-energize the discussion about life on Mars. The young Earth as well as present day Mars, Saturnian Titan, or Jovian Europa have a lack of free oxygen in common. In anaerobic environments iron can act as both an electron donor in its ferrous form and a terminal electron acceptor in its ferric form to support metabolism (Megonigal et al., 2003, and references therein). Furthermore, Fe oxide and hydroxide minerals have the potential to preserve microfossils and physical biomarkers (e.g., Allen et al., 2004). The distribution of Fe between Fe-bearing minerals and its oxidation states can help to characterize and understand ancient environments with respect to the suitability for life by constraining the primary rock type (e.g., olivine- versus non-olivine-bearing basalt), the redox conditions under which primary minerals crystallized (e.g., presence or absence of magnetite), the extent of alteration and weathering (e.g., value of Fe^{3+}/Fe_{Total}), the type of alteration and weathering products (e.g., oxides versus sulfates versus phyllosilicates), and the processes and environmental conditions for alteration and weathering (e.g., neutral versus acid-chloride versus acid-sulfate aqueous process under ambient or hydrothermal conditions) (Morris et al., 2006).

Moessbauer spectroscopy is a powerful tool in analyzing Fe-bearing compounds. The method identifies Fe-bearing minerals, determines Fe oxidation states with high accuracy, quantifies the distribution of Fe between mineralogical phases, and provides clues about crystallinity and particle sizes. It is particularly useful in systems where the

iron oxide may be too low in concentration or in crystallinity to be detected by XRD, for example in soils, sediments, rust and in organisms (Cornell and Schwertmann, 1996, p. 148ff). Moessbauer spectroscopy has for example been used in the characterization of terrestrial hydrothermal springs (Wade et al., 1999).

Moessbauer spectroscopy is a well-established technique in use in laboratories around the world. A miniaturized Moessbauer spectrometer has been developed for spaceflight to investigate planetary surfaces in situ (Klingelhoefer, 1999; Klingelhoefer et al., 1995, 1996, 2003). As part of the payload of NASA's twin Mars Exploration Rovers (MER) it has successfully returned results from the surface of Mars (Morris et al., 2004, 2006; Klingelhoefer et al., 2004) and is available for inclusion in future planetary missions. In the following, after a brief introduction to the principles of Moessbauer spectroscopy, we summarize the MER Moessbauer results with respect to astrobiology. We present new results from laboratory Moessbauer studies on basaltic glass samples exposed at a deep sea hydrothermal vent.

3.2 Moessbauer Spectroscopy

Rudolf Ludwig Moessbauer (Nobel Prize 1961) discovered recoilless absorption and emission of g-rays by specific nuclei in a solid in 1958 (Moessbauer, 1958a, b, 2000). There are numerous reviews and textbooks available of this ''Moessbauer effect'' in general (e.g., Greenwood and Gibb, 1971; Gonser, 1975; Guetlich, et al., 1978), of its applications in mineralogy and geochemistry (e.g., Bancroft, 1973; Hawthorne, 1988; Mitra, 1992; McCammon, 1995), and of the investigation of planetary surfaces in particular (Burns, 1993; Klingelhoefer et al., 1995; Wdowiak et al., 2003). Constraints of

remote Moessbauer spectroscopy such as on the surface of Mars are discussed by Dyar and Schaefer (2004). Here we provide a brief overview.

3.2.1 Moessbauer Effect

When a nucleus of a particular isotope (e.g., ^{57}Fe with an isotopic abundance of 2.14% in natural iron) in an excited state decays to the ground state, separated by the transition energy Et (e.g., 14.4 keV for the transition of the nuclear spin I = 3/2 excited state to the I = 1/2 ground state of ^{57}Fe, Figure 3.1), by emitting g-radiation of the energy E_γ it experiences recoil of energy E_R expressed as $E_R = (E_\gamma^2)/(2Mc^2)$, where M is the mass of the nucleus and c is the velocity of light. Conservation of energy requires that only E_t-E_R is available for E_γ. Likewise, in order to bring an identical nucleus from the ground state into the excited state, radiation with an energy of $E_\gamma = E_t + E_R$ is necessary. The linewidth Γ' of the emitted γ-radiation can be determined with the lifetime τ of the excited state (10^{-7} s for ^{57}Fe) via Heisenberg's uncertainty principle $\Gamma \tau \geq h/2\pi$, where h/2π is Planck's constant divided by 2π. For ^{57}Fe the linewidth $\Gamma = 4.67 \times 10^{-9}$ eV and $E_R = 1.9 \times 10^{-3}$ eV. Because Γ is much less than E_R, it is not sufficient to bridge the energy gap of $2E_R$; resonant emission and absorption of γ-rays is not possible. However, as Moessbauer discovered, when the nucleus is bound rigidly to the crystal lattice of a solid, the crystal as a whole takes up the recoil energy. Recoil energy is thereby transferred to the lattice by exciting phonons (quantum units of lattice vibrations). The energy of excited phonons adds up to E_R on average, but with a certain probability no phonons are excited and emission or absorption processes happen recoilless. Conditions for resonant emission and

absorption of γ-rays are restored. This probability, the recoil-free fraction f, can be expressed as $f = \exp(-k^2\langle x^2\rangle)$, where k is the wave vector of the γ-ray and $\langle x^2 \rangle$ is the mean vibrational amplitude of the nucleus. This f-factor is also referred to as the Lamb–Moessbauer factor or the Debye– Waller factor. The Moessbauer effect has been observed in specific isotopes of over 40 elements. ^{57}Fe Moessbauer spectroscopy is the most widely applied, because of the relative ease of measurement, and because Fe is one of the most abundant and wide-spread elements.
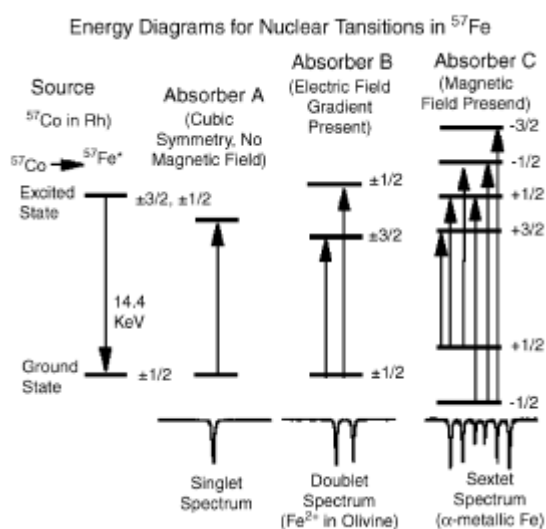
Figure 3.1. Energy level diagram for ^{57}Fe showing emission of 14.4 keV g-rays from a ^{57}Co Moessbauer source and absorption of the g-rays in three different nuclear environments.

3.2.2 A Simple Moessbauer Spectrometer

A simple Moessbauer spectrometer consists of a source emitting the specific g-rays, a sample or absorber to be investigated, and a γ-ray detector (Figure 3.2). The isotope ^{57}Co decays by electron capture with a halflife of 270 days to ^{57}Fe. This happens with a certain probability via the I = 3/2 excited nuclear spin state of ^{57}Fe, emitting the

desired 14.4 keV γ-radiation when finally transitioning to the ground state. Nuclear energy levels are influenced by the chemical environment. If the Moessbauer isotopes in source and absorber reside in different chemical compounds, resonant conditions may be violated. They can be restored by moving the source relative to the absorber with velocity v_s, thereby adding or subtracting energy E_D to E_γ via the Doppler effect $E_D = (v_s/c)E_\gamma$. The x-axis in Moessbauer spectra is therefore labeled in units of velocity (usually mm/s) rather than energy. The detector may be installed in line with source and absorber, with the absorber between source and detector (transmission geometry, Figure 3.2). Thin slices or thinly distributed powders of the absorber material have to be prepared to let enough radiation pass through to the detector. Resulting Moessbauer spectra show absorption minima. Alternatively, the detector may be installed on the same side of the absorber as the source (backscattering geometry, Figure 3.2). The detector then records reemitted γ-rays, or may be tuned to detect competing ways of deexcitation such as conversion electrons, or secondary processes such as X-rays. The resulting Moessbauer spectra show reflection maxima.

3.2.3 Moessbauer Parameters

The interaction of a nucleus with its chemical environment affects the nuclear energy levels. Positions of resonant peaks in Moessbauer spectra reflect these changes relative to the source material and can thus be used to determine the character of the chemical environment of the absorber. Different kinds of interaction manifest themselves in three important parameters, which can be extracted from a Moessbauer spectrum.

These hyperfine parameters or Moessbauer parameters are the isomer shift δ, the quadrupole splitting ΔE_Q, and the magnetic hyperfine splitting B_{hf}.
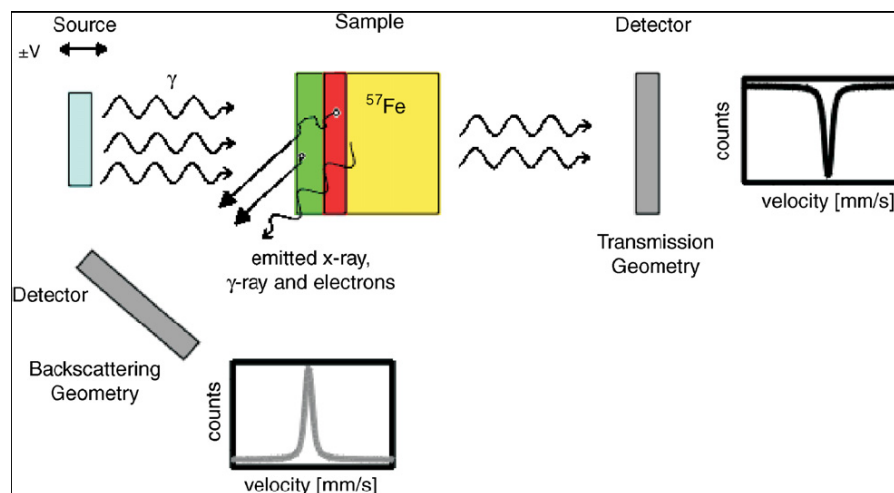
Figure 3.2. A simple Moessbauer spectrometer consisting of a source, a sample or absorber, and a detector. The absorber may be between source and detector (transmission geometry), or on the same side of the absorber as the source (backscattering geometry).

3.2.3.1 Isomer Shift

The isomer shift δ results from electric monopole interaction, i.e., Coulomb interaction of the positive nuclear charge with electrons inside the nuclear region. It can be expressed as $\delta = (4/5)\pi Ze^2 R^2 (\delta R/R)\{|\Psi(0)|_A^2 - |\Psi(0)|_S^2\}$, where Ze is the nuclear charge, R is the mean radius of the nucleus in its ground and excited states, δR is the difference between the radii of excited and ground states, and $|\Psi(0)|^2$ is the electron density at the nucleus of the source (S) or the absorber (A). Isomer shifts thus also vary according to the source material used (e.g., [57]Co in Rh matrix) and have to be cited relative to a common reference material, which in the case of Fe Moessbauer

spectroscopy is commonly pure metallic Fe foil. The isomer shift d can be used to determine the oxidation state of iron in a given absorber. The $\delta R/R$ ratio for [57]Fe is negative, and thus increasing electron density at the nucleus results in a lower value of δ. Only electrons in s-shells have a finite probability of being located at the nucleus. When metallic iron is oxidized to Fe^{2+}, two 4s electrons are removed and δ increases. Further oxidation to Fe^{3+}, however, removes an electron from the 3d shell. The remaining electrons are bound tighter to the nucleus and the electron density at the nucleus increases. As a result, δ values for Fe^{3+}-bearing compounds are lower than for Fe2+-bearing compounds. The ligand-type (e.g., O versus S bound to Fe) and the coordination symmetry (e.g., Fe in tetrahedrally coordinated sites versus Fe in octahedral sites) also influence the electron density and therefore the isomer shift. For Fe bound to O such as in silicates, sulfates, carbonates, etc., isomer shifts for Fe^{2+} cations typically range from 0.75 to 1.3 mm/s in room temperature Moessbauer spectra; isomer shifts for Fe^{3+} cations range from 0.15 to 0.5 mm/s (e.g., Burns and Solberg, 1990; Burns, 1993, 1994).

3.2.3.2 Quadrupole Splitting

Quadrupole splitting ΔE_Q results from electric quadrupole interaction. It is observed only when the nuclear charge is not distributed spherically symmetric (i.e., the nucleus possesses a non-zero quadrupole moment Q) and electron and lattice charges are arranged other than in cubic symmetry, thus producing an electric field gradient at the nucleus interacting with the quadrupole moment. This interaction partially removes the degeneracy of the I = 3/2 excited state of [57]Fe, separating it into two levels with magnetic spin quantum numbers of $m_I = \pm 3/2$ and $\pm 1/2$. The energy difference between these two

levels is $\Delta E_Q = E_Q(\pm 3/2) - E_Q(\pm 1/2) = eQV_{zz}/2$, where V_{zz} is a component of the electric field gradient. Two transitions to the ground state are possible (Figure 3.1), manifesting themselves as two separate resonant peaks (a doublet) in a Moessbauer spectrum. The distance between the two peak centers is equal to ΔE_Q. In the case of combined electric monopole and quadrupole interaction, the location of the center between the two doublet peaks on the x-axis in the Moessbauer spectrum defines the isomer shift δ. The different electronic configurations of, e.g., Fe^{2+} and Fe^{3+} ions and different coordination environments result in different electric field gradients at the nucleus. ΔE_Q values are generally larger for compounds containing Fe^{2+} ions than for compounds containing Fe^{3+}. The combination of isomer shift δ and quadrupole spliting ΔE_Q enables to reliably distinguish between Fe^{2+} and Fe^{3+} ions in mixed-valence compounds (e.g., Burns and Solberg, 1990; Burns, 1993, 1994).

3.2.3.3 Magnetic Hyperfine Splitting

Magnetic hyperfine splitting B_{hf} results from the interaction of a magnetic field at the nucleus, it may be intrinsic or externally applied, with the magnetic dipole moment μ_N of the nucleus. The degeneracy of nuclear states of spin I is completely removed into (2I+1) energy levels (nuclear Zeeman effect) $E_M = -g_N\mu_N m_I B_{hf}$, where g_N is the nuclear Lande´ factor and $m_I = I, I-1,\ldots,-I$. The ground state of ^{57}Fe with $I = 1/2$ splits into two, the excited state with $I = 3/2$ into four levels. Selection rules for magnetic dipole transitions ($\Delta I = 1$, $\Delta m_I = 0, \pm 1$) allow only six transitions, which manifest themselves as six separate resonant peaks (a sextet) in the Moessbauer spectrum (Figure 3.1). The

parameter B_{hf} is the distance between the outermost peak centers of the sextet. In the case of simultaneous electric monopole interaction, electric quadrupole interaction, and magnetic dipole interaction the isomer shift δ can be calculated as $\delta = (1/4)(v_1 + v_2 + v_5 + v_6)$, where enumerated v_6, for example, corresponds to the center position of peak number 6 of a sextet when counted from lower to higher velocity in a Moessbauer spectrum. The quadrupole splitting DEQ can be calculated in most cases as $\Delta E_Q = (1/2)[(v_6 - v_5) - (v_2 - v_1)]$. The magnetic hyperfine field B_{hf} of magnetically ordered compounds may not be observed in a Moessbauer spectrum when particle sizes are in the range of magnetically ordered domains. Thermal excitation may cause the reversal of the magnetization of such one-domain particles. The fluctuations of the magnetization happen with the relaxation time τ, $\tau = t_0 \exp(\kappa V/kT)$, where t_0 is a constant, κ is the magnetic anisotropy energy per unit volume, V is the volume of the particle, and kT is the thermal energy. If the relaxation time is smaller than the lifetime of the Moessbauer transition, the magnetic field sensed by the nucleus of the Moessbauer isotope is reduced to zero. The particles become superparamagnetic. At room temperature this effect is observed for particles o30 nm, i.e., nanocrystalline particles. The magnetic hyperfine splitting B_{hf} may be restored in the Moessbauer spectrum by lowering the temperature of the absorber in the experiment, thereby increasing the relaxation time τ. Nanocrystalline or superparamagnetic iron oxides occur in many environments important in an astrobiological context such as pedogenic weathering environments (e.g., Murad, 1988), the Orgueil carbonaceous chondrite (Wdowiak and Agresti, 1984), hydrothermal vent systems (Agresti et al., 1994; Wade et al., 1999), clays at the Cretaceous-Tertiary (KT) boundary (e.g., Wdowiak et al., 2001), or the surface of Mars (e.g., Morris et al., 1989a, 2000, 2001, 2004, 2006).

3.2.3.4 Relative Areas

Every Fe-bearing compound is characterized by a particular set of the Moessbauer parameters δ, ΔE_Q, and B_{hf}, like a fingerprint. An absorber investigated by Moessbauer spectroscopy may contain several Fe-bearing compounds. Hence a Moessbauer spectrum may be resolved into several single peak, doublet, and sextet subspectral components. The relative subspectral peak area is roughly proportional to the relative amount of Fe in this compound. Deviations from that proportionality arise, because Debye–Waller factors are compound specific. De Grave and Van Alboom (1991) and Eeckhout and De Grave (2003) evaluated Debye–Waller factors for many Fe-bearing minerals. Generally, Fe^{3+} ions have higher Debye–Waller factors than Fe^{2+} ions and an f-factor correction may be applied to account for this difference.

3.2.4 The Miniaturized Moessbauer Spectrometer MIMOS II

The miniaturized Moessbauer spectrometer MIMOS II was specifically designed for planetary missions. Besides miniaturization this involves low power consumption and a rigid design to withstand high acceleration forces and shocks, large temperature variations such as typical during the Martian diurnal cycle, and cosmic radiation. To avoid complicated sample preparation the instrument is set up in backscattering geometry. The instrument is simply applied to the sampling surface. Klingelhoefer et al. (2003) give a detailed description of the instrument. The special features of MIMOS II open up a range of terrestrial applications. It has been used in the monitoring of iron ore production (Klingelhoefer et al., 1998), the monitoring of hydromorphic soils in the field (Klingelhoefer et al., 1999; Feder et al., 2002, 2005), and in situ monitoring of corrosion

and air pollution studies (de Souza et al., 2001, 2002). Due to its set-up in backscattering geometry it is a non-destructive method suitable for the investigation of rare and precious materials, such as archaeological artifacts (Klingelhoefer et al., 2002a, b; de Souza et al., 2003; de Souza, 2004) or Martian meteorites (Schroeder et al., 2004; de Souza, 2004).

3.3 Mars

Martian surface materials contain between 13 and 18 wt% FeO (e.g., Rieder et al., 1997), making it 2 to 3 times more abundant than in Earth's crust. On the basis of that high Fe content Morris et al. (1989b), Knudsen (1989), Knudsen et al. (1990, 1992), and others argued in detail for the use of Moessbauer spectroscopy to investigate the surface of Mars. Moessbauer spectroscopy was recommended for the in situ investigation of the Martian surface in an ESA study on exobiology in the solar system and the search for life on Mars (Westall et al., 2000; Wilson, 1999). The miniaturized Moessbauer spectrometer MIMOS II was part of the payload of the ill-fated ESA Mars Express exobiological lander ''Beagle 2'' (Sims et al., 1999; Pullan et al., 2003). Two miniaturized Moessbauer spectrometers (Klingelhoefer et al., 2003) are part of the payload of the Mars Exploration Rovers ''Spirit'' and ''Opportunity'' (Squyres et al., 2003), conducting successful surface investigations on the planet since January 2004. The primary objective of the Athena science investigation is to explore two sites on the Martian surface where water may once have been present, and to assess past environmental conditions at those sites and their suitability for life (Squyres et al., 2003).

3.3.1 Gusev Crater

Gusev Crater was selected as the landing site for the Mars Exploration Rover (MER) Spirit mission, because the crater could have collected sediments from a variety of sources during its 3.9 Ga history, including fluvial, lacustrine, volcanic, glacial, impact, regional and local aeolian, and global air falls. It may thus be a unique site to investigate the past history of water on Mars, climate and geological changes, and the potential habitability of the planet (Cabrol et al., 2003).

During its primary mission Spirit found no evidence for lacustrine sedimentation in the plains surrounding its landing site (Squyres et al., 2004a). Instead Spirit's Moessbauer spectrometer identified olivine, pyroxene, non-stoichiometric magnetite, and unspecified nanophase iron oxide in rocks and soils.[1] Olivine is usually the first mineral to weather away in aqueous environments (e.g., Eggleton, 1986). The ubiquitous presence of olivine in soil suggests that physical rather than chemical weathering processes currently dominate at Gusev crater (Morris et al., 2004). However, water probably has been involved to a limited degree in the formation of veins, filled vugs, and surface coatings that are associated with rocks at the Spirit landing site (Squyres et al., 2004a; Haskin et al., 2005). Spirit's Moessbauer spectrometer identified crystalline hematite and elevated Fe^{3+}/Fe_{Total} ratios associated with a multilayered coating on a basaltic olivine-bearing rock dubbed Mazatzal (Morris et al., 2004), providing part of the evidence. In that coating, Fe^{2+} in olivine is negatively correlated with Fe3+ in nanophase ferric oxides, requiring alteration of adhering soil or the underlying rock itself (Haskin et al., 2005). Effects of aqueous activity are also seen in subsurface soils exposed in trenches dug using the rover wheels in the intercrater plains. These effects include the

oxidation of Fe^{2+} as is indicated by elevated Fe^{3+}/Fe_{Total} ratios measured in the subsurface soils compared to the topmost soil layer (Haskin et al., 2005; Morris et al., 2006; Wang et al., 2006). The combined evidence implicates interaction with liquid water, but not pools of surface or ground water, or hydrothermal conditions (Haskin et al., 2005). Possible sources of water include precipitation and condensation from the atmosphere (e.g., acid fog) or melting of ground ice during episodes of higher obliquity (Arvidson et al., 2004).

Des Marais et al. (2005) assessed the availability of nutrient elements, energy and liquid water on the Gusev plains. In particular, energy and reducing power to sustain microbial synthesis can be provided by reduced minerals such as olivine, when altered by water. Serpentinization of ultramafic rocks at temperatures <300 °C would end in the production of magnetite and H_2 (Sleep et al., 2004). H_2 acts as a near universal source of energy and reducing power for microorganisms. Chapelle et al. (2002) describe a subsurface hydrogen-based methanogenic microbial community in deeply buried igneous rocks on Earth. The Fe-bearing mineralogy of dark soils derived from Moessbauer spectra from both MER landing sites, Gusev Crater and Meridiani Planum, is essentially identical and contains olivine, pyroxene, nanophase iron oxide and non-stoichiometric magnetite as described above. Yen et al. (2005) conclude that olivine-bearing precursor rocks may be wide-spread on the surface of Mars. Magnetite forms also by solely igneous processes and its presence alongside olivine does not necessarily infer that it was formed by serpentinization processes as described above (Schroeder et al., 2005). Des Marais et al. (2005) conclude, that, despite the current sparsity of water, because of the potential of mafic and ultramafic terrains to sustain chemosynthetic microorganisms in subsurface

environments, the Gusev Crater plains and related terrains merit closer scrutiny in future orbiter and lander missions.

On sol 156 after landing at Gusev Crater MER Spirit left the plains and started ascending into the Columbia Hills, rising about 90m above the surrounding plains (Arvidson et al., 2006). The Columbia Hills are composed of older material than the surrounding plains. Rocks in the Columbia Hills are diverse in composition, some outcrop rocks exhibit layered structures (Squyres et al., 2006). Iron oxidation ratios Fe^{3+}/Fe_{Total} of rocks in the Columbia Hills range from 0.2 to 0.9, i.e., from little alteration comparable to rocks encountered in the plains to highly altered. Well-crystalline hematite and goethite were identified by Moessbauer spectroscopy in highly altered rocks, providing evidence for aqueous processes. Goethite in particular provides mineralogical proof for aqueous processes because it has structural hydroxide and is formed under aqueous conditions (Morris et al., 2006). However, Columbia Hills outcrops and rocks do not represent lacustrine sediments (Squyres et al., 2006). They may have formed by the aqueous alteration of basaltic rocks, volcaniclastic materials, and/or impact ejecta by solutions that were rich in acid-volatile elements (Ming et al., 2006).

3.3.2 Meridiani Planum

Meridiani Planum was selected as the landing site for the MER Opportunity mission because of the detection of hematite from orbital observations by the Mars Global Surveyor TES (Christensen et al., 2000, 2001). Hematite formation in most cases involves aqueous processes. At its landing site in _20m diameter Eagle crater, Opportunity discovered flat-lying, finely laminated sedimentary rocks, which contained

abundant sulfate salts (Squyres et al., 2004b). These rocks provide in situ evidence for an ancient aqueous environment at Meridiani Planum, where conditions were suitable for biological activity for a period of time in martian history (Squyres et al., 2004c). Key to these findings is the identification of jarosite within the sedimentary rocks by Opportunity's Moessbauer spectrometer (Klingelhoefer et al., 2004). Jarosite is an iron hydroxide sulfate mineral, whose general formula can be written $(K, Na, H_3O)(Fe_{3-x}Al_x)(SO_4)_2(OH)_6$, where x<1. Other cations such as Pb are possible. Jarosite provides mineralogical in situ evidence for the presence of water on Mars and for aqueous acid sulfate processes under oxidizing conditions. The average outcrop matrix contains ~2 wt% H2O within the jarosite alone (Klingelhoefer et al., 2004). Jarosite forms only under low pH conditions (5 or less) (e.g., Catling, 2004) and puts thus strong contraints on the chemistry and mineralogy of sedimentary outcrop material at Meridiani Planum (Clark et al., 2005), the diagenesis of the sedimentary outcrop formations (McLennan et al., 2005), and the geochemical modeling of evaporation processes on Mars (Tosca et al., 2005). Knoll et al. (2005) give an astrobiological perspective on Meridiani Planum. Although the high levels of acidity inferred from the presence of jarosite would have challenged prebiotic chemical reactions thought to have played a role in the origin of life on Earth, microbial populations on Earth have adapted to low pH levels and episodic water limitation. Fe^{2+} is soluble under low pH and thus would have been available as an electron donor for microbial metabolism. Hence the Meridiani plain may have been habitable during the time deposition of the outcrop material took place.

Dispersed throughout the sedimentary rocks are mmsized spherules, which are interpreted to be concretions formed by postdepositional diagenesis, again involving

liquid water (Squyres et al., 2004c). The spherules are eroded from the rocks and cover large parts of the Meridiani plains (Soderblom et al., 2004). Measurements with Opportunity's Moessbauer spectrometer showed, that the spherules are hematite-rich (Klingelhoefer et al., 2004) and are thus the source for the hematite observed from orbit. The occurrence of sulfates and iron oxides, both of which can preserve chemical, textural and microfossil signatures (e.g., Allen et al., 2004; Fernandez-Remolar et al., 2005), make Meridiani Planum a prime candidate for a Mars sample return mission (Knoll et al., 2005).

Based on mineralogy and jarosite occurence, the Tinto river system in Spain, an extreme acidic environment under the control of iron, provides an analogous habitat for Meridiani Planum on Earth (Ferna´ ndez-Remolar et al., 2004). The site may facilitate the understanding of Meridiani mineral precipitation and diagenesis. At Rio Tinto a microbial ecosystem thrives based on the iron cycle (Gonza´ lez-Toril et al., 2003). Biosignature and microfossils are preserved in iron oxides in the sedimentary rocks. The site has been extensively studied by Moessbauer spectroscopy to allow for comparison with data obtained from Meridiani Planum (Ferna´ ndez-Remolar et al., 2005). Jarosite also forms during acid-sulfate alteration of volcanic rocks. Jarositic tephra on Mauna Kea, Hawaii, are also well-studied by Moessbauer spectroscopy (Morris et al., 1996).

A single rock, dubbed Bounce Rock, discovered on the plains of Meridiani Planum is completely unrelated to the ubiquitous sedimentary outcrop rocks. It was likely ejected from a crater ~75km southwest from Opportunity's landing site (Squyres et al., 2004b). Moessbauer spectra identified the only Fe-bearing mineral as pyroxene (Klingelhoefer et al., 2004). The spectra are unlike any other Moessbauer spectrum

obtained on Mars to date, but similar to spectra taken in laboratories on Earth from meteorites related to Mars. The Moessbauer spectra and data from Opportunity's Alpha Particle X-ray Spectrometer (APXS) (Rieder et al., 2004) of ''Bounce'' rock combined revealed the first basaltic shergottitic rock on Mars (Rodionov et al., 2004; Zipfel et al., 2004; Squyres et al., 2004b), similar in mineralogical and chemical composition to Lithology B of the shergottite meteorite EETA 79001. The shergottites are a subgroup of a larger group of meteorites whose origin has been interpreted to be Mars. Bounce rock is the first rock related to these Martian meteorites discovered on Mars itself, adding further evidence to their origin, and hence shows that exchange of matter—and possibly life or prebiotic chemical compounds— between Mars and Earth occurred.

The recent findings from MER and the European orbiter Mars Express (e.g., Formisano et al., 2004) combined prompted one commentator to say: ''Given what we now know about Mars, planetary protection considerations require the assumption that Martian life exists, until we learn otherwise'' (Kargel, 2004).

3.4 Loihi deep sea mount

Deep sea hydrothermal vents and the surrounding oceanic basaltic crust have been hypothesized as the possible origin of life on the prebiotic Earth and provide Earth-bound analogues to possible subsurface biospheres on Mars and Europa. The pressure, temperature, temperature gradients, lack of sunlight and oligotrophic nature of these surroundings are extreme in nature and force life to incorporate alternate methods of metabolism for survival. It is thermodynamically possible for chemolithotrophs and chemolithoautotrophs to utilize the large energy potential found in the form of Fe^{2+} to

Fe^{3+} transitions within the basaltic glass found in oceanic crust and seamount pillow basalts. Iron is the leading nutrient candidate in the basaltic glass as an electron donor due to its relative abundance (~12 wt% Fe-Total), high degree of reduced iron (~90% Fe2+) and energy yield per reaction. Thus, the use of Moessbauer spectroscopy as a tool to measure this potential yield can ultimately lead to an upper limit on energy available for biomass production in a particular environment.

Weathering rates of basaltic glass in seawater has been an ongoing study with early work done by Moore (1966) describing the palagonitization of pillow basalts taken offshore near Hawaii. However, continued laboratory studies of the weathering rinds on both natural and synthetic basalts has produced a wide array of rates of palagonitization varying from 10_4 to 70 mm/1000 years (Techer et al., 2001). Numerous experiments (e.g., Advocat et al., 1991) have shown that dissolution of natural and synthetic glasses depend on three main factors: (1) temperature and pH of the surrounding solution, (2) hydrolysis of the glass matrix and (3) the secondary mineral phases generated by the weathering eventually sealing the fresh glass off from further weathering. One can argue that over the past several decades, a fourth method of dissolution/alteration has been discovered in the form of microbiology (e.g., Ross and Fisher, 1986; Thorseth et al., 1992, 1995; Furnes et al., 1996; Giovannoni et al., 1996; Torsvik et al., 1998; Furnes and Staudigel, 1999; Furnes et al., 2001). Daughney et al. (2004) report microbiota enhanced removal of Mn and Fe from natural basalt when compared to abiotic controls, furthering the theory that microbes play an important role in chemical cycling between the oceanic basalt crust and seawater (Staudigel and Hart, 1983). Agresti et al. (1994), using Moessbauer spectroscopy, identified superparamagnetic Fe oxide material at deep sea

smoker vents, which is correlated with anaerobic bacteria found to thrive there. Bailey et al. (2004) have cultured several strains of Fe-oxidizing bacteria from various basalt surfaces with SEM data showing significant colonization of fresh basalt after a one year exposure to hydrothermal vent water in Hawaii.

Biotic alteration of basaltic glass competes with abiotic alteration in the deep biosphere as bottom seawater interacts with the glass to form palagonite, an oxidized, hydrated form of basaltic glass (Thorseth et al., 1991). Numerous researchers have shown that photomicrographs of pillow basalt thin sections allow for quantification and identification of various types of alteration (e.g. Torsvik et al., 1998; Furnes and Staudigel, 1999; Fisk et al., 1998). Furnes and Staudigel (1999) took several samples from DSDP/ODP drill holes and quantified the amount of abiotic vs biotic alteration in glass margins from pillow basalts. Their results show that 60–85% of total alteration in the upper 250m of oceanic crust can be attributed to biological alteration. This trend gradually decreases down to approximately 10% biological alteration at 550m depth where temperature, oxygen availability, and porosity limit biological growth and effects.

To study the effects of iron in basaltic glass on microbial communities, several synthetic basalt glasses of varying composition and oxidation states were created in platinum crucibles in a molybdenum heating element furnace. The raw starting material for the synthetic glasses was quenched tholeiitic basalt glass taken from an active lava flow from the Pu'u O'o vent, Kilauea Volcano, Hawaii, USA. The raw material was then powdered in a disc mill and remelted at 1450 1C to achieve homogeneity and lack of crystal structure. Some glass samples were also amended with other nutrients necessary for survival such as apatite (a phosphate-rich mineral) and reduced manganese, another

potential electron donor, but these fall outside the realm of this study. The iron oxidation state of each glass substrate was either unaltered from its natural state or oxidized by firing at sub-solidus temperatures (700 1C) for 4 h prior to remelting, yielding samples containing primarily reduced and oxidized iron, respectively.

The substrates were again powdered and sewn into sachets with 50 mm mesh and housed in open 400 PVC tubes. Each different type of glass was exposed for one year on Loihi Seamount, Hawaii in a diffuse hydrothermal vent field at the base of the Tower Vents inside Pele's Pit (water temp ~10 °C, ambient ~3 °C). The PVC tubes were placed into active hydrothermal vents using the Pisces V submersibles operated by the Hawaii Undersea Research Laboratory (HURL). The samples were collected in the following year after a 13-month deployment. Upon retrieval, fine-grained sediment in the sample, predominately composed of starting material but enriched in secondary mineral phases (iron oxyhydroxides and clays) and altered glass (palagonite) created in the weathering process of the fresh glass, was separated from the bulk sample by immersion in distilled, deionized (DDI) water, sonicated to separate secondary mineral phases from nucleation sites on the glass and suspending the fines in DDI water followed by suction filtration through 0.22 mm Teflon filters.

The iron oxidation state of the fine fraction of glass was analyzed via Moessbauer spectroscopy using a common laboratory transmission setup, and compared to the bulk oxidation state of the coarse remaining material, which is believed to have negligible amounts of weathering due to large grain size to gauge reaction rates and weathering over a 1 year time period. The Moessbauer spectra were evaluated fitting ferric and ferrous-bearing phases with Voigt lineshapes. In accordance with De Grave and Van Alboom,

(1991) and Morris et al. (1995) the ratio $f(Fe^{3+})/ f(Fe^{2+}) = 1.21$ was used. Figure 3.3 and Table 3.1 show an initial Fe^{3+}/Fe_{Total} ratio of 0.13 (Sample 2) and 0.70 (Sample 4) percent in the bulk natural and oxidized glasses, respectively. The fine fraction, representing a higher degree of alteration/weathering, shows an increase of the Fe^{3+}/ Fe_{Total} ratio to 0.17 in the natural glass (Sample 1) and 0.72 in the oxidized glass (Sample 3). The increase of Fe^{3+} by 4% over 1 year in the bulk natural sample is in good agreement with theoretical estimates (see below), but the change is low in comparison to the errors for relative peak areas, usually quoted as 72% absolute. The observed increase of Fe^{3+} in the oxidized glass (2%) is smaller than in the natural glass, which is as expected from the reduced availability of Fe^{2+} to start with. Repeated measurements with different velocity settings on the same samples confirm the observed trends.
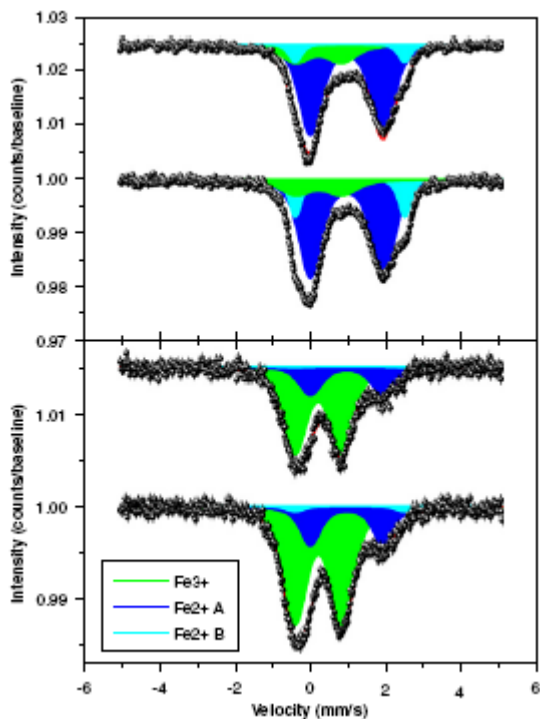
Figure 3.3. Moessbauer spectra of basaltic glass samples exposed for 1 year at the Loihi seamount, from top: Sample # 1, natural glass, fine fraction; sample # 2, natural glass, coarse fraction; sample # 3, oxidized glass, fine fraction; sample # 4, oxidized glass, coarse fraction. Spectra are offset for clarity.

Table 3.1. Moessbauer parameters, area ratios for Fe^{2+} and Fe^{3+} bearing subspectral components, and Fe^{3+}/Fe_{Total} rations of Mossbauer spectra obtained from basaltic glass samples exposed at the Loihi deep sea hydrothermal mount.

Sample	Fe^{3+}			Fe^{2+} A			Fe^{2+} B			Fe^{3+}/Fe_{Total}
	δ (mm/s)	ΔE_Q (mm/s)	A (%)	δ (mm/s)	ΔE_Q (mm/s)	A (%)	δ (mm/s)	ΔE_Q (mm/s)	A (%)	
1. Natural Glass (fines)	[0.31][abc]	[1.23]	17d	[1.05]	[1.92]	74	[1.13]	[2.89]	8	0.17
2. Natural Glass (coarse)	[0.31][abc]	[1.23]	13	1.05	1.92	71	1.13	2.89	15	0.13
3. Oxidized Glass (fines)	0.30	1.25	72	[1.05]	[1.92]	28	[1.13]	[2.89]	1	0.72
4. Oxidized Glass (coarse)	0.31	1.25	70	[1.05]	[1.92]	27	[1.13]	[2.89]	3	0.70

[a] Values in square brackets are constraints used in fitting processes
[b] Isomer shifts, d, are quoted relative to pure metallic Fe foil
[c] Uncertainties of d and DEQ are in 0.02 mm/s
[d] The uncertainty of peak area ratios are +/- 2% absolute

Calculating potential biomass yields from chemolithoautotrophic growth is an extremely difficult and complex problem. Several papers aimed at quantifying this type of biomass production have been generated (e.g., Battley, 1998). Bach and Edwards (2003) used results from Heijnen and Van Dijken (1992) to estimate that up to $48\pm21\times10^{10}$ g cellular C per year are created through aerobic and anaerobic iron and sulfur oxidation. Building upon this previous work, initial estimates of the rate of iron oxidation on Loihi within our crushed synthetic basaltic glasses have been shown to be about 3% per year. Using this oxidation rate and the aerobic Fe oxidation values set forth by Bach and Edwards (2003) (292 ± 117 kJ/g C produced, ΔG of 66.2 kJ/mole Fe oxidized, a factor of 1:2.2 in g C biomass: g dry weight of cells), a total of approximately 3×10^{-2} g cellular weight/kg fresh basalt glass can be produced per year. Approximately 2.5km^2 of new oceanic crust/year are generated at spreading ridges and if the upper 5m of this new crust is about 10% basalt glass, the total potential biomass production per year over the spreading ridges alone is about 3×10^7 g cellular weight! This is only the maximum upper bound on biomass production, however, from an astrobiology perspective, it shows that there indeed exists energy available from iron oxidation wherever water and Fe-rich rock interact that life can harness for growth and proliferation.

3.5 **Conclusions**

The Moessbauer spectrometers on the Mars Exploration Rovers Spirit and Opportunity were successfully used in the in situ identification and characterization of aqueous minerals such as jarosite and hematite (Klingelhoefer et al., 2004). The

identification of jarosite was crucial to evaluate the habitability of Opportunity's landing site at Meridiani Planum during the formation of the sedimentary outcrop rocks, because jarosite puts strong constrains on pH levels (Knoll et al., 2005). Its identification is also crucial for the evaluation of analogous habitats that can be studied on Earth such as the Rio Tinto system in Spain (Ferna´ ndez- Remolar et al., 2004, 2005). Fe oxidation states and Fe3+/ FeTotal ratios provide further evidence for aqueous processes on Mars (Haskin et al., 2005). In contrast, the identification of olivine in rocks and soils on the Gusev crater plains provide evidence for the long-term sparsity of water in that area on Mars (Morris et al., 2004). On the other hand, aqueous alteration of olivine may provide an energy source for microbial metabolism (Des Marais et al., 2005).

Moessbauer spectroscopy supported the identification of the first rock on Mars, which is actually similar in elemental and mineralogical composition to Martian meteorites discovered on Earth (Rodionov et al., 2004; Zipfel et al., 2004; Klingelhoefer et al., 2004; Squyres et al., 2004b).

Although Moessbauer spectroscpy cannot detect life directly, the identification of Fe-bearing minerals is crucial in the hunt for it. Iron oxides such as hematite, and Febearing sulfates can preserve microfossils (e.g., Allen et al., 2004; Ferna´ ndez-Remolar et al., 2005). So-called biominerals comprise Fe oxides such as magnetite, as well as sulfides, carbonates, and phosphates of iron (Cornell and Schwertmann, 1996). Moessbauer spectroscopy thus remains an important contact instrument to choose rocks in situ that merit further analysis in sophsiticated laboratories inside future rovers, or, on Earth after Mars sample return.

Results from Moessbauer spectroscopy confirm estimates of biomass yield from the utilization of the Fe^{2+}/Fe^{3+} redox potential in basaltic glass by chemolithoautotrophs at deep sea hydrothermal vent systems. While not all aqueous oxidation of iron within basaltic glass is evidence for life, the iron does present an energy source for chemolithoautotrophic growth and relative proportions of Fe^{2+}/Fe^{3+} allow for a measure of potential energy for use by a microbial community. Such measurements are just one example of how the technique can help to understand habitats, which are possibly analogous to sub-ice environments on Europa and Jupiter's other icy moons Ganymede and Calisto.

The potential for the application of Moessbauer spectroscopy within the field of astrobiology is by far not exhausted.

3.6 Acknowledgments

Chapter 3 is a formatted version of the published work: C. Schröder, B. Bailey, G. Klingelhöfer and H. Staudigel. (2006) Fe Mössbauer spectroscopy as a tool in astrobiology. *Planetary and Space Science*. 54(15):1622-1634. The dissertation author

was the second author of this paper and completed work for this paper including creation

of basaltic glasses, deployment, collection and processing of fines, calculations of

potential biomass production and writing of several sections of the paper.

3.7 References

Advocat, T., Crovisier, J.L., Vernaz, E., Ehret, G., Charpentier, H., 1991. Hydrolysis of R7T7 nuclear waste glass in dilute media: Mechanisms and rate as a function of pH. Mater. Res. Soc. Symp. Proc. 212, 57–64.

Agresti, D.G., Wdowiak, T.J., Wade, M.L., 1994. Moessbauer spectroscopy as a tool in the search for evidence of past life on Mars. Hyperfine Interact. 91, 523–528.

Allen, C.C., Probst, L.W., Flood, B.E., Longazo, T.G., Schelble, R.T., Westall, F., 2004. Meridiani Planum hematite deposit and the search for evidence of life on Mars—iron mineralization of microorganisms in rock varnish. Icarus 171, 20–30.

Arvidson, R.E., Anderson, R.C., Bartlett, P., Bell III, J.F., Blaney, D., Christensen, P.R., Chu, P., Crumpler, L., Dvis, K., Ehlmann, B.L., Fergason, R., Golombek, M.P., Gorevan, S., Grant, J.A., Greeley, R., Guinness, E.A., Haldemann, A.F.C., Herkenhoff, K., Johnson, J., Landis, G., Li, R., Lindemann, R., McSween, H., Ming, D.W., Myrick, T., Richter, L., Seelos IV, F.P., Squyres, S.W., Sullivan, R.J., Wang, A., Wilson, J., 2004. Localization and physical properties experiments conducted by spirit at Gusev Crater. Science 305, 821–824.

Arvidson, R.E., Squyres, S.W., Anderson, R.C., Bell III, J.F., Blaney, D., Bruckner, J., Cabrol, N.A., Calvin, W.M., Carr, M.H., Christensen, P.R., Clark, B.C., Crumpler, L., DesMarais, D.J., de Souza Jr., P.A., d'Uston, C., Economou, T., Farmer, J., Farrand, W.H., Folkner, W., Golombek, M., Gorevan, S., Grant, J.A., Greeley, R., Grotzinger, J., Guinness, E., Hahn, B.C., Haskin, L., Herkenhoff, K.E., Hurowitz, J.A., Hviid, S., Johnson, J.R., Klingelhoefer, G., Knoll, A.H., Landis, G., Leff, C., Lemmon, M., Li, R., Madsen, M.B., Malin, M.C., McLennan, S.M., McSween, H.Y., Ming, D.W., Moersch, J., Morris, R.V., Parker, T., Rice Jr., J.W., Richter, L., Rieder, R., Rodionov, D.S., Schroeder, C., Sims, M., Smith, M., Smith, P., Soderblom, L.A., Sullivan, R., Thompson, S.D., Tosca, N.J., Wang, A., Waenke, H., Ward, J., Wdowiak, T., Wolff, M., Yen, A., 2006. Overview of the Spirit Mars exploration Rover Mission to Gusev Crater: landing site to Backstay Rock in the Columbia Hills. J. Geophys. Res. 111, E02S01.

Bach, W., Edwards, K.J., 2003. Iron and sulfide oxidation within the basaltic ocean crust: implications for chemolithoautotrophic microbial biomass production. Geochim. Cosmochim. Acta 67 (20), 3871–3887.

Bailey, B.E., Staudigel, H., Templeton, A., Tebo, B.M., Ryerson, F., Plank, T., Schroeder, C., Klingelhoefer, G., 2004. Biological alteration of basaltic glass with altered composition and oxidation states. EOS Transactions, AGU, 85(47), Fall Meeting Supplement, Abstract B53C- 1006.

Banin, A., Clark, B.C., Wanke, H., 1992. Surface Chemistry and Mineralogy. In: Kieffer, H.H., Jakosky, B.M., Snyder, C.W., Matthews, M.S. (Eds.), Mars. The University of Arizona Press, Tucson, pp. 594–625. Bancroft, G.M., 1973. Moessbauer Spectroscopy— An Introduction for Inorganic Chemists and Geochemists. McGraw Hill, New York.

Battley, E.H., 1998. The development of direct and indirect methods for the study of the thermodynamics of microbial growth. Thermochim. Acta 309, 169–171.

Burns, R.G., 1993. Moessbauer spectral characterization of iron in planetary surface materials. In: Pieters, C.M., Englert, P.A.J. (Eds.), Remote Geochemical Analysis: Elemental and Mineralogical Composition. Cambridge University Press, Cambridge, pp. 539–556.

Burns, R.G., 1994. Mineral Moessbauer spectroscopy: correlations between chemical shift and quadrupole splitting parameters. Hyperfine Interact. 91, 739–745.

Burns, R.G., Solberg, T.C., 1990. Crystal structure trends in Moessbauer spectra of ^{57}Fe-bearing oxide, silicate and aluminosilicate minerals. In: Coyne, L.M. (Ed.), Structure of Active Sites in Minerals. ACS Symposium Series vol. 415. pp. 262–283.

Cabrol, N.A., Grin, E.A., Carr, M.H., Sutter, B., Moore, J.M., Farmer, J.D., Greeley, R., Kuzmin, R.O., Des Marais, D.J., Kramer, M.G., Newsom, H., Barber, C., Thorsos, I., Tanaka, K.L., Barlow, N.G., Fike, D.A., Urquhart,M.L., Grigsby, B., Grant, F.D., de Goursac, O., 2003. Exploring Gusev Crater with Spirit: review of science objectives and testable hypotheses. J. Geophys.l Res. 108 (E12), 8076.

Catling, D.C., 2004. On Earth, as it is on Mars? Nature 429, 707–708.

Chapelle, F.H., O'Neill, K., Bradley, P.M., Methe´ , B.A., Ciufo, S.A., Knobel, L.L., Lovley, D.R., 2002. A hydrogen-based subsurface microbial community dominated by methanogens. Nature 415, 312–315.

Christensen, P.R., Bandfield, J.L., Clark, R.N., Edgett, K.S., Hamilton, V.E., Hoefen, T., Kieffer, H.H., Kuzmin, R.O., Lane, M.D., Malin, M.C., Morris, R.V., Pearl, J.C., Pearson, R., Roush, T.L., Ruff, S.W., Smith, M.D., 2000. Detection of crystalline hematite mineralization on Mars by the Thermal Emission Spectrometer: evidence for nearsurface water. J. Geophys. Res. 105, 9623–9642.

Christensen, P.R., Morris, R.V., Lane, M.D., Bandfield, J.L., Malin, M.C., 2001. Global mapping of Martian hematite deposits: remnants of waterdriven processes on early Mars. J. Geophys. Res. 106, 23873–23886.

Clark, B.C., Morris, R.V., McLennan, S.M., Gellert, R., Jolliff, B., Knoll, A.H., Squyres, S.W., Lowenstein, T.K., Ming, D.W., Tosca, N.J., Yen, A., Christensen, P.R., Gorevan, S., Brueckner, J., Calvin, W., Dreibus, G., Farrand, W., Klingelhoefer, G., Waenke, H., Zipfel, J., Bell III, J.F., Grotzinger, J., McSween, H.Y., Rieder, R., 2005. Chemistry and mineralogy of outcrops at Meridiani Planum. Earth Planet. Sci. Lett. 240, 73–94.

Cornell, R.M., Schwertmann, U., 1996. The Iron Oxides. VCH Verlagsgesellschaft mbH, Weinheim, Germany. Daughney, C.J., Rioux, J.P., Fortin, D., Pichler, R., 2004. Laboratory investigation of the role of bacteria in the weathering of basalt near deep sea hydrothermal vents. Geomicrobiol. J. 21, 21–31.

De Grave, E., Van Alboom, A., 1991. Evaluation of ferrous and ferric Moessbauer fractions. Phys. Chem. Miner. 18, 337–342.

Des Marais, D.J., Walter, M.R., 1999. Astrobiology : exploring the origins, evolution, and distribution of life in the universe. Ann. Rev. Ecol. Systemat. 30, 397–420.

Des Marais, D.J., Clark, B.C., Crumpler, L.S., Farmer, J., Grotzinger, J.P., Haskin, L.A., Knoll, A.H., Landis, G.A., Moersch, J., Schroeder, C., Wdowiak, T., Yen, A.S., Squyres, S.W., 2005. Astrobiology and the Basaltic Plains in Gusev Crater. Lunar Planet. Sci. 36 (2353) (CD-ROM).

De Souza Jr., P.A., 2004. Extraterrestrial and terrestrial outdoor applications of Moesbauer Spectroscopy. Doctoral Thesis. Johannes Gutenberg-Universitaet, Mainz, Germany. De Souza Jr., P.A., Klingelhoefer, G., Bernhardt, B., Schroeder, C., Guetlich, P., Morimoto, T., 2001. On-line and in-situ characterization of iron phases in particulate matter. In: Proceedings of the Air & Waste Management Association's 94th Annual Conference'' (Air & Waste Management Associaiton'94th Annual Conference & Exhibition, Orlando, Florida, USA, June 24–28, 2001). Air & Waste Management Association, Pittsburgh, PA, USA, pp. 1–11.

De Souza Jr., P.A., de Macedo, M.C.S., de Queiroz, R.S., Klingelhoefer, G., 2002. Atmospheric corrosion investigation in industrial, marine and rural environments in South-East Brazil. Hyperfine Interact. 139/140, 183–191.

De Souza Jr., P.A., Bernhardt, B., Klingelhoefer, G., Guetlich, P., 2003. Surface analysis in archaeology using the miniaturized Moessbauer Spectrometer MIMOS II. Hyperfine Interact. 151/152, 125–130.

Schaefer, M.W., 2004. Moessbauer spectroscopy on the surface of Mars: constraints and expectations. Earth Planet. Sci. Lett. 218, 243–259.

Eeckhout, S.G., De Grave, E., 2003. Evaluation of ferrous and ferric Moessbauer fractions. Part II. Phys. Chem. Miner. 30, 142–146.

Eggleton, R.A., 1986. The relation between crystal structure and silicte weathering rates. In: Colman, S.M., Dethier, D.P. (Eds.), Rates of Chemical Weathering of Rocks and Minerals. Academic Press, London, pp. 21–40.

Feder, F., Klingelhoefer, G., Rolard, F., Bourrie, G., 2002. In situ Moessbauer spectroscopy and soil solution monitoring to follow spatial and temporal iron dynamics. 17th World Congress of Soil Science, Bangkok, Symposium 8, 1654.

Feder, F., Trolard, F., Klingelhoefer, G., Bourrie, G., 2005. In situ Moessbauer spectroscopy: evidence for green rust (fougerite) in a gleysol and its mineralogical transformations with time and depth. Geochim. Cosmochim. Acta 69 (18), 4463–4483.

Fernandez-Remolar, D., Gomez-Elvira, J., Go´ mez, F., Sebastian, E., Martı´ in, J., Manfredi, J.A., Torres, J., Gonzalez Kesler, C., Amils, R., 2004. The Tinto River, an extreme acidic environment under control of iron, as an analog of the Terra Meridiani hematite site of Mars. Planet. Space Sci. 52, 239–248.

Fernandez-Remolar, D.C., Morris, R.V., Gruener, J.E., Amils, R., Knoll, A.H., 2005. The Rı´o Tinto Basin, Spain: mineralogy, sedimentary geobiology, and implications for interpretation of outcrop rocks at Meridiani Planum, Mars. Earth Planet. Sci. Lett. 240, 149–167.

Fisk, M.R., Giovannoni, S.J., Thorseth, I.H., 1998. Alteration of oceanic volcanic glass: textural evidence of microbial activity. Science 281, 978–980.

Formisano, V., Atreya, S., Encrenaz, T., Ignatiev, N., Giuranna, M., 2004. Detection of methane in the atmosphere of Mars. Science 306, 1758–1761.

Furnes, H., Staudigel, H., 1999. Biological mediation in ocean crust alteration: how deep is the deep biosphere? Earth Planet. Sci. Lett. 166, 97–103.

Furnes, H., Thorseth, I.H., Tumyr, O., Torsvik, T., Fisk, M.R., 1996. Microbial activity in the alteration of glass pillow lavas from Hole 896A. In: Alt, J.C., Kinoshita, H., Stokking, L.B., Michael, P.J. (Eds.), Proceedings of the Ocean Drilling Prog., Sci. Results. College Station, Texas, pp. 191–206.

Furnes, H., Staudigel, H., Thorseth, I.H., Torsvik, T., Muehlenbachs, K., Tumyr, O., 2001. Bioalteration of basaltic glass in the oceanic crust. Geochemistry, Geophysics, Geosystems 2, Paper no. 2000GC000150.

Giovannoni, S.J., Fisk, M.R., Mullins, T.D., Furnes, H., 1996. Genetic evidence for endolithic microbial life colonizing basaltic glass/seawater interfaces. In: Alt, J.J., Kinoshita, H., Stokking, L.B., Michael, P. (Eds.), Proc. Ocean Drilling Prog., Sci. Results. College Station, Texas, pp. 207–214.

Gonser, U. (Ed.), 1975. Moessbauer Spectroscopy. Topics in Applied Physics, vol. 5. Springer, Berlin.

Gonzalez-Toril, E., Llobet-Brossa, E., Casamayor, E.O., Amann, R., Amils, R., 2003. Microbial ecology of an extreme acidic environment, the Tinto River. Appl. Environ. Microbiol. 69 (8), 4853–4865.

Greenwood, N.N., Gibb, T.C., 1971. Moessbauer Spectroscopy. Chapman & Hall Ltd., London. Guetlich, P., Link, R., Trautwein, A., 1978. Moessbauer Spectroscopy and Transition Metal Chemistry. Springer, Berlin.

Haskin, L.A., Wang, A., McSween, H.Y., Clark, B.C., Des Marais, D.J., McLennan, S.J., Tosca, N.J., Hurowitz, J.A., Jolliff, B.J., Farmer, J.D., Yen, A.S., Squyres, S.W., Arvidson, R.E., Klingelhoefer, G., Schroeder, C., de Souza Jr., P.A., Morris, R.V., Ming, D.W., Gellert, R., Zipfel, J., Brueckner, J., Bell III, J.F., Herkenhoff, K., Christensen, P.R., Ruff, S., Blaney, D., Gorevan, S., Cabrol, N.A., Crumpler, L., Grant, J., Soderblom, L., 2005. Water alteration of rocks and soils from the spirit Rover Site, Gusev Crater, Mars. Nature 436, 66–69.

Hawthorne, F.C., 1988. Moessbauer Spectroscopy. In: Hawthorne, F.C. (Ed.), Reviews in Mineralogy. Spectroscopic Methods in Mineralogy and Geology, vol. 18. Mineralogical Society of America, pp. 255–340.

Heijnen, J.J., Van Dijken, J.P., 1992. In search of a thermodynamic description of biomass yields for the chemotrophic growth of microorganisms. Biotechnol. Bioeng. 39, 833–858. Kargel, J.S., 2004. Proof for Water, Hints for Life? Science 306, 1689–1691.

Klingelhoefer, G., 1999. The miniaturized spectrometer MIMOS II. In: Miglierini, M., Petridis, D. (Eds.), Moessbauer Spectroscopy in Materials Science. Kluwer, Amsterdam, pp. 413–426.

Klingelhoefer, G., Held, P., Teucher, R., Schlichting, F., Foh, J., Kankeleit, E., 1995. Moessbauer spectroscopy in space. Hyperfine Interact. 95, 305–339.

Klingelhoefer, G., Fegley Jr., B., Morris, R.V., Kankeleit, E., Held, P., Evlanov, E., Priloutskii, O., 1996. Mineralogical analysis of Martian soil and rock by a miniaturized backscattering Moessbauer spectrometer. Planet. Space Sci. 44, 1277–1288.

Klingelhoefer, G., Campbell, S.J., Wang, G.M., Held, P., Stahl, B., Kankeleit, E., 1998. Iron ore processing—in-situ monitoring. Hyperfine interact. 111, 335–339.

Klingelhoefer, G., Trolard, F., Bernhardt, B., Bourrie, G., Feder, F., Genin, J.-M.R., 1999. The Monitoring of Iron Mineralogy and Oxidation States by Moessbauer Spectroscopy in the Field; the Green Rust Mineral in Hydromorphic Soils. AGU Fall meeting, San Francisco.

Klingelhoefer, G., da Costa, G.M., Prous, A., Bernhardt, B., 2002a. Rock paintings from Minas Gerais, Brazil, investigated by in situ Moessbauer Spectroscopy. Hyperfine interact. C 5, 423.

Klingelhoefer, G., Bernhardt, B., Foh, J., Bonnes, U., Rodionov, D., de Souza Jr., P.A., Schroeder, C., Gellert, R., Kane, S., Guetlich, P., Kankeleit, E., 2002b. The miniaturized Moessbauer spectrometer MIMOS II for extraterrestrial and outdoor applications: a status report. Hyperfine interact. 144/145, 371–379.

Klingelhoefer, G., Morris, R.V., Bernhardt, B., Rodionov, D., de Souza Jr., P.A., Squyres, S.W., Foh, J., Kankeleit, E., Bonnes, U., Gellert, R., Schroeder, C., Linkin, S., Evlanov, E., Zubkov, B., Prilutski, O., 2003. Athena MIMOS II Moessbauer spectrometer investigation. J. Geophys. Res. 108 (E12), 8067.

Klingelhoefer, G., Morris, R.V., Bernhardt, B., Schroeder, C., Rodionov, D.S., de Souza Jr., P.A., Yen, A., Gellert, R., Evlanov, E.N., Zubkov, B., Foh, J., Bonnes, U., Kankeleit, E., Guetlich, P., Ming, D.W., Renz, F., Wdowiak, T., Squyres, S.W., Arvidson, R.E., 2004. Jarosite and Hematite at Meridiani Planum from Opportunity's Moessbauer Spectrometer. Science 306, 1740–1745.

Knoll, A.H., Carr, M.H., Clark, B.C., Des Marais, D.J., Farmer, J.D., Fischer, W.W., Grotzinger, J.P., Hayes, A., McLennan, S., Malin, M., Schroeder, C., Squyres, S.W., Tosca, N.J., Wdowiak, T., 2005. An astrobiological perspective on Meridiani Planum. Earth Planet. Sci. Lett. 240, 179–189.

Knudsen, J.M., 1989. Moessbauer spectroscopy of ^{57}Fe and the evolution of the solar system. Hyperfine Interact. 47, 3–31.

Knudsen, J.M., Mørup, S., Galazkha-Firedman, J., 1990. Moessbauer spectroscopy and the iron on Mars. Hyperfine Interact. 57, 2231–2236.

Knudsen, J.M., Madsen, M.B., Olsen, M., Vistisen, L., Koch, C.B., Mørup, S., Kankeleit, E., Klingelhoefer, G., Evlanov, E.N., Khromov, V.N., Mukhin, L.M., Prilutski, O.F., Zubkov, B., Smirnov, G.V., Juchniewicz, J., 1992. Moessbauer spectroscopy on the surface of Mars. Why? Hyperfine Interact. 68, 83–94.

McCammon, C., 1995. Moessbauer spectroscopy of minerals. In: Ahrens, T.J. (Ed.), Mineral Physics and Crystallography: A Handbook of Physical Constants. American Geophysical Union, Washington, DC, pp. 332–347.

McKay, D.S., Gibson Jr., E.K., Thomas-Keprta, K.L., Vali, H., Romanek, C.S., Clemett, S.J., Chillier, X.D.F., Maechling, C.R., Zare, R.N., 1996. Search for Past Life on Mars: Possible Relic Biogenic Activity in Martian Meteorite ALH84001. Science 273, 924–930.

McLennan, S.M., Bell III, J.F., Calvin, W.M., Christensen, P.R., Clark, B.C., de Souza Jr., P.A., Farmer, J., Farrand, W.H., Fike, D.A., Gellert, R., Ghosh, A., Glotch, T.D., Grotzinger, J.P., Hahn, B., Herkenhoff, K.E., Hurowitz, J.A., Johnson, J.R., Johnson, S.S., Jolliff, B., Klingelhoefer, G., Knoll, A.H., Learner, Z., Malin, M.C., McSween Jr., H.Y., Pocock, J., Ruff, S.W., Soderblom, L.A., Squyres, S.W., Tosca, N.J., Watters, W.A., Wyatt, M.B., Yen, A., 2005. Provenance and diagenesis of the evaporite-bearing Burns formation, Meridiani Planum, Mars. Earth Planet. Sci. Letters 240, 95–121.

Megonigal, J.P., Hines, M.E., Visscher, P.T., 2003. Anaerobic Metabolism: Linkages to Trace Gases and Aerobic Processes. In: Schlesinger, W.H., Holland, H.D., Turekian, K.K. (Eds.), Biogeochemistry. Treatise on Geochemistry, vol. 8. Elsevier-Pergamon, Oxford. Ming, D.W., Mittlefehldt, D.W., Morris, R.V., Golden, D.C., Gellert, R., Yen, A., Clark, B.C., Squyres, S.W., Farrand, W.H., Ruff, S.W., Arvidson, R.E., Klingelhoefer, G., McSween, H.Y., Rodionov, D.S., Schroeder, C., de Souza Jr., P.A., Wang, A., 2006. Geochemical and mineralogical indicators for aqueous processes in the Columbia Hills of Gusev crater, Mars. J. Geophys. Res. 111, E02S12.

Mitra, S., 1992. Applied Moessbauer Spectroscopy: Theory and Practice for Geochemists and Archaeologists. Pergamon Press, Oxford.

Moore, J.G., 1966. Rate of palagonitation of submarine basalt adjacent to Hawaii. US Geol. Sun. Prof: Patw HO-D, 163–171.

Morris, R.V., Agresti, D.G., Lauer Jr., H.V., Newcomb, J.A., Shelfer, T.D., Murali, A.V., 1989a. Evidence for pigmentary hematite on Mars based upon optical, magnetic, and Moessbauer studies of superparamagnetic (nanocrystalline) hematite. J. Geophys. Res. 94, 2760–2772.

Morris, R.V., Agresti, D.G., Shelfer, T.D., Wdowiak, T.J., 1989b. Mossbauer backscatter spectrometer: a new approach for mineralogical analysis on planetary surfaces. Lunar Planet. Sci. 20, 723–724.

Morris, R.V., Golden, D.C., Bell III, J.F., Lauer Jr., H.V., 1995. Hematite, pyroxene, and phyllosilicates on Mars: implications from oxidized impact melt rocks from Manicouagan Crater Quebec, Canada. J. Geophys. Res. 100, 5319–5328.

Morris, R.V., Ming, D.W., Golden, D.C., Bell III, J.F., 1996. Occurrence of jarositic tephra on Mauna Kea, Hawaii: Implications for the ferric mineralogy of the Martian

surface. In: Dyar, M.D., et al. (Eds.), Mineral Spectroscopy: A Tribute to Roger G. Burns. Geochem. Soc. Spec. Publ. vol. 5. pp. 327–336.

Morris, R.V., Golden, D.C., Bell III, J.F., Shelfer, T.D., Scheinost, A.C., Hinman, N.W., Furniss, G., Mertzman, S.A., Bishop, J.L., Ming, D.W., Allen, C.C., Britt, D.T., 2000. Mineralogy, composition, and alteration of Mars Pathfinder rocks and soils: evidence from multispectral, elemental, and magnetic data on terrestrial analogue, SNC meteorite, and Pathfinder samples. J. Geophys. Res. 105 (E1), 1757–1817.

Morris, R.V., Golden, D.C., Ming, D.W., Shelfer, T.D., Jørgensen, L.C., Bell III, J.F., Graff, T.G., Mertzman, S.A., 2001. Phyllosilicate-poor palagonite dust from Mauna Kea Volcano (Hawaii): a mineralogical analogue for magnetic Martian dust? J. Geophys. Res. 106, 5057–5083.

Morris, R.V., Klingelhoefer, G., Bernhardt, B., Schroeder, C., Rodionov, D.S., de Souza Jr., P.A., Yen, A., Gellert, R., Evlanov, E.N., Foh, J., Kankeleit, E., Guetlich, P., Ming, D.W., Renz, F., Wdowiak, T., Squyres, S.W., Arvidson, R.E., 2004. Mineralogy at Gusev Crater from the Moessbauer Spectrometer on the Spirit Rover. Science 305, 833–836.

Morris, R.V., Klingelhoefer, G., Schroeder, C., Rodionov, D.S., Yen, A., Ming, D.W., de Souza Jr., P.A., Fleischer, I., Wdowiak, T., Gellert, R., Bernhardt, B., Evlanov, E.N., Zubkov, B., Foh, J., Bonnes, U., Kankeleit, E., Guetlich, P., Renz, F., Squyres, S.W., Arvidson, R.E., 2006. Moessbauer mineralogy of rock, soil, and dust at Gusev Crater, Mars: Spirit's journey through weakly altered olivine basalt on the plains and pervasively altered basalt in the Columbia Hills. J. Geophys. Res. 111, E02S13.

Moessbauer, R.L., 1958a. Kernresonanzfluoreszenz von Gammastrahlung in Ir191. Z. Phys. 151, 124–143. Moessbauer, R.L., 1958b. Kernresonanzabsorption von Gammastrahlung in Ir191. Naturwissenschaften 45, 538–539.

Moessbauer, R.L., 2000. The discovery of the Moessbauer effect. Hyperfine Interact. 126, 1–12.

Murad, E., 1988. Properties and behavior of iron oxides as determined by Moessbauer spectroscopy. In: Stucki, J.W., Goodman, B.A., Schwertmann, U. (Eds.), Iron in Soils and Clay Minerals. Reidel, Dordrecht, Netherlands, pp. 309–350.

Pullan, D., Sims, M.R., Wright, I.P., Pillinger, C.T., Trautner, R., 2003. Beagle 2, An Exobiological lander for the Mars Express mission. ESA SP-1240, December 2003.

Rieder, R., Economou, T., Waenke, H., Turkevich, A., Crisp, J., Brueckner, J., Dreibus, G., McSween Jr., H.Y., 1997. The chemical composition of Martian soil and rocks returned by the mobile Alpha Proton X-ray spectrometer: preliminary results from the X-ray mode. Science 278, 1771–1774.

Rieder, R., Gellert, R., Anderson, R.C., Brueckner, J., Clark, B.C., Dreibus, G., Economou, T., Klingelhoefer, G., Lugmair, G.W., Ming, D.W., Squyres, S.W., d'Uston, C., Waenke, H., Yen, A., Zipfel, J., 2004. Chemistry of rocks and soils at Meridiani Planum from the alpha particle X-ray spectrometer. Science 306, 1746–1749.

Rodionov, D., Schroeder, C., Klingelhoefer, G., Morris, R.V., Bernhardt, B., de Souza Jr., P.A., Yen, A., Renz, F., Wdowiak, T., Squyres, S.W., and the Athena Science Team, 2004. Moessbauer investigation of 'Bounce Rock' at Meridiani Planum on Mars—Indications for the first Shergottite on Mars. Meteor. Planet. Sci. 39 (NR8, Suppl.), A91, (67th Annual Meteoritical Society Meeting 2004).

Ross, K.A., Fisher, R.V., 1986. Biogenic grooving on glass shards. Geology 14, 571–573. Rothschild, L.J., Mancinelli, R.L., 2001. Life in extreme environments. Nature 409, 1092–1101.

Schroeder, C., Klingelhoefer, G., Tremel, W., 2004. Weathering of Febearing minerals under Martian conditions, investigated by Moessbauer spectroscopy. Planet. Space Sci. 52 (11), 997–1010.

Schroeder, C., Klingelhoefer, G., Morris, R.V., Rodionov, D.S., de Souza Jr., P.A., Ming, D.W., Yen, A.S., and the Athena Science Team, 2005. Weathering of basaltic rocks from the Gusev plains up into the Columbia hills from the perspective of the MER Moessbauer spectrometer. Lunar Planet. Sci. 36 (2309) (CD-ROM).

Sims, M.R., Pillinger, C.T., Wright, I.P., Dowson, J., Whitehead, S., Wells, A., Spragg, J.E., Fraser, G., Richter, L., Hamacher, H., Johnstone, A., Meredith, N.P., de la Nougerede, C., Hancock, B., Turner, R., Peskett, S., Brack, A., Hobbs, J., Newns, M., Senior, A., Humphries, M., Keller, H.U., Thomas, N., Lingard, J.S., Underwood, J.C., Sale, N.M., Neal, M.F., Klingelhoefer, G., Ng, T.C., 1999. Beagle 2: A proposed exobiology lander for ESA's 2003 Mars Express Mission. Adv. Space Res. 23 (11), 1925–1928.

Sleep, N.H., Meibom, A., Fridriksson, T., Coleman, R.G., Bird, D.K., 2004. H2-rich fluids from serpentinization: geochemical and biotic implications. Proc. Natl Acad. Sci. 101, 12818–12823.

Soderblom, L.A., Anderson, R.C., Arvidson, R.E., Bell III, J.F., Cabrol, N.A., Calvin, W., Christensen, P.R., Clark, B.C., Economou, T., Ehlmann, B.L., Farrand, W.H., Fike, D., Gellert, R., Glotch, T.D., Golombek, M.P., Greeley, R., Grotzinger, J.P., Herkenhoff, K.E., Jerolmack, D.J., Johnson, J.R., Jolliff, B., Klingelhoefer, G., Knoll, A.H., Learner, Z.A., Li, R., Malin, M.C., McLennan, S.M., McSween, H.Y., Ming, D.W., Morris, R.V., Rice Jr., J.W., Richter, L., Rieder, R., Rodionov, D., Schroeder, C., Seelos IV, F.P., Soderblom, J.M., Squyres, S.W., Sullivan, R., Watters, W.A., Weitz, C.M., Wyatt, M.B., Yen, A., Zipfel, J., 2004. Soils of Eagle Crater and Meridiani Planum at the opportunity Rover landing site. Science 306, 1723–1726.

Squyres, S.W., Arvidson, R.E., Baumgartner, E.T., Bell III, J.F., Christensen, P.R., Gorevan, S., Herkenhoff, K.E., Klingelhoefer, G., Madsen, M.B., Morris, R.V., Rieder, R., Romero, R.A., 2003. Athena Mars rover science investigation. J. Geophys. Res. 108 (E12), 8062.

Squyres, S.W., Arvidson, R.E., Bell III, J.F., Brueckner, J., Cabrol, N.A., Calvin, W., Carr, M.H., Christensen, P.R., Clark, B.C., Crumpler, L., Des Marais, D.J., d'Uston, C., Economou, T., Farmer, J., Farrand, W., Folkner, W., Golombek, M., Gorevan, S., Grant, J.A., Greeley, R., Grotzinger, J., Haskin, L., Herkenhoff, K.E., Hviid, S., Johnson, J., Klingelhoefer, G., Knoll, A., Landis, G., Lemmon, M., Li, R., Madsen, M.B., Malin, M.C., McLennan, S.M., McSween, H.Y., Ming, D.W., Moersch, J., Morris, R.V., Parker, T., Rice Jr., J.W., Richter, L., Rieder, R., Sims, M., Smith, M., Soderblom, L.A., Sullivan, R., Waenke, H., Wdowiak, T., Wolff, M., Yen, A., 2004a. The Spirit Rover's Athena Science Investigation at Gusev Crater, Mars. Science 305, 794–799.

Squyres, S.W., Arvidson, R.E., Bell III, J.F., Brueckner, J., Cabrol, N.A., Calvin, W., Carr, M.H., Christensen, P.R., Clark, B.C., Crumpler, L., Des Marais, D.J., d'Uston, C., Economou, T., Farmer, J., Farrand, W., Folkner, W., Golombek, M., Gorevan, S., Grant, J.A., Greeley, R., Grotzinger, J., Haskin, L., Herkenhoff, K.E., Hviid, S., Johnson, J., Klingelhoefer, G., Knoll, A., Landis, G., Lemmon, M., Li, R., Madsen, M.B., Malin, M.C., McLennan, S.M., McSween, H.Y., Ming, D.W., Moersch, J., Morris, R.V., Parker, T., Rice Jr., J.W., Richter, L., Rieder, R., Sims, M., Smith, M., Soderblom, L.A., Sullivan, R., Waenke, H., Wdowiak, T., Wolff, M., Yen, A., 2004b. The opportunity Rover's Athena Science investigation at Meridiani Planum, Mars. Science 306, 1698–1703.

Squyres, S.W., Grotzinger, J.P., Arvidson, R.E., Bell III, J.F., Calvin, W., Christensen, P.R., Clark, B.C., Crisp, J.A., Farrand, W.H., Herkenhoff, K.E., Johnson, J.R., Klingelhoefer, G., Knoll, A.H., McLennan, S.M., McSween, H.Y., Morris, R.V., Rice, J.W., Rieder, R., Soderblom, L.A., 2004c. In situ evidence for an ancient aqueous environment at Meridiani Planum, Mars. Science 306, 1709–1714.

Squyres, S.W., Arvidson, R.E., Blaney, D.L., Clark, B.C., Crumpler, L., Farrand, W.H., Gorevan, S., Herkenhoff, K.E., Hurowitz, J., Kusack, A., McSween, H.Y., Ming, D.W., Morris, R.V., Ruff, S.W., Wang, A., Yen, A., 2006. The Rocks of the Columbia Hills. J. Geophys. Res. 111, E02S11.

Staudigel, H., Hart, S.R., 1983. Alteration of basaltic glass: processes and significance for the oceanic crust-sewater budget. Geochim. Cosmochim. Acta 47, 337–350.

Techer, I., Lancelot, J., Clauer, N., Liotard, J.M., Advocat, T., 2001. Alteration of a basaltic glass in an argillaceous medium: The Salagou dike of the Lodeve Permian Basin (France). Analogy with an underground nuclear waste repository. Geochim. Cosmochim. Acta 65 (7), 1071–1086.

Thorseth, I.H., Furnes, H., Tumyr, O., 1991. A textural and chemical study of Icelandic palagonite of varied composition and its bearing on the mechanism of the glass-palagonite transformation. Geochim. Cosmochim. Acta 55, 731–749.

Thorseth, I.H., Furnes, H., Heldal, M., 1992. The importance of microbiological activity in the alteration of natural basaltic glass. Geochim. Cosmochim. Acta 56, 845–850. Thorseth, I.H., Furnes, H., Tumyr, O., 1995. Textural and chemical effects of bacterial activity on basaltic glass: an experimental approach. Chem. Geol. 119, 139–160.

Torsvik, T., Furnes, H., Muehlenbachs, K., Thorseth, I.H., Tumyr, O., 1998. Evidence for microbial activity at the glass-alteration interface in Oceanic Basalts. Earth Planet. Sci. Lett. 162, 165–176.

Tosca, N.J., McLennan, S.M., Clark, B.C., Grotzinger, J.P., Hurowitz, J.A., Knoll, A.H., Schroeder, C., Squyres, S.W., 2005. Geochemical modeling of evaporation processes on Mars: Insight from the sedimentary record at Meridiani Planum. Earth Planet. Sci. Lett. 240, 122–148.

Waoechtershaoeuser, G., 1988. Before enzymes and templates: theory of surface metabolism. Microbiol. Rev. 52 (4), 452–484. Waoechtershaoeuser, G., 1992. Groundworks for an evolutionary biochemistry: the Iron–sulphur world. Prog. Biophys. Mol. Biol. 58, 85–201.

Wade, M.L., Agresti, D.G., Wdowiak, T.J., Armendarez, L.P., Farmer, J.D., 1999. A Moessbauer investigation of iron-rich terrestrial hydrothermal vent systems: lessons for Mars exploration. J. Geophys. Res. 104 (E4), 8489–8507.

Walker, J.C.G., 1979. The early history of oxygen and ozone in the atmosphere. Pure Appl. Geophys. 117, 498–512.

Wang, A., Haskin, L.A., Squyres, S.W., Jolliff, B.L., Crumpler, L., Gellert, R., Schroeder, C., Herkenhoff, K., Hurowitz, J., Tosca, N.J., Farrand, W.H., Anderson, R., Knudson, A.T., 2006. Sulfate deposition in subsurface regolith in Gusev crater, Mars. J. Geophys. Res. 111, E02S17. Wdowiak, T.J., Agresti, D.G., 1984. Presence of a superparamagnetic component in the Orgueil meteorite. Nature 311, 140–142.

Wdowiak, T.J., Armandarez, L.P., Agresti, D.G., Wade, M.L., Wdowiak, Y., Claeys, P., Izett, G., 2001. Presence of an iron-rich nanophase material in the upper layer of the Cretaceous-Tertiary boundary clay. Meteor. Planet. Sci. 36, 123–133.

Wdowiak, T.J., Klingelhoefer, G., Wade, M.L., Nunez, J.I., 2003. Extracting science from Moessbauer spectroscopy on Mars. J. Geophys. Res. 108 (E12), 8097.

Westall, F., Brack, A., Hofmann, B., Horneck, G., Kurat, G., Maxwell, J., Ori, G.G., Pillinger, C., Raulin, F., Thomas, N., Fitton, B., Clancy, P., Prieur, D., Vassaux, D., 2000. An ESA study for the search for life on Mars. Planet. Space Sci. 48, 181–202.

Wilson, A. (Ed.), 1999. Exobiology in the Solar System & The Search for Life on Mars. European Space Agency, SP-1231, October 1999.

Yen, A.S., Gellert, R., Schroeder, C., Morris, R.V., Bell III, J.F., Knudson, A.T., Clark, B.C., Ming, D.W., Crisp, J.A., Arvidson, R.E., Blaney, D., Brueckner, J., Christensen, P.R., DesMarais, D.J., de Souza Jr., P.A., Economou, T.E., Ghosh, A., Hahn, B.C., Herkenhoff, K.E., Haskin, L.A., Hurowitz, J.A., Joliff, B.L., Johnson, J.R., Klingelhoefer, K., Madsen, M.B., McLennan, S.M., McSween, H.Y., Richter, L., Rieder, R., Rodionov, D., Soderblom, L., Squyres, S.W., Tosca, N.J., Wang, A., Wyatt, M., Zipfel, J., 2005. An integrated view of the chemistry and mineralogy of martian soils. Nature 436, 49–54.

Zipfel, J., Anderson, R., Brueckner, J., Clark, B.C., Dreibus, G., Economou, T., Gellert, R., Klingelhoefer, G., Lugmair, G.W., Ming, D., Rieder, R., Squyres, S.W., d'Uston, C., Waenke, H., Yen, A., and the Athena Science Team, 2004. APXS Analyses of Bounce Rock— The First Basaltic Shergottite on Mars. Meteor. Planet. Sci. 39 (NR8, Suppl.), A118, (67th Annual Meteoritical Society Meeting 2004).

Chapter 4

Utilization of substrate components during basaltic glass colonization by *Pseudomonas* and *Shewanella* isolates

Brad Bailey[a*], Alexis Templeton[b], Hubert Staudigel[a], Bradley M. Tebo[c]

[a]Institute of Geophysics and Planetary Physics, Scripps Institution of Oceanography, University of California, San Diego, CA 92093
[b]Department of Geological Sciences, University of Colorado, Boulder, CO 80309
[c]Division of Environmental and Biomolecular Systems, Oregon Health & Science University, Beaverton, OR 97006
*. Corresponding Author Address: 9500 Gilman Drive, M/C 0225, La Jolla, CA, 92093. bebailey@ucsd.edu.

Abstract

Many recent studies have shown that submarine basaltic rocks can host a diverse, well-developed microbial community and yet the ocean crust has been shown to be extremely oligotrophic, especially below its surface. This study demonstrates that iron-oxidizing and -reducing bacterial strains, isolated from Loihi Seamount, are able to utilize different nutrients (phosphate), electron donors (reduced iron as Fe(II)) and electron acceptors (oxidized iron as Fe(III)) found within basaltic glasses. To test whether microbial life is able to acquire specific required nutrients and energy sources directly from basaltic substrates under nutrient-limiting conditions, we prepared three different basaltic glass substrates: one amended with increased levels of phosphate (apatite), one with predominantly Fe(III) and one with predominantly Fe(II) and exposed these glasses in an annular reactor to a suite of metal-oxidizing and reducing isolates and a microbial mat consortium. Lithoautotrophic growth of *Pseudomonas* LOB-7, an obligate Fe(II)

oxidizing bacterium, was found on all basaltic substrates in excess of that found on a background borosilicate glass, while enhanced growth was observed on the apatite infused glass over other basaltic substrates when phosphate was absent in the growth medium. Anaerobic, heterotrophic growth of Shewanella 601R-1 with lactate revealed an ~2x increase in cell growth on the Fe(III)-enriched basalt. A parallel experiment performed using a natural inoculum from a Fe(III)-rich microbial mat revealed enhanced growth on all basalt surfaces over the background borosilicate glass. These results indicate that basaltic substrates could be an attractive substrate for microbial colonization under minimal nutrient conditions and suggests that enhanced growth of the colonizing bacteria may result from the nutrient content of the basalt.

4.1 Introduction

Until recently, the upper basaltic oceanic crust has been considered largely oligotrophic and unsuitable for the development of life. Yet microscopic and chemical studies of volcanic glass revealed that it is likely that there is a thriving microbial biosphere (Thorseth et al., 1992; for a complete review see Staudigel et al. 2008 and references therein) that leaves characteristic textures that dominate glass alteration in the upper 500m of the oceanic crust (e.g. Furnes et al., 1996; Furnes and Staudigel, 1999). The biogenic origin of these textures has been supported by a range of geochemical arguments and molecular probes (Staudigel, et al., 2008). Additionally, a multitude of recent molecular and microbiological studies have begun to phylogenetically characterize this deep biosphere at both hydrothermal spreading ridge axes (e.g. Thorseth et al., 2001; Huber et al., 2002; Lysnes et al., 2004a & 2004b; Mason et al, 2007; Santelli et al., 2008;

Mason et al., 2009; Santelli et al., 2009) and seamounts (e.g. Emerson and Moyer, 2002; Templeton et al., 2005; Mason et al., 2007; Santelli et al., 2008; Mason et al., 2009). While it is clear that a wide diverse seafloor basalt biosphere exists and that those textures discussed above are of biological origin, no specific microbes have been identified as those responsible for basalt bioalteration (although Fe(II)-oxidizing bacteria have been suggested as likely contributors, e.g. Edwards et al., 2004), and in particular no clear indication has been found for the controls of these biological functions. Several first order questions remain about these overall bioalteration processes: How do the biotextures relate to surface biofilms associated with submarine volcanic rock surfaces? What is the energy source? Where does the carbon come from? How do these microbes obtain critical nutrients in these oligotrophic environments?

It is widely speculated that the very large content of reduced transition metals in volcanic glass (Fe (II); Mn (II)) might offer a significant energy source when oxidized by O_2 or nitrate in seawater (Bach and Edwards, 2003). Indeed, several studies demonstrate the presence of Fe(II)- and Mn(II)-oxidizing microbes in submarine volcanic settings (e.g. Templeton et al., 2005; Emerson et al., 2007; Mason et al., 2007; Santelli et al., 2008) and that microbes do form biofilms on glass (e.g. Staudigel et al., 1995) and volcanic rock (e.g. Daughney, et al., 2004, Rogers and Bennett, 2004). Microbially mediated digestion of these basaltic materials may release reduced metals and possibly some nutrients that may be used to drive carbon fixation and primary productivity (e.g. Stevens and McKinley, 1995; Edwards et al., 2004; Rogers and Bennett, 2004). However, while there is much circumstantial evidence, it remains to be demonstrated that

microbes can directly obtain reduced transition metals or other nutrients from volcanic rock through colonization and direct interaction with the glass.

In this study we explored the ability of marine microorganisms to colonize and directly utilize particular nutrients (phosphate) and energy sources (Fe(II)/Fe(III) as the primary electron donor/acceptor in this setup) from silicate glass surfaces of specific composition. We used a natural Fe(III)-rich microbial inoculum and microbial isolates, specifically Fe(II)-oxidizing strains of *Pseudomonas* and a Fe(III)-reducing *Shewanella sp.* obtained from the hydrothermally active Loihi Seamount (Hawai'i). In our experiments, we explore the role of substrate Fe(II)/Fe(III) as a key redox pair that may provide energy for autotrophic carbon fixation and the role of substrate-based phosphate as a nutrient under nutrient-starved conditions. Experiments were designed to specifically explore how the concentration of Fe(II), Fe(III) or PO_4 in specifically formulated glasses would control the colonization density of biofilms that formed with 30-113 days of growth in oligotrophic annular reactors. Our observations of microbial colonization and biofilm density show a strong correlation between substrate composition and the microbial metabolic function of the isolates studied.

4.2 Methods and Materials

4.2.1 Basalt substrates

Colonization studies were carried out using polished sections of three distinct glass compositions mounted with epoxy on a standard borosilicate microscope slide. Basalt glass substrates were all derived from a natural tholeiitic basaltic glass (sample number: HSHI-16) that was quenched from an active lava flow on Kilauea Volcano, Hawai'I (Pu'U Oo; 11-21-2002). This glass was powdered in a disc mill and split into three separate batches for chemical modification (see Table 1). The first batch was remelted to yield our "Normal" Basalt (NB). The Oxidized Basalt (OB) was prepared by firing the glass powder at subsolidus temperatures (750-850°C) and re-ground three consecutive times in order to oxidize Fe(II) to Fe(III) as much as possible. The Apatite Basalt (AB) was prepared using NB and amended with 5 wt% of apatite ($Ca_5(PO_4)_3(OH)_{0.33}F_{0.33}Cl_{0.33}$) crystals (< 97um). All substrates were fused in a bottom loading furnace at 1450°C for 30 mins in a platinum crucible for homogenization purposes and to resorb crystalline material and vesicles. The silicate melt was then poured into graphite molds and annealed at temperatures of 850°C and 450°C for 15 mins each to relieve internal stresses and minimize shattering during sectioning and polishing. The basalts were then placed side by side and cut into 60 mm thick thin-sections and polished such that the resultant slide had all four types of substrates aligned on one slide (NB, OB, AB, borosilicate). Major element compositions of these glasses were determined by electron microprobe for major element analysis; Fe speciation within the glass was determined by Mössbauer spectroscopy (Table 1; Schroeder et al., 2006).

4.2.2 Bacterial Communities, Isolation and Media

Bacterial isolation and experiments are all based on a modified Wolfe's mineral medium (Wolin et al., 1963) which is an artificial seawater medium described in Emerson and Moyer (1997; hereafter referred to as "MMWM"), and prepared with 18.3 MW DDI water. The MMWM medium was prepared by using (per 1L of 18.3 MW DDI water: 27.5g NaCl, 5.38g $MgCl_2(6H_2O)$, 0.72g KCl, 0.2g $NaHCO_3$, 1.4g $CaCl_2$, 1.0 NH_4Cl, 0.05 K_2HPO_4. The solution was then autoclaved and amended with 1ml of vitamin solution (per 200ml 18.3 MW DDI water: 20mg biotin, 4mg niacin, 2mg thiamin, 4mg pABA, 2mg pantothenic, 20mg pyridoxine, 2mg B12, 4mg riboflavin, 4mg folic acid, filter sterilized) and 1ml trace elements (per 1L 18.3 MW DDI water: 10mg $CuSO_4$-$5H_2O$, 44mg $ZnSO_4$-$7H_2O$, 20mg $CoCl_2$-6H2O, 13mg Na_2MoO_4-$2H_2O$, filter sterilized and the pH adjusted to 7.6). Dissolved CO_2 was the only carbon source available for the aerobic experiments to promote autotrophy. For anaerobic experiments, MMWM was de-oxygenated by bubbling with N_2, and Na-lactate (100mM final concentration) was added as the carbon and energy source. For the phosphate-limited experiment, K_2HPO_4 was excluded from the basal medium.

For our experiments, we used two bacterial strains and a sub-sample from a natural microbial community harvested from an iron oxyhydroxide microbial mat. *Pseudomonas* sp. strain LOB-7 is an obligate, Fe(II)-oxidizing, lithoautotrophic rod-shaped bacterium, which was isolated from a low-temperature Fe-oxyhydroxide-rich mat on Loihi Seamount off the southeast coast of the Big Island of Hawai'i (Templeton, unpublished data). *Shewanella* strain 601R-1 is a Fe(III)-reducing bacterium isolated at room temperature from the Upper Hiolo Vents on Loihi Seamount.   Anaerobic

enrichment cultures used MMWM with 10mM poorly-crystalline ferric oxides (prepared after Frederickson et al., 1998) as the sole electron acceptor and 10mM Na-lactate as the primary e-donor. The strain was isolated through dilution to extinction. Sequencing and BLAST (McGinnis and Madden, 2004) of this isolate's 16S rRNA region revealed that its 16S rRNA structure is 99% similar to *Shewanella loihica* PV-4, another facultative Fe(III)-reducing strain isolated from Loihi Seamount (Gao et al. 2006). The bacterial enrichment, 05PV610R3 (hereafter 610R3), came from an Fe-rich microbial floc found on Nafanua, the central cone of Vailulu'u Seamount (Staudigel et.al., 2006). This enrichment was originally for Fe(II)-oxidizers as it was microaerophilic with no added carbon; however, some heterotrophy and iron reduction may have been present under those conditions. Diversity studies have been completed on the original sample from this site collected 3 months later from which this enrichment was inoculated (Sudek et al., 2009).

4.2.3 Experiments

All incubation experiments were carried out in an autoclaved, 1L annular reactor (Biosurface Technologies, Model 1120 LS) in the dark at 17°C, in the (laboratory) atmosphere (passive exposure to air was filtered through a 0.22 mm syringe filter) or in a 100% N_2-filled glove bag for the anaerobic *Shewanella* experiment, flushing nitrogen every 4 days. Each bacterial culture was grown under microaerophilic conditions (LOB-7 and 610R3) or anaerobically (601-R1) in 10ml syrum vials and were inoculated at stationary phase. As the experiments compare one surface to another within an isolated

experiment and not across experiments, the initial concentration of bacteria was not measured upon inoculation. Experimental conditions were:

1) FeOx(+p) - Fe(II)-oxidizing *Pseudomonas* isolate LOB-7 , on MMWM media, 30 days in air;

2) FeOx(-p) - Fe(II)-oxidizing *Pseudomonas* isolate, LOB-7, on MMWM (-)PO_4, 30 days in air on MMWM without phosphate;

3) FeRed - Fe(III)-Reducing *Shewanella* isolate, 601R-1, 30 days on anoxic MMWM (+)lactate (in N_2);

4) Enrichment - a microbial community, 610R3, on MMWM in air with multiple samples taken at time intervals up to 113 days; and

5) An abiotic control was carried out over 30 days with MMWM medium to demonstrate sterility of the system and to explore the potential for abiotic authigenic mineral deposition.

Determination of growth was based on total cell counts performed using 4',6-diamidino-2-phenylindole (DAPI) (Porter and Feig, 1980) on a Zeiss Axioplan Universal Compound Microscope with a mercury fluorescent light source. We counted at least three independent areas defined by the field of vision with a diameter of 0.23 mm. Uncertainties were determined as the 2 sigma variation in counts between these fields. Cell counts were also carried out on the borosilicate glass and the epoxy-mounting medium to obtain an iron and phosphate-free substrate background. We plotted cell counts on background glass and cell counts on basaltic glass substrates in Figure 4.1. The uncertainties of the cell count values are reported as 2s (standard deviation from triplicate

measurements). During cell counts via light microscopy, false positive counts from autofluorescence were minimized due to the distinct rod shapes of the cells; however, the small size of the cells associated with oxides and secondary minerals could have artificially increased cell counts in the final tally.
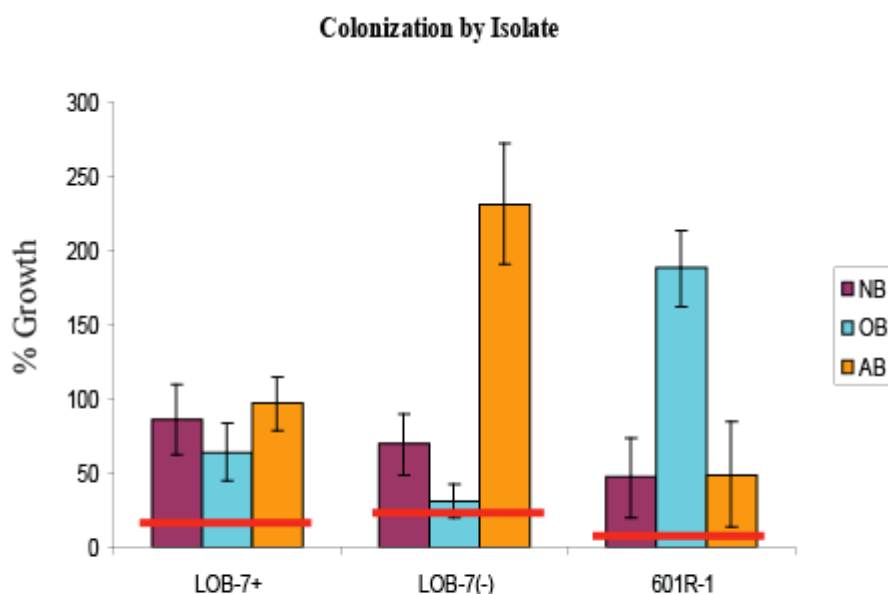
Figure 4.1. Cell counts on various basalt and background substrates after growth for 30 days. All numbers have been normalized to background counts on the borosilicate glass. LOB-7(+) is an obligate autotrophic Fe(II)-oxidizing *Pseudomonas* isolate on EM media with PO_4 added in. LOB-7(-) is the same *Pseudomonas* Fe(II)-oxidizer on EM media without PO_4 added to the media. 601R-1 is inoculated with a, iron-reducing *Shewanella* strain. NB = normal basaltic glass, OB = oxidized basaltic glass, AB = apatite basaltic glass. The red line indicates an upper bound on error calculations for background counts made on the borosilicate glass. Error bars represent 2s. No discernable difference in cell counts were observed under normal conditions. However, under PO_4 starving conditions, a dramatic increase of approximately 225% growth over background and an almost 200% increase over normal basalt was witnessed on the apatite doped basalts. A similar effect was witnessed on the oxidized basalts using 601R-1 given the much higher degree of available Fe(III) within the basalt substrate.

4.3 Results

The chemical composition of the three glasses (NB, OB and AB) were determined by electron microprobe (Table 4.1). These analyses confirmed that the bulk concentration of most elements were similar to Normal Basalt and only the concentrations of phosphorus and the Fe(III)/Fe(total) ratios were significantly altered. Schroeder et al., (2006) determined a Fe(III)/Fe(total) ratio of 0.70 in the oxidized glass by Moessbauer spectroscopy while this ratio is 0.13 in the natural glass. Phosphate concentration in the apatite-doped basalt was increased to 2.22% compared to 0.35% in the natural material. Some small non-resorbed apatite remained visible in the glass.

Table 4.1. Major element analysis by microprobe of the amended basaltic glass after processing. Elements are reported as oxides and numbers are given in weight %.

Sample Name	SiO_2	TiO_2	Al_2O_3	Cr_2O_3	Fe_2O_3	FeO	MnO	MgO	CaO	Na_2O	K_2O	P_2O_5	Total
Normal Basalt	51.92	2.39	13.53	0.05	1.73	9.55	0.14	7.05	10.68	1.89	0.39	0.32	99.62
Oxidized Basalt	51.50	2.42	13.52	0.07	8.69	3.35	0.14	6.99	10.65	1.86	0.38	0.31	99.88
Apatite Basalt	49.25	2.23	12.75	0.03	1.64	9.04	0.17	6.68	13.09	1.81	0.38	2.22	99.27

All biological experiments resulted in preferred colonization on the basalt surfaces compared to the background borosilicate glass (Figures 4.1 and 4.2) even though FeOx(-p) cell counts are within the uncertainty of the background colonization for the oxidized basalt (Figure 4.1). T-Test statistical analysis on these data show that each of the basaltic data sets are statistically different from the background glass sample where most values were between 0.08-0.13 and the largest t-test result was 0.19. Two of the experiments showed substantially enhanced growth. The Fe(II)-oxidizing *Pseudomonas* LOB-7 grew 2-2.5x better on the PO_4-doped basalt relative to the other basalts. Similarly,

the Fe(III)-reducing *Shewanella* 601R-1 grew ~2x better on the Fe(III)-rich basalt (OB) (with its four-fold high amount of Fe(III)) than the other basalts. This shows that, at least in an anaerobic environment, our strain of *Shewanella* can use Fe (III) from basalt as an electron acceptor. The abiotic experiment revealed no significant precipitation or detritus on the glass surfaces after 30 days and showed little to no alteration in SEM images (data not shown).

610R3 Cell Counts
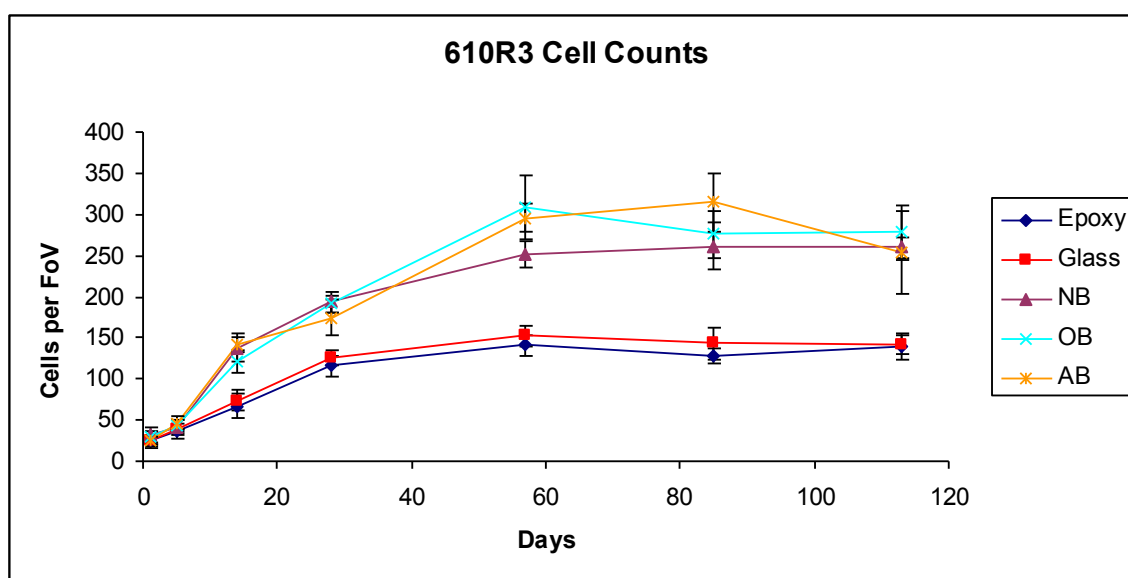
Figure 4.2. A 115 day enrichment culture using 610R3 microbial community as an inoculum where cells were counted on each substrate at various intervals and are reported in cells counted per field of view (0.23 mm). Cellular growth in all cases was higher on basaltic substrates than background borosilicate glass and the embedding epoxy. Error bars represent 2σ.

The Fe-rich microbial mat 610R3 collected from Vailulu'u Seamount was used to directly inoculate the annular reactor containing seven identical sets of basalt slides. Slides were sequentially harvested at Day 1, 5, 14, 28, 57, 85 and 113, respectively. Cell counts from this experiment (Figure 4.2) show that there is no discernable difference between basalt substrates. However, there is a clear preference for colonization of any of

the basalt glasses relative to borosilicate glass and epoxy. Overall the system reaches a steady-state cell abundance after about 60 days. We attempted to characterize the microbial communities associated with each glass slide but were unable to extract sufficient DNA.

Figure 4.3 displays four scanning electron microscope (SEM) photomicrographs taken from FeOx(+p) where scattered single cells formed on the borosilicate glass (Figure 4.3A), surrounding epoxy (Figure 4.3B), natural basalt (Figure 4.3C) and oxidized basalt (Figure 4.3D). Each biofilm consists of a discontinuous monolayer of the Fe(II)-oxidizing *Pseudomonas* isolate; however, the basalt substrates clearly indicate a greater density of cells versus the nutrient-poor epoxy and borosilicate glass. Similar features and densities of the Fe(III)-reducing *Shewanella* 601R-1 were seen on the oxidized basalt (data not shown).
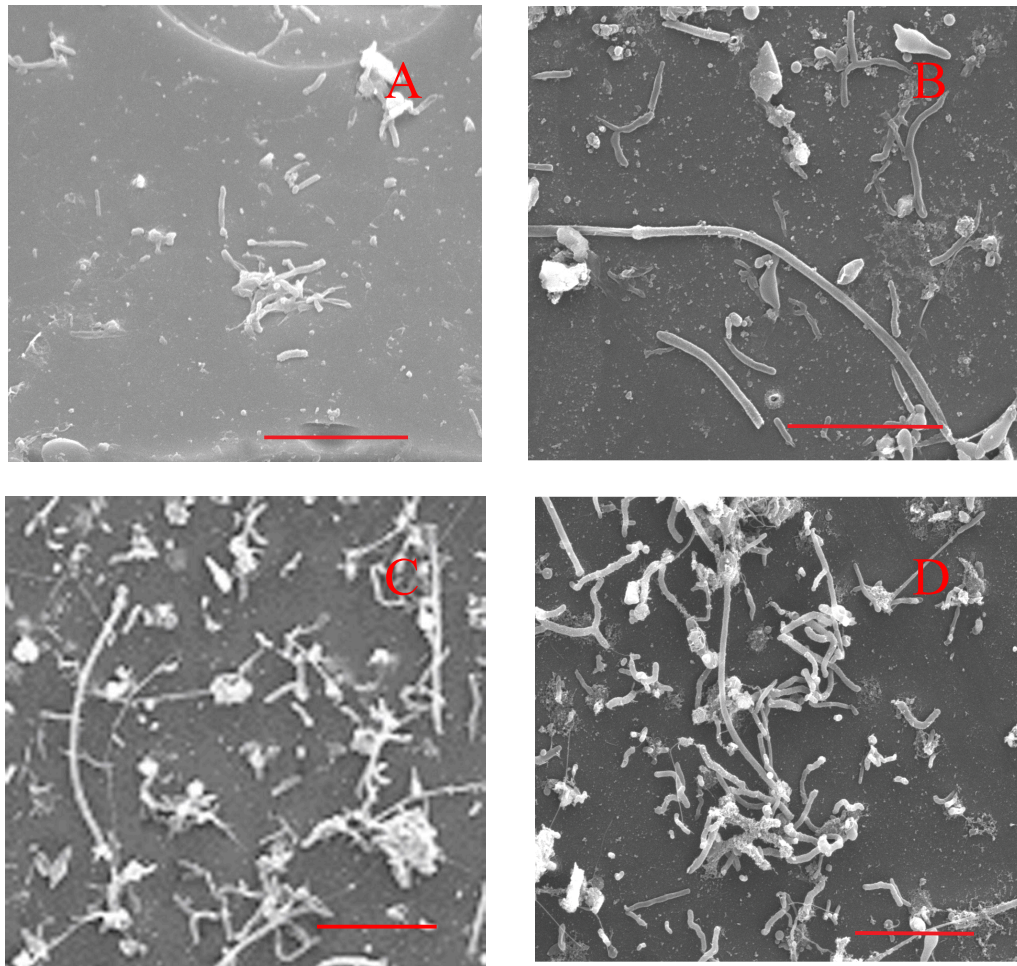
Figure 4.3. SEM photomicrographs of various glass types colonized with *Pseudomonas* isolate LOB-7(+). All photos are taken from the same experiment after a 42 day incubation period. (A) Borosilicate glass. (B) Surrounding epoxy. (C) Normal basalt. (D) Oxidized basalt. Cell coverage on each basalt surface is much higher than on borosilicate glasses and the surrounding epoxy. Scale bars represent 10μm.

4.4 Discussion

The potential for preference of some microbes to colonize and grow on particular substrate compositions basaltic glass base-composition colonization and growth in nutrient-limiting environments has far reaching implications for a deep subsurface biosphere. The abundance of bioalteration textures in basalts from the oceanic crust suggests that microbial processes dominate, or at least play an important role in the alteration of basaltic glass (e.g. Thorseth et al., 19911992; Furnes and Staudigel, 1999; Staudigel et al., 2008). These microbial activities are important, as the resultant glass alteration dominates the low temperature geochemical fluxes between seawater and the extrusive oceanic crust. (Staudigel and Hart, 1983). The mechanisms and driving forces behind this dissolution/alteration are largely hypothesized to be organic ligands and local environment pH changes (e.g. Rogers et al., 2001; Buss et al., 2007; Wu et al., 2008), however). However, the focus of most of our discussion keys in on how compositional characteristics of basalt might provide particular nutrients and energy in the form of electron donor/acceptors by taking advantage of elements within the basaltic glass matrix (e.g. Rogers et al., 1998; 2001).

While our study does not necessitate actual release of Fe from the glass matrix for electron transfer, we do observe an increase in iron on the surface of the glasses compared to abiotic controls . This suggests that microbial activity mediates the release of some Fe from the glass surfaces microbial Fe release from mineral surfaces is . Maurice et al. (2001a, 2001b) reported that an aerobic *Pseudomonas mendocina* bacterium has the ability to enhance mineral dissolution in kaolinites (0.04 wt% Fe_2O_3) in a Fe-limiting setting and additionally releases significant amounts of Al and Si when

compared to a non-Fe-limited environment. Buss et al. (2007) showed significant surface alteration and pitting when subjected to siderophores and Brantley et al. (2001) show an enhanced Fe release from mineral surfaces which is additionally isotopically light when in the presence of bacteria/siderophores. Kalinowski et al. (2000) report that Fe release from hornblende is accelerated by up to a factor of ~20 in the presence of bacteria.

Fe(II) is probably the most attractive energy source in basalts since basalts typically contain 10-12 wt% Fe and 90% of this is Fe(II) which is capable of supporting the growth of chemolithoautotrophic Fe(II)-oxidizing bacteria (e.g. Edwards et al. 2003, Bach and Edwards 2003). Bach and Edwards (2003) propose that up to 48 ± 21 x 10^{10} g of cellular carbon is produced per year within ridge flanks due to Fe and S oxidation. The potential biomass associated with this subsurface environment can have a significant impact on chemical cycling within the deep oceanic crust. Additionally, energy may be derived from Fe(III) reduction when coupled to organic carbon oxidation. Fresh basalt contains typically about 1 wt% Fe(III) and bulk altered basaltic alteration products crusts host ~15-25 wt% Fe(III) (Alt and Honnorez, 1984; Staudigel et al., 1996). This Fe(III) can act as a terminal electron acceptor which is crucial to electron flow in anaerobic microbial metabolism. Without access to nitrate, coupling oxidation of lactate to reduction of ferric iron results in favorable energy yields within the given constraints of our experiments:

$$C_3H_5O_3^- + 12Fe^{3+} + 3H_2O = 3CO_2 + 11H^+ + 12Fe^{2+} \quad \Delta G°=\text{-846 kJ/mol}$$
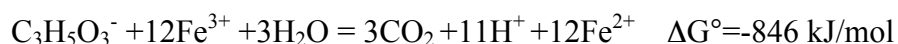
Stapleton et. al. (2005) report on several strains of *Shewanella* capable of metal reduction (including Fe(III)) within marine sediments and active iron-rich hydrothermal vent sites.

The importance of Fe redox related metabolism of basalt hosted microbial communities has been shown to potentially support a massive subsurface microbial ecosystem (e.g. Stevens and McKinley, 1995; Bach and Edwards, 2003; Edwards et al., 2003), but so far it has been uncertain whether microbes access the Fe passively through interactions with hydrothermal solutions or whether they are actively involved in interactions with the substrates themselves. This distinction is important as active hydrothermal venting in a volcanic system is restricted in time and space, and therefore microbial activity would only occur during initial eruption and along ridge/active seamount flanks. In contrast the basaltic substrates themselves are much more common and available for much longer time (i.e. until subduction or burial), well beyond termination of volcanic activity, and thus microbial activity could continue throughout the entire lifespan of the substrate if the microbe/mineral interaction was active instead of passive. Furthermore, there is a wide range of geochemical and microbe-functional implications associated with active vs passive interactions. Active microbial dissolution of substrates can be a much more efficient mechanism of utilization and chemical fluxes from basalt alteration may be profoundly altered when mediated by microbial activities. Passive interactions or dissolution as a convenient by-product of other cellular mechanisms would ultimately result in lower geochemical fluxes.

These results indicate that the presence of basalt in the environment is beneficial for the growth of the microbes and the consortia used in our experiments. Although the scope of these experiments may not point to a unique nutrient or energy source given the complex major and trace element composition of basalt, more specific experiments could be carried out to delineate particular metabolic requirements. For example, future

experiments could focus on pure silica glasses amended with phosphate or iron to target specific elements required for growth. However, it is fair to say that (1) several components in basaltic glass may be readily available for microbial utilization and/or consumption, and (2) most critical chemical components are available in abundances well above the concentration in the media. Hence, future studies should examine other potential nutrient candidates or electron donor/acceptor pairs that occur in basalts and which could be utilized by microbes (e.g. Mn, S, U, Mo) for growth and metabolism.

The goal of our study was to explore the extent to which microbes directly interact with substrates by simulating oligotrophic conditions and by providing them with nutrients or energy sources from the glass itself. All of our basaltic glasses provided a more attractive growth substrate than borosilicate glass (except FeOx(-p) in which error bars overlap between oxidized basalt and background). The results presented here indicate that single isolates grew better on substrates that contained the needed nutrients (i.e., phosphate) or electron donor/acceptor (Fe(II)/Fe(III)) during nutrient-poor or starving conditions. In fact, it is very likely that these microbes are able to utilize the P or Fe(II)/Fe(III) directly from the basaltic glass and that substrate composition positively affects the overall growth potential in oligotrophic environments. While not specifically tested in this set of experiments, it should be noted that the operating assumption is that if the microbe would not grow if it can not access the necessary element within the enclosed system via media, utilizing them from the rock matrix or otherwise, it would not grow.

4.4.1 Iron Cycling in Auto- and Heterotrophic Growth

Cells were seen on nearly all surfaces within the annular reactor chamber with varying degrees of coverage with both the obligate Fe(II)-oxidizing autotroph LOB-7 (Figure 4.3) and the microbial community 610R3.   However, in most cases, more growth/colonization was observed on the basaltic substrates than any other surface present in the system indicating a strong preference for the basalt substrate.   We infer that this results from the higher concentration of Fe(II) in the basalts. Additionally the two experiments FeOx(+p) and the enrichment 610R3, from a natural Fe(III)-rich environment, grown on MMWM revealed that no enhanced growth on any one basaltic substrate relative to the other basaltic surfaces (Figures 4.1 and 4.2), suggesting that the amount of Fe(II) present in all substrates was enough to sustain biological productivity in the form of lithoautotrophy.

In PO_4 experiments FeOx(+p) and FeOx(-p) (Figure 4.1), some (background) colonization of LOB-7 was witnessed observed on the borosilicate glass. While no iron was present in the given medium, trace quantities of Fe may be derived from the (biotic or abiotic) dissolution of the basalt slides that were present in the system or the inoculum itself, possibly providing LOB-7 with the necessary iron for growth. on the borosilicate slide. Alternatively, cells may have initially grown on the basalt surface and detached ultimately settling out on the borosilicate slide or cells were deposited directly onto these surfaces with the initial inoculum. Additionally, it is not known if there were may have been trace quantities of P or Fe in the borosilicate glasses or if we observed random settling of cells that is not related to the substrate. Thus, while we don't quite understand the reasons why there are any cells on the borosilicate glass, the basaltic substrate appears

to provide a better growth medium for initial lithoautotrophic colonizers may possibly providing a foundation upon which other cells could attach, grow and form a biofilm..

The experiment with the enrichment culture (Figure 4.2) was designed to determine whether a community of Fe(II)-oxidizing bacteria would preferentially colonize a particular substrate. In the annular reactor, the MMWM medium plus the basalt and no other added electron donor effectively provided a growth environment that enriched for lithoautotrophs. Whether the concentration of Fe(II) in the glass was sufficient or the microorganisms are extremely adept at utilizing the Fe(II) in the substrate is not clear. The end result was that it was not possible to distinguish differences between each type of basalt which suggests that given that both Fe(II)-oxidizers and Fe(III) reducers were likely present; the various basaltic substrates all provided enough Fe(II)/Fe(III) to support biological growth from oxidation and reduction. The microbial growth leveled off after ~60-80 days which is likely due to a nutrient (likely carbon/CO_2 through passive exposure to air, fixed N, vitamins or perhaps even a quorum sensing limitation on growth) limitation within the growth medium. However, it is important to note that it was not likely a limitation on P given that all basalts, including the phosphate buffed substrate, exhibited similar cell counts.

The Fe-Red experiment completed with the Fe(III)-reducing *Shewanella sp.* 601R-1 revealed preferred colonization of the Fe(III)-enriched (oxidized) basaltic glass over other substrates. Gao et al. (2006) showed that using lactate as a carbon source, *Shewanella sp.* PV-4 strain, which is phylogenetically similar to our 601-R1 strain, is capable of reducing Fe(III), Mn(IV), Co(III), U(VI), Cr(VI) and fumarate. The oxidized basalt was previously characterized by Schroeder et.al. (2006) who measured a

Fe^{3+}/Fe^{total} ratio of 0.70 compared to 0.12 in the natural glass. Thus, this basalt contains the largest source of oxidized Fe within our system and therefore presents the most attractive target substrate for 601R-1 to colonize in an electron acceptor limited environment.

4.4.2 Nutrient Leaching from Apatite Infused Basaltic Glass

The role of phosphate-containing substrates in the environment has been well studied in terrestrial environments. In particular, in anoxic, carbon-rich, phosphorus- and nitrogen-poor ground waters, feldspars with apatite inclusions appear to be preferentially colonized over other similar substrates without such inclusions (e.g. Rogers and Bennett 2004, Rogers et. al. 1998, Stillings et.al. 1996, Welch et. al. 2002). Rogers et al (1998) showed in a one-year exposure experiment that microcline ($KAlSi_3O_8$) with 0.24% P_2O_5 was heavily colonized and weathered by microbes whereas a microcline with no detectable phosphorus was not.

Our FeOx(-p) laboratory inoculation corroborates findings from terrestrial systems: less growth was observed on substrates when phosphate was limiting (e.g. Rogers et al., 1998). The apatite-doped basaltic glass hosts an ~7x increase in phosphate concentration and results in a near 2.5x cell density on the substrate surface when compared against the normal basalt. In the FeOx(-p) experiment (Figure 4.1), the apatite basalt (AB) was significantly more colonized compared to the other basalts suggesting two things: 1) our MMWM (+)PO_4 media (~0.3mM K_2HPO_4) is not phosphate-limited as evidenced by the similar growth patterns across all basalts and 2) the MMWM (-)PO4 experiment reveals that LOB-7 is able to leach phosphate out of a silicate matrix. Our

study did not address the mechanism by which this bioleaching utilization occurs or whether it is an abiotic dissolution/diffusion or a potentially biologically mediated exchange reaction of which the microbes take advantage. Several studies have shown that the presence of microbes increases the release of Fe and P due to microbe-mineral interactions, hypothesized to occur due to the production of organic acids and metal chelaters/ligands which break down the silicate matrix and release the needed elements (e.g. Duff *et.al.* 1963, Rogers and Bennett 2004, Stillings et.al. 1996,). Welch et. al. (2002) found that apatite dissolution is a function of pH and organic ligand content. Barker et al. (1998) found that microbes create a microenvironment in which pH in the immediate vicinity of the cells may be substantially different from the surrounding medium. Applying this concept to our own findings where the solution pH never varied more than 0.1 pH, suggests whether through organic ligands, acids, or abiotic passive dissolution, dissolution enhancement could accelerate nutrient leaching and/or weathering by several orders of magnitude (Welch et. al. 2002).

4.5 Conclusions

These studies have shown that microbial life is capable of obtaining required elements directly from basaltic glass in nutrient- and energy-limiting environments. These laboratory results are in agreement with previous *in situ* and laboratory work done in terrestrial systems (Edwards et al., 2004), on phosphate-rich feldspars (Rogers et al., 1998) and crushed basalt exposed in aquifers within the Columbia River Basalt Group (Stevens and McKinley, 1995). The enhanced growth on the basaltic glasses over the

borosilicate glass in all cases suggest that nutrients present within the basaltic silicate matrix are beneficial for metabolic activity and cell proliferation.

The glasses amended with apatite or altered with respect to Fe oxidation state tested whether substrate composition could affect the microbial community composition associated with surface colonization by selecting for organisms capable of utilizing specific nutrients or energy sources within the glass. Both Fe(II)-oxidizing *Pseudomonas sp.* LOB-7 and Fe(III)-reducing *Shewanella sp.* 601R-1 appear to be adept at accessing iron and phosphate directly within the silicate matrix and consequently showed enhanced growth on the glass containing the elements needed for metabolism relative to the borosilicate glass. The similar growth patterns across the various basalts for *Pseudomonas sp.* LOB-7 and the natural sample inoculum from an Fe-rich site on MMWM medium indicated that our 3 basalts contained sufficient reduced iron, even for the Fe(III)-enriched (oxidized) basalt (approx. 23/77% Fe(II)/Fe(III)), for cells to grow. This demonstrates the efficiency with which the microbes are able to obtain elements from the glass matrix. The ability to leach nutrients or use energy sources found in rocks may be a specific adaptation of certain microbes, which may have potentially led to specialized endo- and epi-lithic bacterial communities.

4.6 Acknowledgements

assistance and facilities were essential to the formulation of glass substrates. Any opinions, findings and conclusions or recommendations expressed in this material are those of the author(s) and do not necessarily reflect the views of these agencies.

Chapter 4 is a formatted version of the published work: Bailey B., Templeton A. S., Staudigel H., Tebo B. M. (2009). Utilization of substrate components during basaltic glass colonization by Pseudomonas and Shewanella isolates. Geomicrobiol. J. 26, 648–656. doi: 10.1080/01490450903263376.   The dissertation author was the primary investigator and author of this paper.

4.7 References

Bach, W. and K.J. Edwards. (2003) Iron and sulfide oxidation within the basaltic ocean crust: Implications for chemolithoautotrophic microbial biomass production. *Geochimica et Cosmochimica Acta*., **67**:3871-3887.

Barker, W.W., S.A. Welch, S. Chu, J.F. Banfield. (1998) Experimental observations of the effects of bacteria on aluminosilicate weathering. *American Mineralogist*. **83**: 1551-1563

Duff, R. B., D. M. Webley, and R. 0. Scott. (1963) Solubilization of minerals and related materials by 2-ketogluconic acid-producing bacteria. *Soil Science*. **95**:105-114.

Edwards, K.J., D.R. Rogers, C.O. Wirsen, and T.M. McCollom. (2003) Appl. Environ. Microbiol. **69(5)**:2906-2913

Emerson D and C.L. Moyer. (1997) Isolation and characterization of novel iron-oxidizing bacteria that grow at circumneutral pH. *Applied and Environmental Microbiology*. **63**;4784–4792.

Fisk, M. R., S. J. Giovannoni, and I. H. Thorseth**.** (1998) Alteration of oceanic volcanic glass: textual evidence of microbial activity. Science **281:**978-980.

Furnes, H. and Staudigel, H., (1999) Biological mediation in ocean crust alteration: how deep is the deep biosphere? *Earth and Planetary Science Letters.* **166**:97–103.

Gao, H, A. Obraztova, N. Stewart, R. Popa, J.K. Fredrickson, J.M. Tiedje, K.H. Nealson and J. Zhou. (2006) *Shewanella Loihica* sp. nov., isolated from iron-rich microbial mats in the Pacific Ocean. *Int. J. Syst. Evol. Microbiol.* 56:1911-1916

Krumbein, W.E. and K. Jens. (1981) Biogenic rock varnishes of the Negev Desert (Israel) an ecological study of iron and manganese transformation by cyanobacteria and fungi. *Oecologia* **50**:25–38.

Mason, O.U., U. Stingl, L.J. Wilhelm, M.M. Moeseneder, C.A. Di Meo-Savoie, M.R. Fisk and S.J. Giovannoni. (2007) The phylogeny of endolithic microbes associated with marine basalts. *Environmental Microbiology.* **9**:2539-2550

Maurice, P.A., M.A. Vierkorn, L.E. Hersman, J.E. Fulghum and A. Ferryman. (2001a) Enhancement of kaolinite dissolution by an aerobic Pseudomonas mendocina bacterium. *Geomicrobiology Journal.* **18**:21-35.

Maurice, P.A., M.A. Vierkorn, L.E. Hersman, J.E. Fulghum and A. Ferryman. (2001b) Dissolution of well and poorly ordered kaolinites by an aerobic bacterium. *Chemical Geology.* **180**:81-97.

Myers, C.R. and K.H. Nealson. (1988) Bacterial manganese reduction and growth with manganese oxide as the sole electron acceptor. *Science.* **240**(4857):1319-1321

Rogers, J.R, P.C. Bennett and W.J. Choi. (1998) Feldspars as a source of nutrients for microorganisms. *American Mineralogist.* **83**:1532-1540.

Rogers, J.R. and P.C. Bennett. (2004) Mineral stimulation of subsurface microorganisms: release of limiting nutrients from silicates. *Chemical Geology.* **203**: 91-108

Rogers, K.L., and J.P. Amend. (2006) Archaeal diversity and geochemical energy yields in a geothermal well on Vulcano Island, Italy. *Geobiology* **3**(4):319-332

Ross, K.A. and R.V. Fisher. (1986) Biogenic grooving on glass shards. *Geology.* **14**:571-573

Santelli, C., B. Orcutt, E. Banning, C. Moyer, W. Bach, H. Staudigel, K. Edwards. (2008) Abundance and diversity of microbial life in the ocean crust. *Nature* 453: 653-656.

Stapleton Jr, R.D., Z.L. Sabree, A.V. Palumbo, C.L. Moyer, A.H. Devol, Y. Roh, and J. Zhou. (2005) Metal reduction at cold temperatures by Shewanella isolates from various marine environments. *Aquatic Microbial Ecology.* **38**:81-91

Stillings, L.L., J.I. Drever, S.L. Brantley, Y. Sun, and R. Oxburg. (1996) Rates of feldspar dissolution at pH 3-7 with 0-8 mM oxalic acid. Chemical Geology. **132**:79-89

Staudigel, H. and S. Hart. (1983) Alteration of basaltic glass: Mechanisms and significance for the oceanic crust-seawater budget. *Geochimica et Cosmochimica Acta*. **47**:337-350.

Staudigel H, A. Yananos, R. Chastain, G. Davies, E.A. Verdurmen, P. Schiffman, R. Boucier, H. De Barr. (1998) Biologically mediated dissolution of volcanic glass in seawater. *Earth and Planetary Science Letters*. **164**; 233–244.

Stevens, T. O., and J. P. McKinley. (1995) Lithoautotrophic microbial ecosystems in deep basalt aquifers. *Science* **270:**450-454.

Tebo B.M., W.C. Ghiorse, L.G. van Waasbergen, P.L. Siering, R. Caspi. (1997) Bacterially mediated mineral formation: insights into manganese(II) oxidation from molecular genetic and biochemical studies. In *Geomicrobiology: Interactions Between Microbes and Minerals*, ed. JF Banfield, KH Nealson, Washington, DC: Mineral. Soc. Am. pp. 225–66.

Thorseth, I.H., H. Furnes and M. Heldahl, (1992) The importance of microbiological activity in the alteration zone of natural basaltic glass. *Geochimica et Cosmochimica Acta* **55**:731–749.

Thorseth, I.H., H. Furnes, O. Tumyr, (1995) Microbes play an important role in the alteration of oceanic crust *Chemical Geology*. **126:**137-146.

Torsvik T, H. Furnes, K. Muehlenbacks, I.H. Thorseth, O Tumyr. (1998) Evidence for microbial activity at the glass-alteration interface in oceanic basalts. *Earth and Planetary Science Letters*. **162**:165–176.

Welch, S.A., A.E. Taunton, J.F. Banfield. (2002) Effect of microorganisms and microbial metabolites on Apatite Dissolution. *Geomicrobiology Journal*. **19**:343-367

Chapter 5

An Interlaboratory Comparison of DNA-Based Methods for Assessing Microbial Diversity of Seafloor Basalts

Beth Orcutt[a], Brad Bailey[b], Bradley M. Tebo[c], Hubert Staudigel[b], Katrina J. Edwards[a]

[a]Geomicrobiology Group, Department of Biological Sciences, Marine Environmental Biology, University of Southern California, 3616 Trousdale Boulevard, Los Angeles, California 90089-0371, USA.
[b]Institute of Geophysics and Planetary Physics, Scripps Institution of Oceanography, Univ. of CA, San Diego, La Jolla, CA 92093-0225, USA
[c]Division of Environmental and Biomolecular Systems, Oregon Health & Science University, Beaverton, OR. 97006, USA

Abstract

We present an interlaboratory comparison between full-length 16S rRNA sequence analysis and terminal restriction length polymorphism (T-RFLP) for basalt-hosted microbial communities on seafloor basaltic lavas, with the goal of evaluating how similarly these two different DNA-based methods in two independent labs would estimate the microbial diversity of these basalt samples. Two samples were selected for these analyses based on differences detected in the overall levels of microbial diversity between them.   Richness estimators indicate that TRFLP analysis significantly underestimates the richness of the relatively high-diversity seafloor basalt microbial community: at least 50% of species from the high-diversity site are missed by TRFLP. However, both methods reveal similar dominant species from the samples, and they predict similar levels of relative diversity between the two samples. Importantly, these results suggest that DNA-extraction or PCR-related bias between the two laboratories is

minimal. We conclude that TRFLP may be useful for relative comparisons of diversity between basalt samples, for identifying dominant species, and for estimating the richness and evenness of low-diversity, skewed populations of seafloor basalt microbial communities, but may miss a majority of species in highly diverse sample

5.1 Introduction

Application of the proper metrics for assessing, measuring, and quantifying microbial populations in complex natural systems is a current and long-standing challenge in microbial diversity (reviewed in Hughes et al., 2001). Community genetic fingerprinting methods, such as terminal restriction fragment length polymorphism (TRFLP; Liu et al., 1997), have been used repeatedly to investigate comparative community composition owing to the procedure being relatively rapid, high-throughput and inexpensive. For highly diverse microbial communities, however, there are conflicting results whether different fingerprinting methods determine similar (for example, Hartmann et al., 2005) or different (for example, Danovaro et al., 2006) levels of diversity, although part of the disagreement between methodological approaches may be due to focusing in some cases on the coding 16S rRNA gene and in others on the more highly variable, non-coding intergenic regions of the DNA sequence. In addition, the utility of fingerprinting methods to accurately calculate community diversity in complex communities has been criticized due to inability of the methods to detect low abundance (<1% of the community), rare taxa (Dunbar et al., 2000; Blackwood et al., 2003; Engebretson and Moyer, 2003; Bent et al., 2007). Recent innovations, such as pyrosequencing, now suggest that microbial communities contain even greater diversity

than previously accepted (Sogin et al., 2006, Huber et al., 2007). It is unknown if this diverse "rare biosphere" correlates to diversity in ecological or biogeochemical function, though it is suggested that the it serves as a reservoir of genomic innovation to allow microbial communities to adapt to changing environmental conditions (Sogin et al., 2006). If fingerprinting methods exclude rare taxa, are they useful for predicting metabolic potential in a microbial ecosystem?

A further challenge for microbial ecologists is the reproducibility of microbial biodiversity surveys on similar samples using different methods. As one example, surveys conducted on similar deep marine subsurface sediments using different methods have resulted in contradictory interpretations of whether the domain *Bacteria* or *Archaea* dominate the deep biosphere microbial community (Biddle et al., 2006, Inagaki et al., 2006, Schippers and Neretin, 2006, Sørensen and Teske, 2006, Lipp et al., in press). In order to assess global and local biodiversity patterns and to correctly correlate microbial community form with function, it is essential that methods are accurate, even is biased (Hughes et al., 2006).

In the present study, two independent laboratories utilized different approaches that target the 16S rRNA gene to evaluate diversity of seafloor basalt samples, for the purposes of cross-comparing methods and interlaboratory biases in biodiversity assessments. Previous studies have shown that seafloor basalts harbor some of the most diverse microbial communities on Earth (Santelli et al., 2008). Here, a set of two seafloor basalt samples collected from the Lō`ihi Seamount (Figure 5.1) were analyzed independently by both TRFLP analysis and 16S rRNA gene clone libraries as well as *in silico* TRFLP analysis of the 16S rRNA sequences. Commonly used diversity indices

were applied to the results of both the community fingerprinting analysis by TRFLP as well as to the similarity matrices calculated from the gene sequences. As compared to previous computer simulated comparisons between TRFLP patterns and 16S rRNA sequences (Liu et al., 1997; Engebretson and Moyer, 2003; Blackwood et al., 2007) and comparisons between restriction digests of 16S rRNA gene clones amplified from soils (Dunbar et al., 1999, 2000), this study evaluated empirically-derived diversity assessments generated independently from the same samples.

5.2 Materials and Methods

5.2.1 Sample Collection

As described previously (Santelli et al., 2008) the basaltic lava samples for this study were collected from distinct pillow lava outcrops around the big island of Hawai'i during cruise KOK 02-24 on R/V *Ka'imikai-o-Kanaloa* in November 2002 using the remotely-operated *Pisces V* submersible. Rock samples were placed in bioboxes containing distilled freshwater, allowed to fill with ambient bottom seawater, sealed to minimize contamination from the upper water column, and brought to the surface for immediate processing. Upon retrieval shipboard, basalt samples were handled aseptically using flame- and/or ethanol-sterilized equipment. One portion of the sample was stored at -80 $^{\circ}$C in a sterile Whirlpak™ bag for 16S rRNA clone library construction at the Woods Hole Oceanographic Institute (WHOI); the other portion was stored in sterile cryovials at -80C for TRFLP analysis at the Scripps Oceanographic Institute (SIO).
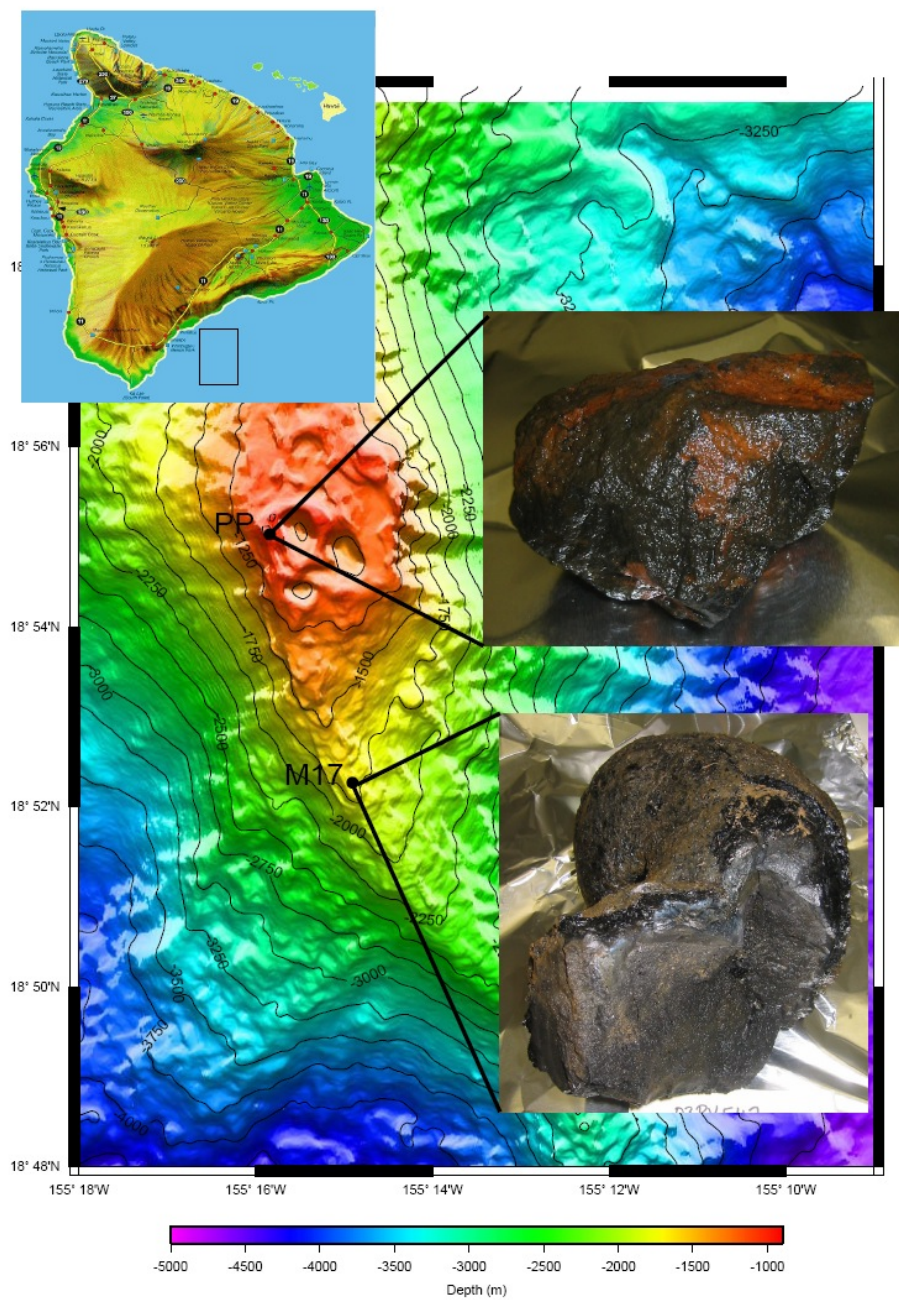
Figure 5.1. Photographs of rock surfaces used in this study. Rock PV549-X2 was taken from Pisces Peak (PP) and rock PV547-X3 was taken from marker #17 (M17). (inset photo of Big Island modified from http://www.liz-randol.com/pdf/map_bigi_lg.gif)

5.2.2 T-RFLP Analysis

DNA was extracted from samples using the QBioGene FASTDNA SPIN kit for Soil (http://www.QBioGene.com , Catalog #6560-200) and purifying/desalting resultant DNA with a microcon centrifugal filter device (http://www.millipore.com, Cat# 42416). The 16S rRNA gene was amplified via polymerase chain reaction (PCR) using universal PCR primers with an annealing temperature of 56°C. The forward primer 68F (5- TNA NAC ATG CAA GTC GRR CG) was fluorescently labeled on the 5' end with 6-FAM (6-carboxyfluorescein); the reverse primer was 1492R (5 -RGY TAC CTT GTT ACG ACT T). PCR amplification products were visualized and assayed for size by 1% gel electrophoresis against a 1-kb ladder DNA standard. Fluorescently labeled PCR products were then digested for 6 to 8 h with various restriction enzymes: AluI, HaeIII, HhaI, MboI, MspI, and RsaI (New England Biolabs, Beverly, Mass.). The array of end-labeled SSU rDNA fragments was separated by polyacrylamide gel electrophoresis against the Genescan-500 ROX size standard with an ABI model 377 automated DNA sequencer, and the data were analyzed with the Genescan software (Applied Biosystems, Foster City, Calif.). Electrophoretic resolution of the TRFLP fragments ranged from 50-500 base pairs (bp) in length. For the application of richness estimators, it was assumed that the detection limit of the TRFLP analysis (i.e. a peak height of ~15 fluorescence units) corresponded to one PCR amplicon; all peaks were then divided by this value to calculate the frequency or abundance of the various OTUs. The use of higher cutoff criteria (i.e. ~50 fluorescence units as used in Danovaro et al., 2006) resulted in exclusion of small peaks/rare abundance and was not further pursued.

5.2.3 16S rRNA Gene Clone Library Construction and in-silico *T-RFLP Analysis*

Procedures for creating 16S rRNA gene clone libraries from the two samples have been presented previously (Santelli et al., 2008). The sequences used in this study (from Santelli et al., 2008) are deposited in GenBank under the accession number EU491020-EU491090 (from Lō`ihi South Rift) and EU491091-EU491336 (from Lō`ihi Pisces peak). The computer program DOTUR (Schloss et al., 2005) was used to calculate species richness estimators from genetic sequence distances using a 97% sequence similarity definition. Using the add-on program tRF-cut (Ricke et al., 2005) for ARB (Ludwig et al., 2004), an *in silico* TRFLP digestion of the nearly-full length 16S rRNA sequences was performed using the restriction enzyme presets in the program for *AluI, HaeIII, HhaI, MboI, MspI,* and *RsaI* assuming that the 68F primer as above was the labeled primer. The predicted fragments were then grouped by base-pair length to generate abundance curves replicating a TRFLP pattern. Fragments of the same size were grouped into one operational taxonomic unit (OTU); the frequency of each OTU was assumed from the number of sequences in each OTU.

5.2.4 Calculation of Diversity Indices

The number and abundance of OTUs calculated in the various datasets were used to evaluate classical non-parametric richness and evenness indices, including the abundance-based coverage (ACE) species richness estimator (Chao and Lee, 1992), the Chao1 species richness estimator (Chao, 1984), the Shannon-Weaver Index of diversity (*H'*; calculated as formulated in Schloss et al., 2005), the Shannon evenness index (*J'*;

calculated as formulated in Schloss et al., 2005), and the Simpson index of diversity (*D*,
calculated as formulated in Schloss et al., 2005).

5.3 Results

Two seafloor basalt samples were the focus of this comparative study, which had
recently been identified as representing relatively high- and low-diversity end members
among a suite of basalt samples from Hawaii (Figure 5.1, Santelli et al., 2008). The
"high diversity" sample originated from the Pisces Peak location on the Lō`ihi Seamount
off the south coast of the big island of Hawai'i (sample PV549X2). The "low diversity"
end member was collected from the South Rift location on the south end of Lō`ihi
(sample PV547X3).

16S rRNA gene clone libraries were constructed in one lab (see Materials and
Methods below) from the two samples. From the clone library data, which contained 246
sequences from the high diversity sample and 71 sequences from the low diversity
sample, the microbial diversity and richness were estimated from sequence alignments
using the program DOTUR (Schloss et al., 2005) at a 97% sequence similarity definition
for species, as described elsewhere (Santelli et al., 2008). To allow comparison of the
clone library data with the measured TRFLP analyses conducted in a separate laboratory
(see below), an *in silico* terminal restriction digestion was performed on the clone library
sequences (Ricke et al., 2005) to generate theoretical fragment patterns that could be
directly compared with the measured TRFLP patterns. Figures 2 and 3 present the
measured and predicted TRFLP patterns from the South Rift and Pisces Peak samples,
respectively.
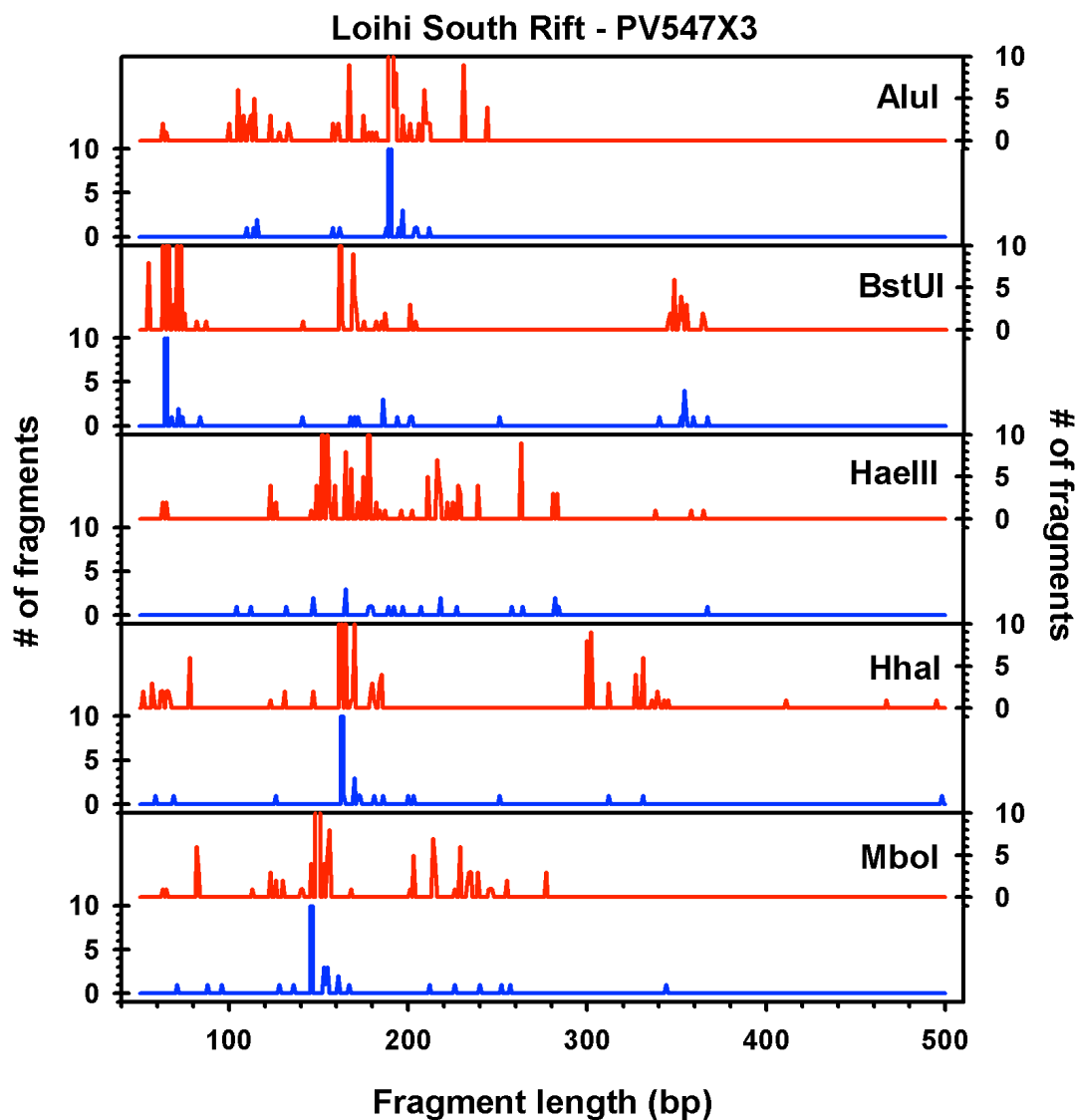
Figure 5.2. Comparison of TRFLP patterns from the South Rift sample. Red lines indicate the measured TRFLP patterns with the respective enzymes and correspond to the axes on the right side of graph; blue lines indicate TRFLP patterns generated from *in silico* digest of nearly full-length 16S rRNA sequences using the tRF-cut program in ARB and correspond to axes on left side of graph. Some peaks are larger than y-scale given, small y-scales given to highlight rare OTUs (shorter peaks).
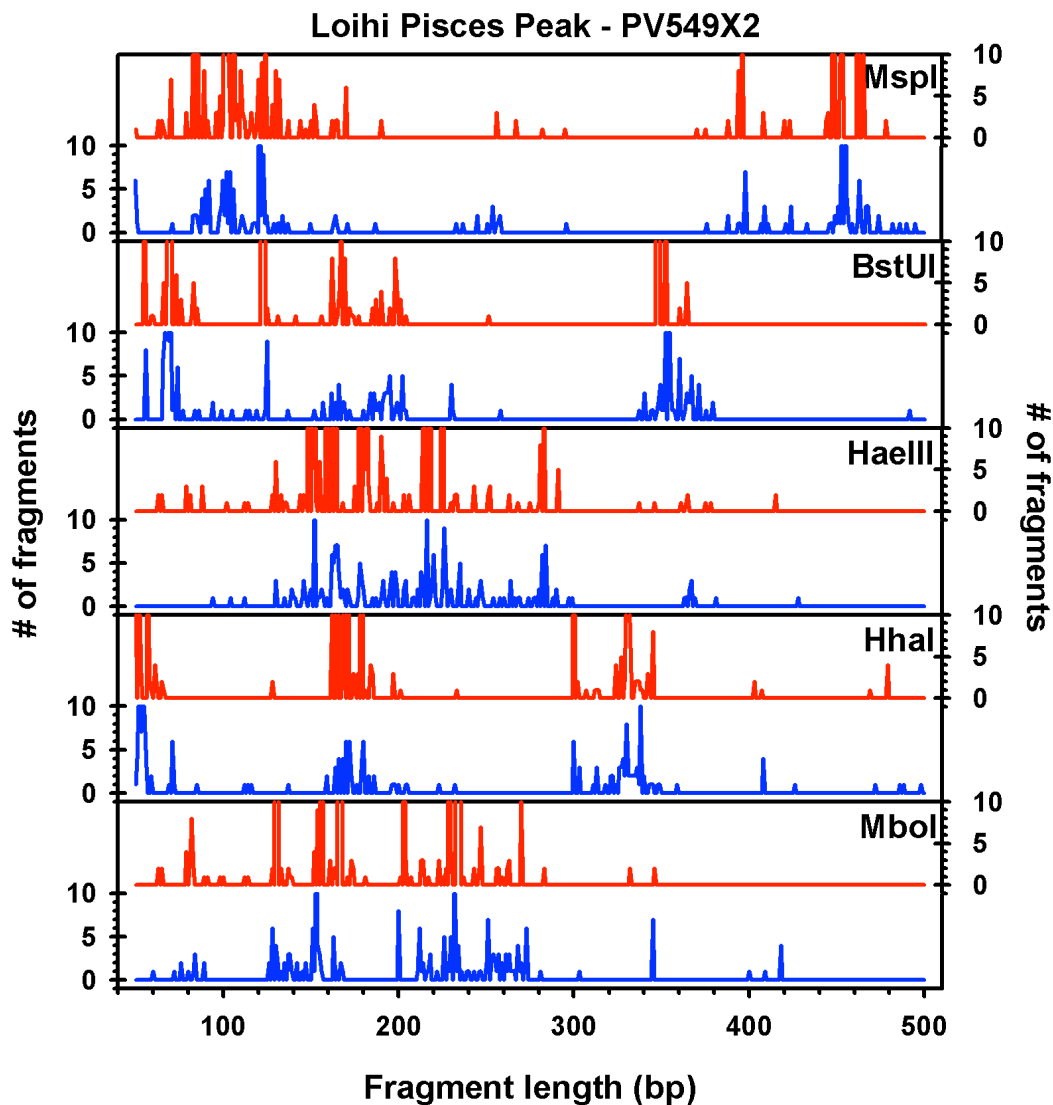
Figure 5.3. Comparison of TRFLP patterns from the Pisces Peak sample. Red lines indicate the measured TRFLP patterns with the respective enzymes and correspond to the axes on the right side of graph; black lines indicate TRFLP patterns generated from *in silico* digest of nearly full-length 16S rRNA sequences using the tRF-cut program in ARB and correspond to axes on left side of graph. Some peaks are larger than y-scale given, small y-scales given to highlight rare OTUs (shorter peaks).

To evaluate how each method predicted microbial community diversity, a suite of classical non-parametric richness and evenness indices were calculated from the observed OTU distribution generated by each of the sampling methods (Table 5.1). As shown previously (Santelli et al., 2008), estimates based on clone library sequence alignments

via DOTUR indicated that the Pisces Peak sample had higher richness with roughly 400 species (from ACE and Chao1) as compared to the South Rift basalt, which was estimated to support approximately 100 species (from ACE and Chao1). Calculation of the Shannon-Weaver index (H') and the Simpson index (D) from the sequence alignments also indicated that the Pisces Peak sample had a higher diversity than the South Rift basalt (respectively, diversity index of 4.77 versus 1.83 for H' and 0.0071 versus 0.38 for D). In addition, the Shannon evenness index (J') indicated that the Pisces Peak sample had a more even microbial population (i.e. index closer to 1) than the South Rift sample.

Table 5.1. Diversity and evenness indices calculated from various methods for the two seafloor basalt samples considered in this study.

Notes:

a: ACE, predicted species richness using Abundance-based Coverage Estimator, calculated using formulation from Chao et al. (1992)

b: Chao, predicted species richness using Chao1 estimator, calculated using formulation from Chao et al. (1992)

c: Shannon H', Shannon Weaver Index of diversity, higher numbers indicate higher diversity, calculated using formulation from Schloss et al. (2005)

d: Shannon J', Shannon evenness, values can range from 0 to 1, with 1 representing perfect evenness, calculated using formulation from Schloss et al. (2005)

e: Simpson, Simpson Index of diversity, values can range from 0 to 1 with higher values indicating a skewed population with dominant members, calculated using formulation from Schloss et al. (2005)

f: S_{obs}, observed OTUs

g: number of OTUs with only one member

h: number of OTUs with only two members

i: DOTUR, based on neighbor-joining alignment at 97% sequence similarity of nearly full length 16S rRNA sequences in ARB following application of a filter for bacteria for the positions 1218-42590 and the Jukes Cantor correction.

j: *is*TRFLP$_{<500}$: estimated using the TRFLP fragments less than 500 bp long generated from the *in silico* digest of the sequences recovered from 16S rRNA clone library; average of 5 digests with different restriction enzymes ± standard deviation of the average

k: *is*TRFLP$_{all}$: estimated using all of the TRFLP fragments generated from the *in silico* digest of the sequences recovered from 16S rRNA clone library; average of 5 digests with different restriction enzymes ± standard deviation of the average

l: TRFLP: estimated from the actual TRFLP fragments; average of 5 digests with different restriction enzymes ± standard deviation of the average

Sample	measure	ACE[a]	Chao[b]	Shannon H'[c]	Shannon J'[d]	Simpson[e]	S_{obs}[f]	n_1[g]	n_2[h]
Pisces Peak	DOTUR[i]	404	416	4.77	0.95	0.0071	148	104	19
	*is*TRFLP$_{<500}$[j]	141±22	189±21	4.03±0.2	0.91±0.02	0.022±0.008	84±9	42±7	15±3
	*is*TRFLP$_{all}$[k]	169±26	168±25	4.16±0.2	0.91±0.02	0.020±0.08	96±11	50±8	17±4
	TRFLP_50fu[l]	**25±2**	**23±2**	**2.55±0.2**	**0.84±0.04**	**0.10±0.03**	**21±3**	**4±1**	**4±4**
	TRFLP_15fu[l]	**76±14**	**69±10**	**3.08±0.2**	**0.76±0.04**	**0.08±0.02**	**59±10**	**17±4**	**15±6**
South Rift	DOTUR[i]	110	87.3	1.83	0.58	0.38	24	20	2
	*is*TRFLP$_{<500}$[j]	100±74	92±51	1.93±0.5	0.66±0.15	0.31±0.15	19±3	15±3	1±1
	*is*TRFLP$_{all}$[k]	86±19	91±31	1.92±0.2	0.62±0.05	0.32±0.08	22±2	17±2	2±1
	TRFLP_50fu[l]	**13±4**	**13±4**	**1.81±0.4**	**0.75±0.13**	**0.26±0.15**	**11±2**	**4±2**	**4±1**
	TRFLP_15fu[l]	**47±8**	**43±7**	**2.50±0.5**	**0.70±0.13**	**0.17±0.11**	**35±4**	**11±3**	**9±2**

When calculating species richness from the predicted *in silico* TRFLP OTU distributions (*is*TRFLP, Table 5.1), the ACE and Chao1 estimates were similar to the DOTUR-derived value for the low diversity sample from South Rift, but the predicted species richness for the high diversity sample from Pisces Peak was significantly lower, with a predicted richness of roughly 170 species as compared to ~400. Additionally, the Shannon *H'* and Simpson richness indices estimated lower richness from the *in silico* TRFLP OTU distributions for the Pisces Peak sample, but similar values were calculated for the South Rift sample by both methods. Notably, the calculation of species evenness (*J'*) was similar by either method for both samples.

The prediction of species richness from the ACE and Chao1 estimators from the measured TRFLP analysis was significantly lower than from the other methods for both samples, with a predicted ~70 species in the Pisces Peak basalt and ~45 species in the South Rift basalt (Table 5.1). The Shannon and Simpson richness indices also estimated significantly lower diversity for the Pisces Peak sample from the measured TRFLP patterns than from the other methods; however, the species evenness prediction (*J'*) was similar but slightly lower. In contrast, for the lower diversity South Rift sample, the Shannon and Simpson richness indices estimated from the measured TRFLP data predicted a slightly more diverse community than estimated using the other gene based and *is*TRFLP methods. Although the OTU sample sizes (S_{obs}, Table 5.1) for the low diversity sample are relatively small, they are still expected to be significant enough that the ACE and Chao1 richness estimators are not biased by sample size (i.e. S_{obs} is greater than the square root of twice the estimate of richness; Colwell and Coddington, 1994).

When doing a peak-by-peak correlation between the measured TRFLP fragment peaks and those predicted from the *in silico* digestion of the clone library sequences (Figures 5.2 and 5.3, Table 5.2), 37 and 72 % of the peaks from the measured TRFLP patterns can be correlated perfectly or within 1-2 bp to peaks predicted from the *in silico* digestion for the South Rift and Pisces Peak samples, respectively. The viability of correlating peaks offset by 1-2 bp is validated by the variation between true and observed fragments based on the relative composition of the DNA sequences (Kaplan and Kitts, 2003). When weighted by frequency of appearance of a particular fragment, this corresponds to 67 and 92 %, respectively, of PCR amplicons from the measured TRFLP analysis being matched by fragments in the *in silico* TRFLP analysis. While the dominant species were recovered in both analyses, a larger proportion of rare species was recovered in the clone library data. Roughly one third to one half of the TRFLP peaks predicted from the *in silico* digestion are not matched in the measured TRFLP analysis.

Table 5.2. Peak-to-peak correlation between measured TRFLP patterns and predicted TRFLP patterns from an *in silico* digestion of 16S rRNA clone library data.

	50fu South Rift %	15fu South Rift %	50fu Pisces Peak %	15fu Pisces Peak %
TRFLP peaks perfect match	8±10	12±4	56±11	42±4
TRFLP peaks off by 1-2bp	37±29	25±13	32±12	30±4
TRFLP peaks not matched	55±20	63±12	12±7	28±3
TRFLP "species" identified	75±9	67±11	93±3	92±3
in silico peaks perfect match	6±8	24±13	15±4	29±4
in silico peaks off by 1-2bp	20±15	45±15	8±3	21±4
in silico peaks not matched	74±7	30±7	77±3	50±6

5.4 Discussion

Seafloor basalts harbor some of the most diverse microbial communities on Earth (Santelli et al., 2008). Previous analysis indicates that the two samples used in this study represent both relatively low (Lō`ihi South Rift basalt) and high (Lō`ihi Pisces Peak basalt) diversity end-members (Santelli et al., 2008). A major goal of the present study was to evaluate how similarly two different DNA-based methods (i.e. TRFLP and 16S rRNA gene clone libraries) in two independent labs would estimate the microbial diversity of these basalt samples. The comparison of richness estimators calculated from the two datasets reveals that TRFLP analysis significantly underestimated the richness of the relatively high-diversity seafloor basalt microbial community (Table 5.1). Depending

on the richness estimator considered, richness predicted by TRFLP analysis for the low-diversity sample was roughly the same (using Shannon and Simpson indices) or lower (ACE and Chao1 estimators) than the richness predicted by sequence similarity. Although the richness estimates were different between the two methodologies, the predictions of community evenness were similar. It should be emphasized that the diversity indices calculated based on 16S rRNA gene clone similarity used a definition of 97 % similar sequence for determining the number of species. If a higher threshold had been used (i.e. 99% sequence similarity), the number of species predicted from the clone library data would have been even greater. The 97 % cut-off is a commonly recognized level for comparative analysis in environmental microbial communities. Nonetheless, it is likely that at least 50% of species from the Pisces Peak samples are missed by TRFLP (Table 5.2), as rarefaction analysis of the sequence similarity data for this sample (from Santelli et al., 2008), which is a measure of the number of species observed per sampling effort, indicates that more sampling would be needed to measure the full diversity of the sample.

There are at least two reasons why the richness estimated by TRFLP is lower than that estimated from clone library sequence alignment, as suggested previously for simulated comparisons of TRFLP and clone sequences (Engebretson and Moyer, 2003; Blackwood et al., 2007). The first explanation is that TRFLP misses the majority of rare species, likely due to detection limits for resolving unique sequence variants, for example, if the 16S rRNA gene from a rare species did not generate enough fluorescently-labeled PCR amplicons for the TRFLP analysis to detect. Table 5.1 lists the number of species that were observed only once (n_1) or twice (n_2) in the various

methods. For instance, in the clone libraries, 104 and 20 different species were observed only once in the Pisces Peak and South Rift samples, respectively, whereas only 17 and 11 species, respectively, were observed only once in the measured TRFLP analysis from both samples. This trend is also evident in Figures 2 and 3, where more small peaks appear in the *in silico* TRFLP patterns than in the measured TRFLP patterns.

The second explanation for the lower estimations of richness from TRFLP as compared to the clone library data is the occurrence of binning in TRFLP, where two different species are counted as one in TRFLP OTU because they generate the same size fragment. This can be shown empirically in the *in silico* TRFLP analysis of the clone library data. For example, the peak seen in the *in silico BstUI* digestion of the Pisces Peak sample at a fragment size of 70 bp (Figure 5.3) contains predicted fragments derived from a diverse range of species from the phyla *Bacteriodetes*, *Firmicutes*, and *Planctomycetes* as well as the Alpha-, Delta-, and Gamma- divisions of the phyla *Proteobacteria* (data not shown). *BstUI* digestion generates 70 bp fragments from fourteen different species as defined by gene sequence similarity, which in the predicted TRFLP analysis would be binned as one peak, or species. In the high-diversity sample from Pisces Peak, the degree of binning is evident in the difference between the richness estimators calculated from the sequence alignment and the *in silico* digestions (Table 5.1). For instance, the *in silico*-based calculations predict nearly two-thirds less richness when estimated by the ACE and Chao1 estimators. For comparison, in randomly simulated microbial communities with richness levels of 100 species, the restriction enzymes considered in this study would correctly assign 60 % or less of the expected OTUs (Engebretson and Moyer, 2003). Both of the above trends of binning and

exclusion of rare taxa are also evident in a comparison of diversity indices calculated by TRFLP and restriction digestion of 16S rRNA gene clones in soils (Dunbar et al., 1999, 2000).

Although there are differences between the two methodological approaches to examining diversity of seafloor basalts, it is notable that both methods retrieved similar dominant species from the samples, and that they predicted similar levels of relative diversity between the two samples. For instance, as shown in Figure 5.2, the major species that dominated the low-diversity South Rift sample was retrieved by both methods, regardless of the enzyme considered for TRFLP. Similarly, the measured and *in silico* TRFLP patterns from the Pisces Peak sample are qualitatively similar, with dominant peaks often matching between the two methods (Figure 5.3). Although predicting a much lower richness level, the calculation of richness from the measured TRFLP analyses also indicates that the Pisces Peak basalt microbial community is more diverse than the South Rift basalt community (Table 5.1). Importantly, these results suggest that there was minimal apparent DNA-extraction or PCR-related bias between the two laboratories. This is rarely evaluated in molecular diversity studies and is often a considerable uncertainty in making cross-comparisons between studies.

Results of these studies indicate that TRFLP could be useful for relative comparisons of diversity between samples, for identifying dominant species, and for estimating the richness and evenness of low-diversity, skewed populations of seafloor basalt microbial communities. This observation supports the claim by Engebretson and Moyer (2003) that TRFLP is a robust technique for identifying dominant populations and for calculating diversity statistics in low diversity communities. Furthermore, these

findings verify that TRFLP will miss the majority of low abundance taxa in highly-diverse communities.

5.5 Acknowledgments

Chapter 5, in full, is a formatted version of the published work: Orcutt B., Bailey B.E., Staudigel H., Tebo B., Edwards KJ. (2009) An interlaboratory comparison of 16S rRNA gene-based terminal restriction fragment length polymorphism and sequencing methods for assessing microbial diversity of seafloor basalts. Environmental Microbiology, 11(7), 1728-1735. DOI: 10.1111/j.1462-2920.2009.01899.x. The dissertation author was the second author of this paper and completed work for this paper including sample collection and processing, t-RFLP on genomic DNA, and power spectrum density calculations for statistical analysis.

5.6 References

Bent, S.J., J.D. Pierson, L.J. Forney. (2007) Measuring species richness based on microbial community fingerprints: the Emperor has no clothes. Appl. Environ. Microbiol. **73**: 2399-2401

Biddle J. F., Lipp J. S., Lever M., Lloyd K. G., Sørensen K. B., Anderson K., Fredricks H. F., Elvert M., Kelly T. J., Schrag D. P., Sogin M. L., Brenchley J. E., Teske A., House C. H., and Hinrichs K.-U. (2006) Heterotrophic Archaea dominate sedimentary subsurface ecosystems off Peru. *Proceedings of the National Academy of Science U.S.A.* **103**(10), 3846-3851.

Blackwood, C.B., T. Marsh, S.H. Kim, E. A. Paul. (2003) Terminal restriction fragment length polymorphism data analysis for quantitative comprison of microbial communities. Appl. Environ. Microbiol. **69**: 926-932.

Chao, A. (1984) Non-parametric estimation of the number of classes in a population. Scand. J. Stat. **11**: 265-270.

Chao, A., and S.M. Lee (1992) Estimating the number of classes via sample coverage. J. Am. Stat. Assoc. **87**: 210-217

Colwell, R.K., and J.A. Coddington (1994) Estimating terrestrial biodiversity through extrapolation. Phil. Trans. R. Soc. London B **345**: 101-118.

Danovaro, R., G.M. Luna, A. Dell'Anno, B. Pietrangeli. (2006) Comparison of two fingerprinting techniques, terminal restriction fragment length polymorphism and automated ribosomal intergenic space analysis, for determination of bacterial diversity in aquatic environments. Appl. Environ. Microbiol. **72**: 5982-5989.

Dunbar, J., L.O. Ticknor, C.R. Kuske. (2000) Assessment of microbial diversity in four southwestern United States soils by 16S rRNA gene terminal restriction fragment analysis. Appl. Environ. Microbiol. **68**: 2943-2950

Engebretson, J.L., C. L. Moyer. (2003) Fidelity of select restriction endonucleases in determining microbial diversity by terminal-restriction fragment length polymorphism. Appl. Environ. Microbiol. **68**: 4823-4829.

Hughes, J.B., Hellmann, J.J., Ricketts, T.H., Bohannan, B.J.M. (2001) Counting the uncountable: Statistical approaches to estimating microbial diversity. Appl. Environ. Microbiol. **67**: 4399-4406

Hughes Martiny, J.B., B.J.M. Bohannan, J.H. Brown, R.K. Colwell, J.A. Fuhrman, J.L. Green, M.C. Horner-Devine, M. Kane, J.A. Krumins, C.R. Ruske, P.J. Morin, S. Naeem, L. Øvreas, A.L. Reysenbach, V.H. Smith, and J.T. Staley. (2006) Microbial

biogeography: putting microorganisms on the map. *Nature Reviews Microbiology* 4: 102-112.

Inagaki F., Nunoura T., Nakagawa T., Teske A., Lever M., Lauer A., Suzuki M., Takai K., Delwiche M. E., Colwell F. S., Nealson K. H., Horikoshi K., D'Hondt S., and Jørgensen B. B. (2006) Biogeographical distribution and diversity of microbes in methane hydrate-bearing deep marine sediments on the Pacific Ocean Margin. *Proceedings of the National Academy of Science U.S.A.* **103**(8), 2815-2820

Kaplan, C.W., and C.L. Kitts. (2003) Variation between observed and true terminal restriction fragment length is dependent on true TRF length and purine content. J. Microbiol. Methods **54**: 121-125.

Lipp J. S., Morono Y., Inagaki F., and Hinrichs K.-U. (2008). Prokaryotic biomass in the deep marine subsurface. Nature *In press*.

Liu, W.T., T.L. Marsh, H. Cheng, L.J. Forney. (1997) Characterization of microbial diversity by determining terminal restriction fragment length polymorphisms of genes encoding 16S rRNA. Appl. Environ. Microbiol. **63**: 4516-4522.

Ludwig W., Strunk O., Westram R., Richter L., Meier H., Yadhukumar, Buchner A., Lai T., Steppi S., Jobb G., Förster W., Brettske I., Gerber S., Ginhart A., Gross O., Grumann S., Hermann S., Jost R., König A., Liss T., Lüssmann R., May M., Nonhoff B., Reichel B., Strehlow R., Stamatakis A., Stuckmann N., Vilbig A., Lenke M., Ludwig T., Bode A., and Schleifer K.-H. (2004) ARB: a software environment for sequence data. *Nucleic Acids Research* **32**, 1363-1371.

Ricke, P., S. Kolb, G. Braker. (2005) Application of a newly developed ARB software-integrated tool for in silico terminal restriction fragment length polymorphism analysis reveals the dominance of a novel pmoA cluster in forest soil. Appl. Environ. Microbiol. **61**: 1671-1673

Santelli, C., B. Orcutt, E. Banning, C. Moyer, W. Bach, H. Staudigel, K. Edwards. (2008) Abundance and diversity of microbial life in the ocean crust. Nature 453: 653-656.

Schippers A. and Neretin L. N. (2006) Quantification of microbial communities in near-surface and deeply buried marine sediments on the Peru continental margin using real-time PCR. *Environmental Microbiology* **8**(7), 1251-1260

Schloss. P., and J. Handelsman. (2005) Introducing DOTUR: a computer program for defining operational taxonomic units and estimating species richness. Appl. Environ. Microbiol. **71**: 1501-1506

Sogin, M.L., H.G. Morrison, J.A. Huber, D.M. Welch, S.M. Huse, P.R. Neal, J.M. Arrieta, G.J. Herndl. (2006) Microbial diversity in the deep sea and the underexplored "rare biosphere." Proc. Nat. Acad. Sci. USA **103**: 12115-12120

Sørensen K. B. and Teske A. (2006) Stratified communities of active archaea in deep marine subsurface sediments. *Applied and Environmental Microbiology* **72**(7), 4596-4603

Chapter 6

A First-Order Assessment of Microbial Diversity at Loihi Seamount using Terminal Restriction Fragment Length Polmorphism

Brad Bailey[a,b] *, Craig M. Moyer[c], Alexis Templeton[d], Hubert Staudigel[a], and Bradley M. Tebo[e,f]

[a]Institute of Geophysics and Planetary Physics, Scripps Institution of Oceanography, University of California, San Diego, CA 92093
[b]NASA Solar System Exploration Research Virtual Institute, NASA Ames Research Center, Moffett Field, CA 94035
[c]Biology Department, Western Washington University, Bellingham, WA 98225
[d]Department of Geological Sciences, University of Colorado, Boulder, CO 80309
[e]Marine Biological Research Division, Scripps Institution of Oceanography, University of California, San Diego, CA 92093
[f]Division of Environmental and Biomolecular Systems, Oregon Health & Science University, Beaverton, OR 97006
    *. Corresponding Author Address: brad.bailey@nasa.gov

Abstract

Through the combination of T-RFLP data, clone libraries and isolate data, this study looks at chemosynthetic microbial diversity as functions of spatial and temporal variability across Loihi Seamount and an historic 1877 Mauna Loa submarine eruption. Using T-RFLP and clone libraries from Santelli et al. (2008), we compared bacterial diversity of iron-oxide encrusted microbial mats with samples from the surfaces of native rock samples and a laboratory - remelted natural basaltic glass. Temporal comparisons of the diversity can also be inferred from in situ exposure periods of ~1 week to >125 years. These results indicate that basaltic bacterial communities display low diversity in hydrothermally influenced basalts (Shannon H' index of 1.92) and a high diversity in an open ocean circulation environment (Shannon H' index of 4.16). Basaltic substrates also

appear to select for specific bacterial communities as they exhibit low diversity compared to microbial mats in the immediate area. Additionally, samples with a low exposure time in hydrothermal systems resulted in a low diversity and T-RFLP analyses coupled to isolate data (Templeton et al., 2005; 2009) indicate that metal-oxidizing bacteria may dominate initial active colonization on fresh basalt surfaces.

6.1 Introduction

Over the past two decades the concept of a deep oceanic biosphere has become a target for exploring paradigm-shifting theories that have altered the way we view the biogeochemical world around us. Originally considered lifeless, the oceanic crust now reveals itself as a biome of substantial size and potential impact on the biosphere and associated chemical cycles. Key evidence for the presence of this deep oceanic biosphere comes from microbiological observations from drill holes (Cowen et al. 2003) as well as geologic constraints based on microbial trace fossils suggesting that the deep oceanic biosphere extends at least to a depth of 500m (Furnes and Staudigel, 1999). Biotically-controlled basalt alteration may have a significant effect on Fe, Mn, S and C biogeochemical cycling (Staudigel et al., 2004) and Bach and Edwards (2003) hypothesize that up to ~5 x10^{11} g C/year can be fixed through biomass production associated with iron and sulfur oxidation in the upper ocean crust, which may represent a major contribution to the overall carbon cycle within the oceans. While these findings are likely to be quite consequential, very little is known about the microbial consortia present, their function and impact and how they relate to the formation of trace fossils in the oceanic crust.

The exploration of the deep volcanic oceanic biosphere has come to a very promising start. Many investigators began exploring seafloor microbial communities at mid-ocean ridges (Thorseth et al., 1995; Mason et al., 2008; Santelli et al., 2008; Santelli et al., 2009), backarc volcanic systems (Davis and Moyer, 2008; Huber et al., 2010), and at seamounts (Moyer et al., 1995; Emerson and Moyer 2002; Templeton et al., 2005; Sudek et al 2009). Initial results (Santelli et al., 2008; Mason et al., 2009) reveal that these ecosystems have diverse bacterial communities with a broad spectrum of possible metabolisms present. Culturing efforts are offering a first glimpse at the metabolic capabilities of these microbes focusing on (Fe(II)) and manganese (Mn(II)) oxidation (Edwards et al., 2003; Templeton et al., 2005; Sudek et al., 2009), and the production of siderophores (Sudek et al., 2009), all of which reveal microbial capabilities to utilize volcano-derived sources of energy and nutrients. Edwards et al. (2003) report on several obligate chemolithoautotrophs isolated from weathered rock surfaces and sediments which showed the greatest growth rate and cell densities using basaltic glass as their sole energy source (Fe(II)). Templeton et al. (2009) demonstrated that microbes colonizing glass surfaces likely utilize Mn(II) from hydrothermal fluids as well as from in-situ basalt alteration.

Even with all of the recent work on epilithic and endolithic bacteria on basalts in the ocean basins, several fundamental questions remain. What environmental controls affect bacterial diversity? Which microbes are responsible for basalt dissolution and alteration? How does spatial resolution of microbial diversity differ based on local environment? We begin exploring these questions by utilizing terminal restriction fragment length polymorphism (T-RFLP) and clone libraries of microbial biomass

colonizing basalt surfaces as well as hydrothermal mats. We focused our study on the submarine flanks of Hawaii, using exposures at Loihi seamount and the submarine extension of Mauna Loa volcano with a well-studied series of eruptions in 1877 with vents down at least to about 1000m water depth. All of the sites studied were explored by submersible (and ROV) over many years, with numerous visits allowing for multi-year exposure experiments and the correlation of our results with other coordinated investigations on the same sites and samples. While our study only represents one step along a long path towards understanding microbes and microbe-rock interaction in these environments, we do offer some new insights into the community structure of the main types of materials in such chemosynthetic oligotrophic volcanically hosted ecosystems and how these communities may develop through time.

6.2 Sample Sites

We have chosen two main types of sample sites: an offshore cold water pillow lava with no active hydrothermal input and an iron-dominated hydrothermally active seamount with basalts from the summit, crater rim and a deep rift zone. Loihi is a volcanically-active seamount that hosts several hydrothermal environments dominated by iron-oxide encrusted microbial mats. Loihi is part of the Loa Trend off the SE flank of the big island of Hawaii (described by Garcia et al., 2006), rises from the ~5100m seafloor to a depth of ~956m and is largely composed of pillow basalts and/or talus breccia. The peak of Loihi is characterized by three pit craters with varying degrees of hydrothermal activity (Figure 6.1). Samples for this study's hydrothermal sites were taken from a deep site along the south rift of Loihi (M17) as well as the western rim

(M18) of the southwestern summit pit crater, also known as Pele's Pit (Figure 6.1). All hydrothermal sites are characterized by diffuse hydrothermal vent fields with cold (~1.7-3.5°C), low-flow shimmering water welling up from among the talus. Iron-oxide encrusted microbial mats largely exist as flocculent mats congregated within localized depressions between the talus or pillow lavas. An additional hydrothermal vent microbial mat was used from the base of the Tower Vents (M48). Scanning electron microscopy (SEM) analysis of these mats show long filamentous iron oxide-dominated sheaths coupled to amorphous oxide agglomerations. SEM also reveals twisted stalk and helical structures. These sites contain breccia and pillow basalts that are all stained red with predominantly hydrogenous oxidized iron coatings (Templeton et al., 2009). An additional sample was taken at Pisces Peak (PP), the highest point on Loihi at 956m depth. PP consists of mounds of brecciated talus with characteristic red staining without any apparent hydrothermal activity. Glassy basalts were also collected from the submarine 1877 lava flow in Kealakekua Bay (KKB) (described by Wanless et al., 2006) on the western flank of Mauna Loa (M1, 1033m) (Figure 6.2). This site largely consists of pillow basalt flows and represents a basaltic surface and associated bacterial community with an exposure age of ~125 years and no hydrothermal input. All Loihi basalt and mat samples from this study are listed in Table 1.
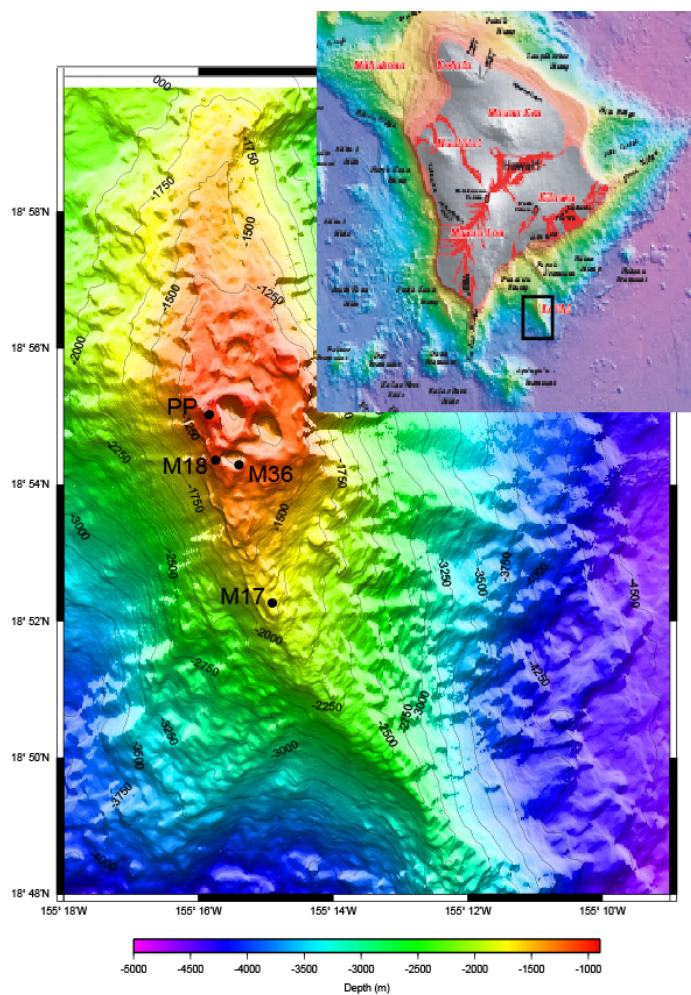
Figure 6.1. Map of Loihi with sample sites. Map .grd data compliments of John R. Smith from SOEST. Insert map modified from Eakins et al.
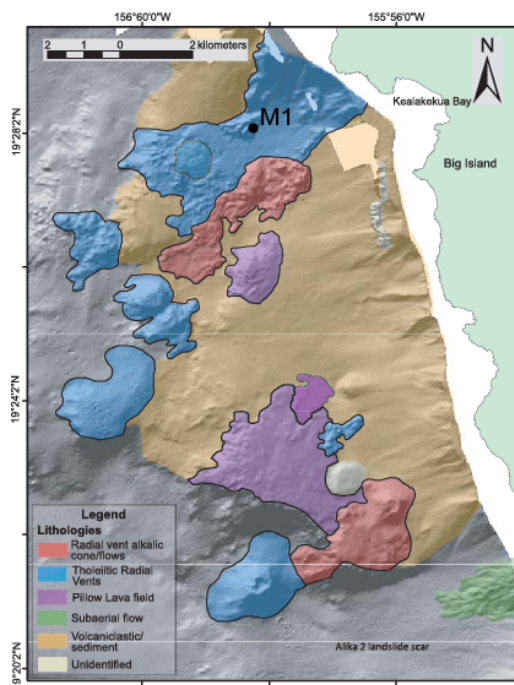
Figure 6.2. Map of 1877 Kealakekua Bay submarine lava flows and sample site. Map modified from Wanless et al. (2006).

Table 6.1. Sample name, type, location, and community diversity

Sample	Sample Type	Sample Site	Site Description	Location	Latitude/Longitude	Depth (m)	Ambient T	**Average Bacterial T-RFs
JV-1*	Culture	Multiple Sites	Iron Oxide Mats	Loihi				1.2 ± 0.5
552X2	Glassy Basalt	M1	Pillow basalts, no venting	Kealakekua Bay	N19°28.020'/W155°58.115'	1033	3.7°C	17.50 ± 3.6
549X2/X3	Glassy Basalt	PP	Breccia, no venting	Loihi – Summit	N18°55.030'/W155°15.886'	956	3.4°C	11.25 ± 2.8
547X3	Glassy Basalt	M17	Pillow basalts, diffuse venting	Loihi - South Rift	N18°52.287'/W155°14.876'	1714	1.7°C	2.25 ± 1.7
SIO10NB	Basaltic Glass Powder							6.0 ± 2.7
548R1	Iron Oxide Mat	M18	Breccia, diffuse venting	Loihi – Western rim	N18°54.420'/W155°15.680'	1104	3.2°C	8.1 ± 3.8
548R3	Iron Oxide Mat	M18	Breccia, diffuse venting	Loihi – Western rim	N18°54.420'/W155°15.680'	1104	3.2°C	9.5 ± 3.3
546R3	Iron Oxide Mat	M48	Thick mats, strong venting	Loihi – Western rim	N18°54.420'/W155°15.680'	1104	3.2°C	
547R1	Iron Oxide Mat	M17	Pillow basalts, diffuse venting	Loihi – South Rift	N18°52.287'/W155°14.876'	1714	1.7°C	14.25 ± 4.7
547R3	Iron Oxide Mat	Uprift M17	Pillow basalts, diffuse venting	Loihi – South Rift	N18°52.287'/W155°14.876'	1714	1.7°C	14.50 ± 3.8

* - Pure culture of JV-1/*Mariprofundus ferrooxidans*. Isolated from and found in several Loihi iron-oxide dominated microbial mats.

** - Average Bacterial T-RFs is a measure of community diversity by determination of numbers of OTUs per restriction enzyme in T-RFLP fingerprints.
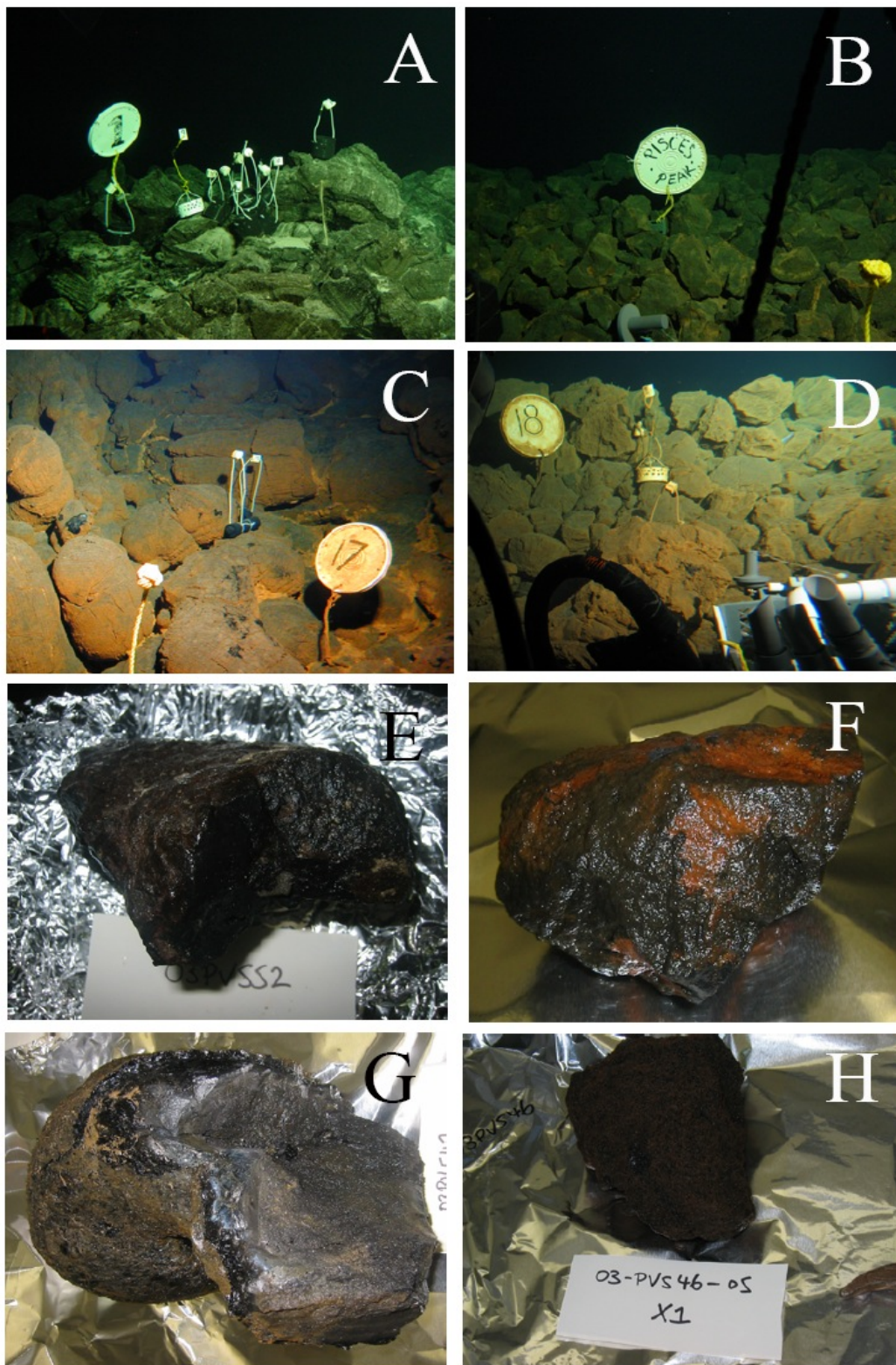
Figure 6.3. Sample site photos of A) Kealakekua Bay: M1, B) Pisces Peak on Loihi: PP, C) Loihi South Rift: M17, D) west crater rim of Pele's Pit on Loihi: M18, and basalt sample photos E) 552X2, F) 549X3, G) 547X3, and H) 546X1.

6.3 Materials and Methods

6.3.1 Sample Collection

All samples were collected by the Pisces IV/V submersibles operated by the Hawaii Undersea Research Laboratory (HURL) on board the R/V Ka'imikai O'Kanaloa (KOK). Rock samples were transported to the surface and protected from shallow seawater contamination via a sealed biobox. Microbial mats were collected via suction sampling and/or sterile PVC tubes sealed with a ball valve. All samples were immediately aseptically split into aliquots and placed in filtered seafloor seawater for culturing, frozen at -80°C for DNA extraction, and preserved via glyceraldehyde/paraformaldehyde for FISH and SEM analyses.

6.3.2 DNA Extraction

DNA was extracted from rock surfaces and microbial mat samples following the procedure developed in Chapter 2 of this dissertation. 2 ml screw cap tubes with O-rings were prepared by filling with 200mg each of acid washed 0.1, 0.5, 2.0 mm zirconium glass beads and then autoclaved. 300 mg of sample was then added to each tube. We then added 580 μl lysis solution (300mM EDTA, 300 mM NaCl, 300 mM Tris buffer, pH 7.5) to the tubes along with 70 μl 15% Sodium Dodecyl Sulfate (SDS), 15ul of Polyadenylic Acid (PolyA, 10mg/ml, Roche Diagnostics Cat. #108626) and 35 μl Dithiothreitol (DTT) (1M DTT in 0.01 M Acetate, Acros Organics Cat. #327190100). The tubes were then homogenized using a Vortexer and incubated at 70°C for 30 mins. After cooling to < 40°C, 14 μl lysozyme (5%) was added. The tubes were again vortexed

and incubated at 37°C for 20 mins. Cells in these tubes were then lysed in the FastPrep FP120A instrument (BioGene, Cat# 6001-120) in two beating cycles at a speed setting of 5.5 for 30 secs and cooled on on ice for 2-4 mins between treatments. We then added 150 µl KCl (1M), vortexed and place on ice for 5 mins. The samples were centrifuged for 5 mins at 14,000 g. Up to 400 µl of clear supernatant was transferred to a Microcon Centrifugal Filter Device (http://www.millipore.com, Cat# 42416) and centrifuged at 1000 g for 15 mins and the filtrate was discarded. We repeated the process until all supernatant has been through the filter. On the last run, we added enough TE buffer (10mM Tris pH 7.5, 1mM EDTA) to have a total volume of 400 µl. To rinse the DNA, we added 400 µl TE buffer to the filter unit and centrifuged at 1000 g for 15 mins and discard filtrate. Invert filter into a clean tube and add 100 µl TE buffer to the filter, centrifuge for 15 mins and discard filter. The DNA was stored at -20°C for later use. DNA yields were quantified via the Picogreen Assay (Invitrogen, Carlsbad, CA, USA, SKU# P11495) and a Perkin Elmer/Tecon HTS 7000 Bio Assay Plate Reader.

6.3.3 Terminal-Restriction Fragment Length Polymorphism (T-RFLP)

The 16S rRNA gene was amplified via polymerase chain reaction (PCR) using universal PCR primers 68F and 1492R. The forward primer 68F was fluorescently labeled on the 5' end with 6-FAM (6-carboxyfluorescein); the reverse primer was 1492R (5'-RGY TAC CTT GTT ACG ACT T). PCR amplification products were visualized and tested for size and purity by 1% gel electrophoresis against a 1-kb ladder DNA standard.

The methodology for producing t-RFLP patterns has been previously described in Emerson and Moyer (2002). The fluorescently labeled primers were digested in a suite

of 8 restriction enzymes (Alu1, BstU1, HaeIII, Hha1, Hinf1, Mbo1, Msp1 and Rsa1 – New England Biolabs, Beverly, MA) overnight and resultant products were cleaned using Sephadex G-50 Gel Filtration (Sigma-Aldrich, Cat# 27.114-4) resin. Cleaned end-labeled fragments were then read out on an ABI PRISM 3100 Genetic Analyzer (Applied Biosystems, Foster City, CA) against the Genescan-500 ROX size standard using a 50cm polyacrylamide electrophoresis capillary. T-RFLP analyses were performed on extracted DNA following procedures outlined by Davis and Moyer (2009) where only fragments between 50-500 were analyzed and the community fingerprints were compared using a Pearson product-moment correlation via BioNumerics (Applied Maths, Sint-Martens-Latem, Belgium). Diversity from T-RFLP fingerprints were calculated after Engebretson and Moyer (2003) by determining averaged detected OTUs (>3% of maximum peak in each pattern) across all 8 restriction enzymes.

6.3.4 Clone Libraries and in-silico T-RF Generation

Cloned DNA sequences from two of these samples have been previously published in Santelli et al. (2008) and are listed in GenBank under accession numbers EU491020-EU491090 (M17 – 547X3) and EU491091-EU491336 (PP – 549X3). An *in-silico* digest of the clone sequences using the TRF-CUT add-on (Ricke et al., 2005) to the ARB phylogenetic analysis tool (see Ludwig et al., 2004 for a review of ARB) was performed using seven restriction enzyme cut sites (Appendix 1) relative to the 49-68F primer site (5- TNA NAC ATG CAA GTC GRR CG) (Orcutt et al. 2009).

6.4 Results

Microbial diversity on four different basaltic glasses along with an iron-dominated microbial mat were compared using T-RFLP to determine diversity and identify major species within the community. Two samples were chosen to coincide with clone library data, reported previously by Santelli et al. (2008), which allows us to phylogenetically identify major terminal restriction fragment (T-RF) peaks in the corresponding samples. The two basalt samples for which clone libraries were completed represent both high and low diversity (Shannon H' indices of 4.16 and 1.92 respectively from Orcutt et al., 2009) within the microbial communities. The low diversity sample from M17, 547X3, shows an unclassified γ-proteobacterium OTU, clone 1_B08 (Accession #: DQ395576) which dominates the clone library (44 out of 71 clones). Approximately 75% of the clones revealed γ-proteobacteria as the dominant class of the microbial community present on the basalt surface, while species richness estimates of this sample were calculated to be ~100 (Santelli et al., 2008; Orcutt et al., 2008). The clone 1_B08 is most closely related (99%) to an uncultured γ-proteobacterium clone from a deep sea coral study on Gulf of Alaska seamounts (Penn et al., 2006), while its closest cultured relative is Mn(II)-oxidizing *Microbulbifer sp.* KBB-1 (accession # DQ412068) which was isolated from Kealakekua Bay basalts (Templeton et al., 2005). The rest of the assigned peaks are predominantly members of the *Proteobacteria* phyla with identification of an oligotrophic Mn-oxidizing *Marinobacter* isolate, LOB-4 (Templeton et al., 2005).

The high diversity basalt sample 549X3 has species richness estimates that predict >400 unique taxa within the given community (Santelli et al., 2008) with a relatively high number of OTUs (11.25 ± 2.8) identified in the T-RFLP pattern. The classifications of the clones/isolates found on this basalt surface (Figure 6.6, Appendix 6.1, Appendix 6.2) are dominated by γ-, δ- and α-proteobacteria. γ-proteobacterium clone 7-D04, whose closest match in BLAST is an uncultured γ-proteobacterium clone Accession #AB015253, is the most abundant member of the community in all t-RFLP patterns from this sample. The a peak at position 56 indicates a *Rhizobiales* clone. The ζ-proteobacterium, *Mariprofundus ferrooxidans* strain PV-1 (Emerson et al., 2007), is present at position 69, clustered with several α– and γ– proteobacterial clones. A majority of the remaining clones are γ-proteobacteria including *Acinetobacter radioresistens* (7_H04), *Marinobacter aqueolei* (7_C07), an oligotrophic Mn-oxidizing *Marinobacter* isolate (LOB-4) (Templeton et al., 2005) and a lithotrophic Fe-oxidizing *Pseudomonas tolassii* (LOB-7).

Figure 6.4 aligns the BstU1 restriction digests from 4 rock surfaces and a corresponding mat sample. Overlapping peaks at position 56 in samples 547X3, 549X3 and 552X2 shows that α-proteobacteria are significant components of the overall community on natural, weathered rock surfaces. However, this peak at position 56 does not occur in either the short-term exposure (SIO10B) nor the mat sample. Additionally, γ-proteobacteria peaks at positions 348 and 352 are present in all samples. Figure 6.5 is a dendogram showing the overall community relationships across several different samples

including two additional Loihi samples from Davis and Moyer (2008) as well as a pure culture of the ζ-proteobacteria originally described by Emerson et al. (2007).

Sample 552X2, collected from the 1877 submarine lava flow, was included in this study to provide a reference basalt to compare against all other basalts associated with Loihi. The 1877 flow represents basalts of known age/weathered surfaces and are unaffected by hydrothermal input from Loihi, resulting in an "open ocean" basalt hosted microbial community. Geochemical data from Wanless et al., (2006), indicate that the 1877 basaltic glasses are of typical tholeiitic composition common to subaerial Mauna Loa lavas. The bacterial community associated with 552X2 basalt is highly diverse (similar in number of peaks when compared to 549X3 t-RFLP pattern), but dominated by α-proteobacteria. While γ-proteobacteria are also in abundance in this sample, two of the three major peaks in this spectrum represent alphas. SIO10B is a glassy basalt powder collected from M18 on the western crater rim. This environment is also cold, but is subject to ambient, low flow, hydrothermal input welling up from between the talus. The community richness found on this basalt is low, comparable with spectra from 547X3, and exhibits 2-3 dominant peaks and few other contributors. Both of these samples possess the Fe-oxidizing isolate LOB-7 (position 348) OTU as either the primary (SIO10B) or secondary (552X2) major peak of the spectra. ζ-proteobacteria is found in SIO10B, but is a minor member of the overall community.
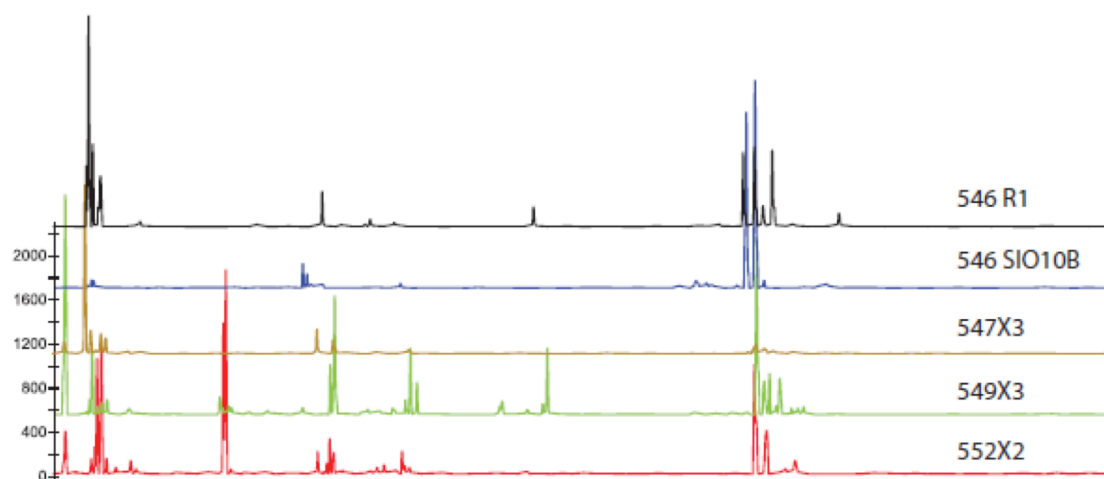
Figure 6.4. T-RFLP comparison for all samples in this study with the BstU1 restriction enzyme. The x-axis is measured from 50-500 bps and the y-axis is in fluorescence units.

FeMO_PV-1_N.	Naha	PV313_b14	1996
FeMO_JV1_N.	Jet Vents, Lower (Ikaika) ~.	PV393_b58	1998
PV546_b1	Upper Rim N of Mkr18	PV546	2003
PV546_b3	Tower Mkr 48	PV546	2003
547x3	South Rift Mkr #17	PV547	2003
549x3	South Point	PV549	2003
552x2	Kealakekua Bay	PV552	2003
PV547_b1	South Rift Mkr 17	PV547	2003
PV547_b3	South Rift Mkr 17	PV547	2003
PV548_b1	Pit Bottom Floc	PV548	2003
646R5	East of Nafanua	PV646	2005
SIO10V	Marker #18	PV546	2003
610R4	Nafanua Mkr #4	PV610	2005

Figure 6.5. T-RFLP dendogram comparing samples from this study along with selected samples from Davis and Moyer (2009).

6.5 Discussion

6.5.1 *Basalt-Hosted Microbial Communities*

Epilithic microbial populations have been shown to be fairly ubiquitous across all basalt environments found on seamounts and submarine lava flows (e.g. Staudigel et al., 2004; Mason et al., 2007; Santelli et al., 2008; Sudek et al., 2009). Previous studies have demonstrated that most basalt hosted microbial communities are quite diverse and that the diversity and overall biomass correlate positively with basalt alteration by oxidative seawater interactions (Santelli et al., 2009). However, this work has revealed that basalts in distinct local environments at Loihi Seamount have their bacterial diversity specifically affected by the unique local environment and not necessarily the degree of alteration associated with the surfaces. There exists a clear distinction in community structure between open-ocean, oxidative seawater interactions with the basalt surfaces and basalt surfaces affected by either diffuse low temperature venting and/or secondary mineral precipitations. Our results of relatively highly diverse community structure associated with basalts that have a primary surficial interaction with open-ocean oxidative seawater corroborate the results found by Santelli et al. (2008); however, low diversity in hydrothermally influenced systems indicates the immediate environment seems to have a marked effect on diversity to the point that only 1-3 species seem to be dominant in these environments. While this sounds immediately intuitive, the differences demonstrated here between the basalt surfaces and the immediate surrounding microbial mats indicate that the unique basaltic chemistry influences the specific bacterial makeup of epilithic bacteria and that the rock surface does not just represent a place for microbial mat to settle out.

Templeton et al. (2009) suggest that biofilms existing within ferromanganese crusts on the basalt surfaces in hydrothermal locations are largely sustained via the surrounding environment by authigenic mineral precipitation and transport of nutrients from the surrounding vent fluids rather than local basalt dissolution. It may be possible that these secondary mineral crusts host very specific microbial populations that out-compete any epilithic microbial populations below the crust resulting in the observed low diversity associated with hydrothermally influenced basalt surfaces. It has been shown across numerous studies that the temporal changes in bacterial abundance, diversity and biogeochemical effects vary across different sample sites and local conditions (Review by Schrenk et al., 2010). It has also been suggested by Templeton et al. (2009) that the similarities in the Hawaii and EPR basalts reported in Santelli et al. (2008) may be the result of the sampling of these ferromanganese crusts on the surfaces. However, this work suggests that the broad diversity found at the EPR correlates much better with the non-hydrothermal basalts around Loihi/Hawaii rather than the basalts with the more developed crust in hydrothermal locales with the corresponding low bacterial diversity. While Santelli et al. (2008) provide a larger global view of bacterial diversity on basalt surfaces, we find that a higher spatial resolution on unique environments will allow for better prediction capabilities when confronted with new samples and exploration sites.

Bacterial diversity on basalts can be affected by the external geochemical environment or by the composition of the substrate: Huber et al. (2002) reported that temperature and fluid chemistry are the most important factors associated with controlling archaeal populations on mid ocean ridge seamounts. Rogers et al., (1998) demonstrated that feldspar substrates with apatite inclusions were more heavily colonized

than feldspars without any phosphate present. Additionally Maurice et al., (2001a, 2001b) showed enhanced mineral dissolution in an iron-containing kaolinite (0.04 wt% Fe2O3) under Fe-limiting conditions. These latter studies suggest that substrate composition is a controlling factor in microbial diversity and activity.

This work describes basaltic glass microbial diversity to a first order degree and identifies several specific microbial species as being the more abundant species present on the basalt surfaces. Diversity analyses of our basalt samples indicate that α- and γ-Proteobacteria represent the dominant members of basalt hosted microbial communities. Several other clades, including δ-, ζ- and ε-Proteobacteria, Nitrospirae, Planctomycetes, Actinobacteria and Acidobacteria, were found on the basalt surface, but clone libraries and t-RFLP patterns both indicate that they represent a much smaller portion of the microbial populace. These findings corroborate previous findings that members of the α- and γ-Proteobacteria clades are the most abundant classes found on basalt surfaces in marine environments (Mason et al., 2007).

Both of the cold (~4°C) non-hydrothermal basalts from PP (549X3) and M1 (552X2) exhibit high diversity evidenced by clone libraries from 549X3 (Santelli et al., 2008; Orcutt et al., 2008) and backed up by comparative t-RFLP peak analysis. No single OTU seems to dominate these microbial populations. Our reference basalt, 552X2, has two of the top three peaks representing α-proteobacteria with an indication that isolate LOB-7 (γ-proteobacteria) as the second highest peak. The dominant T-RF in 552X2 is represented by clone 3_F07 and by isolate LOB-8 (Templeton et al., 2005); however, LOB-8 is only a minor contributor when comparing the spectra between the

rock and mat samples. 3_F07 is phylogenetically related to a *Rhizobiales* clone from a shallow hydrothermal vent system near Japan (Hirayama et al., 2007). This clone was found in all three of the basalts not associated with the pit crater and distinctly absent from the M18 basalt, suggesting that this α-proteobacterium is fairly cosmopolitan across basalt surfaces subject to open ocean circulation; however, it may be that it does not represent an abundant species or cannot thrive in hydrothermally influenced waters. These α- and γ-proteobacteria abundances are similar to microbial communities on EPR basalts characterized in Santelli et al. (2008), as well as basalt epiliths summarized in Mason et al. (2007).

In contrast, the hydrothermally influenced basaltic substrates (547X3 from M17 and 546X1 from M18) show a relatively low bacterial diversity present on the surface when compared to those samples from non-hydrothermal sites. Several environmental factors can contribute to this phenomenon: temperature at depth controlling fluid chemistry, $[O_2]$, salinity, pH, substrate chemistry, as well as tidal heaves controlling exposure to alternatively deep then shallow seawater such as those found on Vailulu'u Seamount (Staudigel et al., 2006). Garcia et al., (1998) determined that Loihi predominantly hosts tholeiitic basalt glasses indicating that any difference in microbial communities between the hydrothermal and non-hydrothermally influenced basalts are likely a result of vent fluid chemistry; however, without specific petrographic evidence that our individual basalts are chemically similar, we cannot rule out substrate composition as a contributing factor to differences between microbial community structure.

Overlapping peaks at position 56 in samples 547X3, 549X3 and 552X2 but absent in 546R1 and SIO10B indicates that α-proteobacteria are significant components of the overall community on natural, weathered rock surfaces but absent in the short term SIO10B experiment and the mat sample. Thus, α-proteobacteria could be interpreted as late colonizers on fresh surfaces and are specifically growing on basaltic surfaces. The high peaks related to δ- and γ-proteobacteria in the short-term exposure SIO10B sample indicate that they may be initial colonizers on fresh surfaces, while the alphas attach once the surface has been colonized/weathered.

6.5.2 *Microbial Mat and Glassy Basalt Community Comparison at M18*

Fe-oxide encrusted microbial mats have been discovered in a variety of deep hydrothermal environments around seamounts and mid-ocean ridges. Scanning electron microscope (SEM) photomicrographs reveal predominantly filamentous tubes and amorphous iron oxyhydroxides (Edwards et al., 2004; Chan et al., 2004; Sudek et al., 2009, this study). Twisted stalk features coupled to T-RFLP data show that the ζ-proteobacterium, *Mariprofundus ferrooxidans* (Emerson et al., 2007), is a contributor to the filamentous mineral structure of several mats in our study, which lends weight to the idea that the subgroup ζ-proteobacteria is found in several environments with access to Fe(II) (Davis et al., 2005; Kato et al., 2009; Emerson and Moyer, 2010; Forget et al., 2010; Edwards et al., 2011). A recent study by Toner et al. (2012) found nanoparticulate ferrihydrite to be dominant across most microbial mats at Loihi and determined long-term stability of the iron mineral phases. This stability could allow for temporal tracking of

the distribution of specific microbes present as the hydrothermal vent/environment evolves over time.

Side by side comparison of the iron oxide microbial mat (546R1) and basalt hosted communities (SIO10B) from M18 (Figure 6.3) reveals low diversity associated with the basalt surface and a much higher diversity within the mat sample. This discrepancy suggests that, under these environmental conditions, basalt surfaces can provide a particular niche in which certain bacterial communities are able to thrive. Edwards et al. (2003) show several isolates that exhibit higher growth and cell densities on basaltic glass than other substrates, which again indicates basalts may host their own independent ecosystems from the surrounding environment. The obligate iron-oxidizing lithoautotroph, LOB-7, appears to be a significant member of each community; however, its larger relative abundance in the rock community suggests that its particular metabolism is well-suited to basalt colonization and inhabitation. This finding infers that chemolithoautotrophs can out-compete the other species present in the microbial mat for surface attachment on basaltic substrates. Whether they are actively leaching Fe as an energy source from the basalt and/or have evolved a surface attachment mechanism remains unclear, but its presence, metabolic processes and apparent abundance on the basalt surface makes it a key suspect in determining who is responsible for basaltic glass alteration and dissolution in these types of environments.

However, even given the apparent substrate's ability to select for specific bacterial communities, there is much debate over where the bulk of the bacterial communities' energy sources come from. Templeton et al. (2009) report that mass balance between Fe- and Mn-oxides within the surface precipitates and concurrent

underlying basalt substrate dissolution indicates that the levels of Fe and Mn within the precipitates are too abundant to have been leached entirely from the underlying basalt substrate. Thus, the most likely source of energy for the basalt-hosted bacteria communities come from particulate and dissolved Fe(II), Mn(II) and carbon from the surrounding fluids/seawater. This supports Huber et al. (2002) in their claim that temperature and fluid chemistry are the major controlling factors in the selection for bacterial growth in the deep ocean. With several lines of evidence to support each claim, it is likely that fluid chemistry and, perhaps to a lesser extent, substrate composition have a role in the selection of specific bacterial growth on basalts in the deep ocean.

6.6 Conclusions

T-RFLP and clone library data from iron-oxide encrusted microbial mats and surfaces of natural and synthetic basalts from the seafloor around Hawaii helped us gather insights into the character and development of active seamount-hosted microbial communities. In particular, hydrothermally influenced basalts show low microbial communities with low diversity (Shannon H' index of 1.92) while basalt surfaces distant from hydrothermal activity show higher diversity (Shannon H' index of 4.16). This general difference is found even in basaltic substrates closely co-located with microbial mats suggesting that basalt surfaces are capable to select for specific bacterial communities that are different from associated mats representing the direct interaction of hydrothermal fluids and seawater. A comparison of T-RFLP data and clone libraries (from Santelli et al., 2008) from natural and synthetic basalt surfaces suggests that early bacterial colonization may predominantly emphasize Fe-oxidation metabolisms. While our study remains at a relatively limited scope these results offer another step towards our understanding of microbial communities in dark, oligotrophic, volcanically-hosted ecosystems and how they may develop through time. It is our hope that this process ultimately will help us link our understanding of microbe-rock interaction in the geological record to a robust understanding of the underlying microbial processes.

6.7 Acknowledgements

Chapter 6 is a formatted version of a paper to be submitted for publication: Bailey B., Moyer C.M., Templeton A.S., Staudigel H., Tebo B.M. Basalt-Hosted Bacterial Community Structure at Loihi Seamount. (in prep). The dissertation author was the primary investigator and author of this paper.

6.8 References

Bach, W. and K.J. Edwards. (2003) Iron and sulfide oxidation within the basaltic ocean crust: Implications for chemolithoautotrophic microbial biomass production. *Geochimica et Cosmochimica Acta.*, **67**:3871-3887.

Chan, C. S., De Stasio, G., Welch, S. A., Girasole, M., Frazer, B. H., Nesterova, M. V., Fakra, S. and Banfield, J. F. (2004). Microbial polysaccharides template assembly of nanocrystal fibers. *Science*, *303*(5664), 1656-1658.

Cowen, J. P., Giovannoni, S. J., Kenig, F., Johnson, H. P., Butterfield, D., Rappé, M. S., Hutnak, M. & Lam, P. (2003). Fluids from aging ocean crust that support microbial life. *Science*, *299*(5603), 120-123.

Davis, R. E., Carney, T., Leal, K., & Moyer, C. L. (2005). Spatial and temporal variability in microbial communities from pre-and post-eruption microbial mats collected from Loihi Seamount, Hawaii. In *AGU Fall Meeting Abstracts* (Vol. 1, p. 1508).

Davis, R.E. and C.L. Moyer. (2008) Extreme spatial and temporal variability of hydrothermal microbial mat communities along the Mariana Island Arc and southern Mariana back-arc system. *Journal of Geophysical Research*. **113**: B08S15

Edwards, K.J., D.R. Rogers, C.O. Wirsen, and T.M. McCollom. (2003) Isolation and Characterization of Novel Psychrophilic, Neutrophilic, Fe-Oxidizing, Chemolithoautotrophic a- and g-Proteobacteria from the Deep Sea. *Applied and Environmental Microbiology*. **69**(5):2906-2913

Edwards, K.J., Bach, W., McCollom, T.M., & Rogers, D.R. (2004). Neutrophilic iron-oxidizing bacteria in the ocean: their habitats, diversity, and roles in mineral deposition, rock alteration, and biomass production in the deep-sea. *Geomicrobiology Journal*, *21*(6), 393-404.

Edwards, K.J., Glazer, B.T., Rouxel, O.J., Bach, W., Emerson, D., Davis, R.E., Toner, B.M., Chan, C., Tebo, B.M., Staudigel, H., & Moyer, C.L. (2011). Ultra-diffuse hydrothermal venting supports Fe-oxidizing bacteria and massive umber deposition at 5000 m off Hawaii. *The ISME Journal*, *5*(11), 1748-1758.

Emerson, D. and C.L. Moyer (2002) Neutrophilic Fe-Oxidizing Bacteria Are Abundant at the Loihi Seamount Hydrothermal Vents and Play a Major Role in Fe Oxide Deposition. *Applied and Environmental Microbiology*. **68**(6):3085-3093

Emerson, D., & Moyer, C. L. (2010). Microbiology of seamounts: common patterns observed in community structure. *Oceanography, 23*.

Emerson D., J.A. Rentz, T.G. Lilburn, R.E. Davis, H. Aldrich, C. Chan, C.L. Moyer. (2007) A Novel Lineage of Proteobacteria Involved in Formation of Marine Fe-Oxidizing Microbial Mat Communities. *PLoS ONE* **2**(8): e667 doi:10.1371/journal.pone.0000667

Engebretson, J.L., C. L. Moyer. (2003) Fidelity of select restriction endonucleases in determining microbial diversity by terminal-restriction fragment length polymorphism. *Applied and Environmental Microbiology.* **68**: 4823-4829.

Forget, N.L., Murdock, S.A., & Juniper, S.K. (2010). Bacterial diversity in Fe‑rich hydrothermal sediments at two South Tonga Arc submarine volcanoes. *Geobiology*, *8*(5), 417-432.

Furnes, H. and Staudigel, H., (1999) Biological mediation in ocean crust alteration: how deep is the deep biosphere? *Earth and Planetary Science Letters.* **166**:97–103.

Furnes, H., H. Staudigel, I.H. Thorseth, T. Torsvik, K. Muehlenbachs and O. Tumyr. (2001) Bioalteration of basaltic glass in the oceanic crust. *Geochem. Geophy. Geosys.* **2**: paper#: 2000GC000150

Garcia, M.O., K.H. Rubin, M.D. Norman, J.M. Rhodes, D.W. Graham, D.W. Muenow and K. Spencer. (1998) Petrology and geochronology of basalt breccia from the 1996 earthquake swarm of Loihi Seamount, Hawaii: magmatic history of its 1996 eruption. *Bulletin of Volcanology.* **59**(8):577-592

Garcia, M. O., Caplan-Auerbach, J., De Carlo, E. H., Kurz, M. D., & Becker, N. (2006). Geology, geochemistry and earthquake history of Lòihi Seamount, Hawaìi's youngest volcano. *Chemie der Erde-Geochemistry*, *66*(2), 81-108.

Huber, J.A., D.A. Butterfield and J.A. Baross. (2002) Temporal Changes in Archaeal Diversity and Chemistry in a Mid-Ocean Ridge Subseafloor Habitat. *Applied and Environmental Microbiology* **68**(4):1585-1594

Huber, J.A., H.V. Cantin. S.M. Huse, S.M. Mark, D.B. Welch, M.L. Sogin and D.A. Butterfield. (2010) Isolated communities of Epsilonproteobacteria in hydrothermal vent fluids of the Mariana Arc seamounts. *FEMS Microbiology Ecology*. **73(**3): 538-549

Kato, S., Hara, K., Kasai, H., Teramura, T., Sunamura, M., Ishibashi, J. I., Kakegawa, T., Yamanaka, T., Kimura, H., Marumo, K., Urabe, T., & Yamagishi, A. (2009). Spatial distribution, diversity and composition of bacterial communities in sub-seafloor fluids at a deep-sea hydrothermal field of the Suiyo Seamount. *Deep Sea Research Part I: Oceanographic Research Papers*,*56*(10), 1844-1855.

Ludwig, W., O. Strunk, R. Westram, L. Richter, H. Meier, Yadhukumar, A. Buchner, T. Lai, S. Steppi, G. Jobb, W. Förster, I. Brettske, S. Gerber, A.W. Ginhart, O. Gross, S. Grumann, S. Hermann, R. Jost, A. König, T. Liss, R. Lüßmann, M. May, B. Nonhoff, B.

Reichel, R. Strehlow, A. Stamatakis, N. Stuckmann, A. Vilbig, M. Lenke, T. Ludwig, A. Bode and K.H. Schleifer. (2004) ARB: a software environment for sequence data. *Nucleic Acids Research.* **32**(4):1363-1371

Mason, O.U., U. Stingl, L.J. Wilhelm, M.M. Moeseneder, C.A. Di Meo-Savoie, M.R. Fisk and S.J. Giovannoni. (2007) The phylogeny of endolithic microbes associated with marine basalts. *Environmental Microbiology.* **9**:2539-2550

Mason, O.U., C.A. Di Meo-Savoie, J.D. Van Nostrand, J. Zhou, M.R. Fisk and S.J. Giovannoni. (2008) Prokaryotic diversity, distribution and insights into their role in biogeochemical cycling in marine basalts. ISME. 3: 231-242

Mason, O. U., Nakagawa, T., Rosner, M., Van Nostrand, J. D., Zhou, J., Maruyama, A., Fisk, M.R. and Giovannoni, S. J. (2010). First investigation of the microbiology of the deepest layer of ocean crust. *PLoS One*, *5*(11), e15399.

Maurice, P.A., M.A. Vierkorn, L.E. Hersman, J.E. Fulghum and A. Ferryman. (2001a) Enhancement of kaolinite dissolution by an aerobic Pseudomonas mendocina bacterium. *Geomicrobiology Journal*. **18**:21-35

Maurice, P.A., M.A. Vierkorn, L.E. Hersman, J.E. Fulghum and A. Ferryman. (2001b) Dissolution of well and poorly ordered kaolinites by an aerobic bacterium. *Chemical Geology*. **180**:81-97

Moore J.G., D.A. Clague, W.R. Normark. (1982) Diverse basalt types from Loihi seamount, *Hawaiian Geology.* **10**:88–92

Moyer, C.L., F.C. Dobbs, D.M. Karl. (1995) Phylogenetic diversity of the bacterial community from a microbial mat at an active, hydrothermal vent system, Loihi Seamount, Hawaii. *Applied and Environmental Microbiology.* **61**: 1555-1562

Orcutt, B. B. Bailey, H. Staudigel, B.M. Tebo and Katrina Edwards (2008) An interlaboratory comparison of DNA-based methods for assessing microbial diversity of seafloor basalts. Submitted to Applied and Environmental Microbiology.

Orcutt, B.N., Bach, W., Becker, K., Fisher, A.T., Hentscher, M., Toner, B.M., Wheat, C.G. & Edwards, K.J. (2010). Colonization of subsurface microbial observatories deployed in young ocean crust. *The ISME journal*, *5*(4), 692-703.

Penn, K., D. Wu, J. A. Eisen, and N. Ward. (2006). Characterization of Bacterial Communities Associated with Deep-Sea Corals on Gulf of Alaska Seamounts. Appl. Environ. Microbio. **72**(2):1680-1683

Ricke, P., S. Kolb, and G. Braker. (2005) Application of a Newly Developed ARB Software-Integrated Tool for In Silico Terminal Restriction Fragment Length

Polymorphism Analysis Reveals the Dominance of a Novel *pmoA* Cluster in a Forest Soil. *Applied and Environmental Microbiology.* **71**:1671-1673.

Rogers, J.R, P.C. Bennett and W.J. Choi. (1998) Feldspars as a source of nutrients for microorganisms. *American Mineralogist.* **83**:1532-1540

Santelli, C., B. Orcutt, E. Banning, C. Moyer, W. Bach, H. Staudigel, K. Edwards. (2008) Abundance and diversity of microbial life in the ocean crust. *Nature* **453**:653-656

Santelli, C., V.P. Edgcomb, W. Bach and K.J. Edwards. (2009) The diversity and abundance of bacteria inhabinting seafloor lavas positively correlate with rock alteration. Environmental Microbiology. **11**: 86-98

Schrenk, M. O., Huber, J. A., & Edwards, K. J. (2010). Microbial provinces in the subseafloor. *Annual Review of Marine Science. 2:* 279-304.

Staudigel, H., B. Tebo, A. Yayanos, H. Furnes, K. Kelley, T. Plank, and K. Muehlenbachs. (2004), The ocean crust as a bioreactor: *in* Wilcock, W.S.D., et al., eds., The subseafloor biosphere at mid-ocean ridges: Washington, D.C., American Geophysical Union Monograph 144, p325–341.

Staudigel H., S.R. Hart, A. Pile, B.E. Bailey, E.T. Baker, S. Brooke, D.P. Connelly, L. Haucke, C.R. German, I. Hudson, D. Jones, A.A. Koppers, J. Konter, R. Lee, T.W. Pietsch, B.M. Tebo, A.S. Templeton, R. Zierenberg, C.M. Young. 2006. Vailulu'u Seamount, Samoa: Life and death on an active submarine volcano. *Proceedings of the National Academy of Sciences.* **103**(17):6448

Sudek, L. A., Templeton, A. S., Tebo, B. M., & Staudigel, H. (2009). Microbial ecology of Fe (hydr)oxide mats and basaltic rock from Vailulu'u Seamount, American Samoa. *Geomicrobiology Journal, 26*(8), 581-596.

Templeton, A., Staudigel, H., and Tebo, B. (2005) Diverse Mn(II)-oxidizing bacteria isolated from submarine basalts at Loihi Seamount. *Geomicrobiology Journal.* **22:** 127–139.

Templeton, A. S., Knowles, E. J., Eldridge, D. L., Arey, B. W., Dohnalkova, A. C., Webb, S. M., Bailey, B.E., Tebo, B.M. & Staudigel, H. (2009). A seafloor microbial biome hosted within incipient ferromanganese crusts. *Nature Geoscience, 2*(12), 872-876.

Thorseth, I.H., T. Torsvik, H. Furnes, K. Muehlenbachs. (1995) Microbes play an important role in the alteration of oceanic crust. Chemical Geology. 126: 137-146.

Toner, B.M., Berquó, T.S., Michel, F.M., Sorensen, J.V., Templeton, A.S., & Edwards, K.J. (2012). Mineralogy of iron microbial mats from loihi seamount. *Frontiers in microbiology*, *3*, 118

Wanless, V.D., M.O. Garcia, F.A. Trusdell, J.M. Rhodes, M.D. Norman, D. Weis, D.J. Fornari, M.D. Kurz, and H. Guillou. (2006) Submarine radial vents on Mauna Loa Volcano, Hawai'i. *Geochem. Geoph. Geosys.* **7**(5)

6.9. Appendices

Appendix 6.1. In-silico restriction digests of clones from 547X3 and 549X3.

This appendix identifies the theoretical cut sites for each clone sequenced from rock surfaces from 547X3 and 549X3. The clone number is on the left; # seqs is the number of times each sequence was counted in the clone library and is related to diversity; "%" is how related the clone is to its closest match in BLAST; "Alu1" through "RsaI" are the restriction enzymes used that results in a fragment length can then be correlated to a T-RFLP electopherogram in order to determine if that species is present in multiple samples.

Appendix 6.1.1. Restriction digests for Basalt 547X3

Clone	# seqs	Classification	Closest match in BLAST	%	ACCESSION	AluI	BstUI	HaeIII	HhaI	MboI	MspI	RsaI
3_B02	1	Acidobacteria	Uncultured bacterium clone P13-79	99	EU287172	168	202	198	523	27	187	430
3_G06	1	Acidobacteria	Uncultured bacterium clone FS266-75B-03	95	DQ513088	161	199	195	183	153	253	450
2_A03	1	Acidobacteria	Uncultured bacterium clone P13-85	96	EU287178	162	152	147	337	154	84	185
7_E11	1	Acidobacteria	Uncultured bacterium clone SS1_B_02_91	96	EU050885	129	67	179	318	251	237	434
7_E09	1	Acidobacteria	Uncultured bacterium clone Cl35cm.1ox.04	96	EF208619	162	202	179	186	1323	256	453
7_A03	1	Acidobacteria	Uncultured sponge symbiont PAUC26f	89	AF186410	199	188	36	172	130	27	413
7_H01	1	Actinobacteria	Uncultured organism clone ctg_CGOAA79	96	DQ395467	197	186	34	170	21	165	411
7_D10	1	Actinobacteria	Uncultured actinobacterium clone AD035	93	EF076144	116	187	190	322	21	85	412
3_F05	2	Actinobacteria	Uncultured actinobacterium clone AD039	93	EF076145	206	195	198	179	45	43	420
7_B11	3	Actinobacteria	Uncultured bacterium clone CV54	94	DQ499303	164	192	130	327	137	92	441
3_C12	2	Actinobacteria	Uncultured organism clone ctg_CGOAA22	97	DQ395502	31	186	139	321	254	26	674
7_B02	3	Actinobacteria	Uncultured bacterium clone Cl75cm.2.13	93	EF208707	204	193	196	633	261	99	418
2_E11	1	Actinobacteria	Uncultured bacterium clone VHS-B4-19	93	DQ394984	205	194	290	338	262	92	37
7_F12	1	Actinobacteria	Uncultured bacterium clone MD2902-B6	96	EU048613	191	195	225	330	263	100	420
3_F02	3	Actinobacteria	Uncultured bacterium clone E17	96	AJ966591	207	364	199	179	264	100	428
3_F08	1	Actinobacteria	Micrococcus luteus strain AUH1	99	EF187229	31	184	187	628	555	122	414
3_A06	1	Actinobacterium	Uncultured organism clone ctg_BRRAA49	92	DQ395394	205	194	290	196	145	100	424
3_C03	1	Alphaproteobacteria	Uncultured bacterium clone S26-96	95	EU287396	144	68	198	53	21	83	393
7_H07	1	Alphaproteobacteria	Uncultured bacterium clone ELB16-042	95	DQ015803	156	66	278	51	72	39	810
3_D08	1	Alphaproteobacteria	Uncultured organism clone MAT-CR-P5-B05	85	EU246200	214	125	199	205	154	111	454
3_F07	6	Alphaproteobacteria	Uncultured Rhizobiales bacterium clone: pltb-vmat-38	94	AB294946	102	56	152	300	200	398	77
3_C11	1	Alphaproteobacteria	Endosymbiont of Acanthamoeba sp. AC305	90	AY549548	102	56	152	863	200	398	781
2_B02	1	Alphaproteobacteria	Uncultured organism clone ctg_CGOAA08	99	DQ395424	167	56	152	472	200	122	785
2_B05	1	Alphaproteobacteria	Roseobacter sp. GAI-109	95	AF098494	220	67	163	311	211	409	392
7_B12	2	Alphaproteobacteria	Bartonella quintana str. Toulouse	90	BX897700	31	168	164	170	212	171	89

Appendix 6.1.2. Restriction digests for Basalt 549X3

Clone	# seqs	Classification	Closest match in BLAST	%	ACCESSION	AluI	BstUI	HaeIII	HhaI	MboI	MspI	RsaI
3_B02	1	Acidobacteria	Uncultured bacterium clone P13-79	99	EU287172	168	202	198	523	27	187	430
3_G06	1	Acidobacteria	Uncultured bacterium clone FS266-75B-03	95	DQ513088	161	199	195	183	153	253	450
2_A03	1	Acidobacteria	Uncultured bacterium clone P13-85	96	EU287178	162	152	147	337	154	84	185
7_E11	1	Acidobacteria	Uncultured bacterium clone SS1_B_02_91	96	EU050885	129	67	179	318	251	237	434
7_E09	1	Acidobacteria	Uncultured bacterium clone C135cm.1ox.04	96	EF208619	162	202	179	186	1323	256	453
7_A03	1	Acidobacteria	Uncultured sponge symbiont PAUC26f	89	AF186410	199	188	36	172	130	27	413
7_H01	1	Actinobacteria	Uncultured organism clone ctg_CGOAA79	96	DQ395467	197	186	34	170	21	165	411
7_D10	1	Actinobacteria	Uncultured actinobacterium clone AD035	93	EF076144	116	187	190	322	21	85	412
3_F05	2	Actinobacteria	Uncultured actinobacterium clone AD039	93	EF076145	206	195	198	179	45	43	420
7_B11	3	Actinobacteria	Uncultured bacterium clone CV54	94	DQ499303	164	192	130	327	137	92	441
3_C12	2	Actinobacteria	Uncultured organism clone ctg_CGOAA22	97	DQ395502	31	186	139	321	254	26	674
7_B02	3	Actinobacteria	Uncultured bacterium clone C175cm.2.13	93	EF208707	204	193	196	633	261	99	418
2_E11	1	Actinobacteria	Uncultured bacterium clone VHS-B4-19	93	DQ394984	205	194	290	338	262	92	37
7_F12	1	Actinobacteria	Uncultured bacterium clone MD2902-B6	96	EU048613	191	195	225	330	263	100	420
3_F02	3	Actinobacteria	Uncultured bacterium clone E17	96	AJ966591	207	364	199	179	264	100	428
3_F08	1	Actinobacteria	Micrococcus luteus strain AUH1	99	EF187229	31	184	187	628	555	122	414
3_A06	1	Actinobacterium	Uncultured organism clone ctg_BRRAA49	92	DQ395394	205	194	290	196	145	100	424
3_C03	1	Alphaproteobacteria	Uncultured bacterium clone S26-96	95	EU287396	144	68	198	53	21	83	393
7_H07	1	Alphaproteobacteria	Uncultured bacterium clone ELB16-042	95	DQ015803	156	66	278	51	72	39	810
3_D08	1	Alphaproteobacteria	Uncultured organism clone MAT-CR-P5-B05	85	EU246200	214	125	199	205	154	111	454
3_F07	6	Alphaproteobacteria	Uncultured Rhizobiales bacterium clone: pltb-vmat-38	94	AB294946	102	56	152	300	200	398	77
3_C11	1	Alphaproteobacteria	Endosymbiont of Acanthamoeba sp. AC305	90	AY549548	102	56	152	863	200	398	781
2_B02	1	Alphaproteobacteria	Uncultured organism clone ctg_CGOAA08	99	DQ395424	167	56	152	472	200	122	785
2_B05	1	Alphaproteobacteria	Roseobacter sp. GAI-109	95	AF098494	220	67	163	311	211	409	392
7_B12	2	Alphaproteobacteria	Bartonella quintana str. Toulouse	90	BX897700	31	168	164	170	212	171	89
3_C05	3	Alphaproteobacteria	Uncultured organism clone ctg_CGOAA09	97	DQ395453	31	68	264	303	212	121	1301
3_B10	2	Alphaproteobacteria	Uncultured bacterium clone S26-96	96	EU287396	144	169	36	53	213	411	394
8_D09c	1	Alphaproteobacteria	Uncultured alpha proteobacterium clone ss1_B_01_63	94	EU050755	85	68	166	53	214	376	89
2_D09	1	Alphaproteobacteria	Uncultured alpha proteobacterium clone L13	92	DQ860071	25	68	266	486	214	131	89
7_D11	1	Alphaproteobacteria	Uncultured bacterium clone P13-82	95	EU287175	183	70	24	488	216	26	659
7_E12	1	Alphaproteobacteria	Uncultured alpha proteobacterium clone MBAE43	93	AJ567596	31	70	24	55	217	26	660
8_H08c	2	Alphaproteobacteria	Uncultured organism clone ctg_NISA128	95	DQ396275	25	68	36	326	226	424	89
8_D11	1	Alphaproteobacteria	Uncultured alpha proteobacterium clone JdFBGBact_40	96	DQ070827	31	68	178	498	226	388	89
8_A05c	1	Alphaproteobacteria	Uncultured alpha proteobacterium clone ss1_B_01_63	93	EU050755	235	68	363	53	226	388	89

Appendix 6.1.2. 549X3 (cont'd).

Clone	# seqs	Classification	Closest match in BLAST	%	ACCESSION	AluI	BstUI	HaeIII	HhaI	MboI	MspI	RsaI
3_C04	1	Bacteroidetes	Uncultured organism clone MAT-CR-P4-B10	88	EU246140	25	68	269	1034	139	395	416
7_B03	1	Bacteroidetes	Uncultured Bacteroidetes bacterium clone MBAE20	90	AJ567581	32	70	185	55	233	104	432
7_H08	1	Bacteroidetes	Flexibacter aggregans strain IFO 15974	94	AB078038	197	69	367	54	254	102	270
7_H02	1	Betaproteobacteria	Nitrosospira multiformis ATCC 25196	97	CP000103	193	348	178	166	126	449	432
3_F12	3	Betaproteobacteria	Curvibacter gracilis	99	AB109889	235	164	178	166	128	71	388
3_B04	4	Betaproteobacteria	Uncultured bacterium clone 661198	98	DQ404920	191	162	28	164	147	98	430
3_H06	1	Caldithrix	Uncultured marine bacterium 159 clone EBAC750-03B02	93	AY458631	163	361	191	330	239	111	446
2_H08	1	Caldithrix	Unidentified bacterium wb1_H02	89	AF317766	207	113	226	198	1325	51	447
2_F02	1	Caldithrix	Uncultured organism clone MAT-CR-P6-G12	85	EU246318	215	71	178	56	1336	258	456
2_B09	1	Chloroflexi	Uncultured bacterium clone FS118-32B-02	88	AY869681	248	66	225	176	40	490	421
3_A11	1	Chloroflexi	Uncultured bacterium clone SS1_B_03_41	97	EU050928	202	72	135	326	42	486	31
8_B08	2	Chloroflexi	uncultured Chloroflexi bacterium clone D92_36	90	AY534100	193	69	227	71	76	164	128
8_G10c	1	Chloroflexi	Uncultured Crater Lake bacterium CL500-11	88	AF316759	211	166	196	168	268	495	426
3_A09	2	Deltaproteobacteria	Uncultured bacterium clone MD2896-B28	97	EU048685	178	94	164	335	89	254	451
2_D04	1	Deltaproteobacteria	Uncultured bacterium clone Kas145B	87	EF203190	116	172	218	54	128	433	81
3_A04	1	Deltaproteobacteria	Pelobacter carbinolicus DSM 2380	84	CP000142	211	68	240	53	130	48	371
3_E07	1	Deltaproteobacteria	Desulfuromonas alkaliphilus strain Z-0531	84	DQ309326	467	69	277	54	131	49	27
7_A07	1	Deltaproteobacteria	Uncultured delta proteobacterium clone AKYH967	94	AY922176	112	180	34	50	133	37	41
3_C02	2	Deltaproteobacteria	Uncultured bacterium clone MD2896-B28	85	EU048685	114	364	162	333	135	121	43
7_F08	1	Deltaproteobacteria	Uncultured delta proteobacterium clone JdFBGBact_5	89	DQ070816	116	202	166	54	138	102	453
7_B09	1	Deltaproteobacteria	Uncultured bacterium clone B78-87	85	EU287051	194	198	551	200	151	278	27
2_D12	1	Deltaproteobacteria	Uncultured delta proteobacterium clone Jt58-30	91	AB189349	194	67	213	52	251	121	409
7_C04	3	Deltaproteobacteria	uncultured delta proteobacterium Sva0853	94	AJ240985	26	349	213	52	251	90	186
3_H10	1	Deltaproteobacteria	Uncultured organism clone ctg_BRRAA88	96	DQ395368	114	349	240	1050	251	90	63
2_C04	1	Deltaproteobacteria	Uncultured delta proteobacterium clone ss1_B_09_96	97	EU050850	26	349	364	52	251	121	409
2_H03	1	Deltaproteobacteria	Uncultured delta proteobacterium clone JTB36	94	AB015242	196	40	366	40	253	123	410
2_F12	1	Deltaproteobacteria	Unidentified bacterium gene clone BD3-7	98	AB015549	196	69	366	54	253	123	410
2_C05	1	Deltaproteobacteria	Uncultured delta proteobacterium clone JdFBGBact_5	93	DQ070816	26	184	166	54	257	112	45
3_H03	2	Deltaproteobacteria	uncultured bacterium clone TopBa32	94	EF999358	114	189	246	52	257	121	415
7_D02	1	Deltaproteobacteria	uncultured bacterium clone TopBa32	93	EF999358	116	191	248	54	259	245	417
2_G02	1	Deltaproteobacteria	Uncultured bacterium clone P13-55	93	EU287148	176	66	26	51	266	100	39
3_G12	1	Deltaproteobacteria	Uncultured delta proteobacterium clone AD027	94	EF076130	178	366	145	52	268	121	451
2_A06	1	Deltaproteobacteria	Uncultured bacterium clone MD2902-B9	94	EU048616	211	200	177	54	268	28	451
3_F03	1	Deltaproteobacteria	Uncultured bacterium clone P13-55	93	EU287148	115	68	26	53	269	102	41
8_D03c	1	Deltaproteobacteria	Uncultured organism clone MAT-CR-M3-B02	86	EU245563	90	202	141	54	270	124	453
7_C08	1	Deltaproteobacteria	Uncultured bacterium clone FS266-91B-03	94	AY869686	116	69	166	54	270	103	205
7_C01	2	Deltaproteobacteria	uncultured bacterium clone BotBa30	85	EF999397	215	70	234	55	272	50	454
7_F01	2	Deltaproteobacteria	Uncultured delta proteobacterium clone MSB-5D3	86	DQ811832	32	371	168	340	273	474	457
3_G05	4	Deltaproteobacteria	Uncultured bacterium clone R4b9	84	AF482443	216	70	235	55	273	50	455
3_B01	8	Deltaproteobacteria	Uncultured bacterium clone S26-84	98	EU287384	993	360	35	338	345	121	43

Appendix 6.1.2. 549X3 (cont'd).

Clone	# seqs	Classification	Closest match in BLAST	%	ACCESSION	AluI	BstUI	HaeIII	HhaI	MboI	MspI	RsaI
7 D01	1	Deltaproteobacteria	Uncultured delta proteobacterium MERTZ_2CM_224	98	AF424215	368	33	94	85	400	118	398
7 D06	1	Deltaproteobacteria	uncultured bacterium clone TopBa32	93	EF999358	170	191	154	54	774	123	417
3 D02	4	Deltaproteobacteria	uncultured bacterium clone TopBa32	89	EF999358	201	67	247	52	775	121	193
3 A05	3	Deltaproteobacteria	Uncultured bacterium clone MD2896-B28	93	EU048685	179	367	146	336	860	123	452
7 H03	1	Deltaproteobacteria	Uncultured bacterium clone Kas164B	83	EF203201	116	371	169	349	1485	123	456
7 E01	1	Firmicutes	Planifilum yunmanesis	82	DQ119659	25	199	229	728	131	468	451
3 A08	1	Firmicutes	Uncultured bacterium clone FS142-17B-02	98	DQ513025	253	115	299	1115	777	296	312
7 A09	1	Gammaproteobacteria	Uncultured gamma proteobacterium clone VHS-B1-32	96	DQ394908	180	184	28	59	35	119	452
3 G03	1	Gammaproteobacteria	Uncultured bacterium clone ORCA-17N118	92	DQ823220	226	258	28	359	35	482	871
7 A04	1	Gammaproteobacteria	Uncultured bacterium clone S26-52	98	EU287352	133	367	28	59	35	468	856
7 G09	1	Gammaproteobacteria	Legionella dresdeniensis type strain W03-356	89	AM747393	34	74	164	46	80	464	269
3 H09	1	Gammaproteobacteria	Uncultured gamma proteobacterium clone VHS-B4-51	92	DQ395013	32	166	214	168	151	451	840
3 F11	2	Gammaproteobacteria	Uncultured gamma proteobacterium clone.JTB254	97	AB015253	32	166	280	168	151	451	840
3 D01	1	Gammaproteobacteria	Uncultured gamma proteobacterium clone AT-s3-68	96	AY225628	33	26	216	527	153	453	841
3 D03	1	Gammaproteobacteria	Uncultured gamma proteobacterium clone Sylt 32	93	AM040128	33	72	216	330	153	104	607
8 B07	1	Gammaproteobacteria	Uncultured gamma proteobacterium clone JTB35	95	AB105250	33	72	216	44	153	104	840
3 B07	7	Gammaproteobacteria	Uncultured bacterium clone P13-70	98	EU287163	118	352	216	527	153	41	840
7 C07	2	Gammaproteobacteria	Marinobacter aquaeolei VT8	99	CP000514	33	352	216	170	153	104	841
3 C07	1	Gammaproteobacteria	Uncultured Ectothiorhodospiraceae bacterium clone MBAE54	92	AJ567603	33	352	216	44	153	421	436
7 E10	1	Gammaproteobacteria	Uncultured bacterium clone S11-46 16S	91	EU287229	33	170	216	330	153	453	841
3 D10	5	Gammaproteobacteria	Uncultured gamma proteobacterium clone Belgica2005/10-130-9	93	DQ351756	33	26	282	26	153	453	842
3 A02	3	Gammaproteobacteria	Colwellia psychrerythraea 34H	99	CP000083	33	352	282	808	153	453	607
3 B06	1	Gammaproteobacteria	uncultured bacterium clone TopBa15	94	EF999348	33	355	219	173	154	106	844
3 F06	1	Gammaproteobacteria	Uncultured gamma proteobacterium clone 9NBGbact_1	98	DQ070789	4	170	369	46	155	455	844
2 E03	1	Gammaproteobacteria	Uncultured gamma proteobacterium clone Belgica2005/10-120-18	95	DQ351749	34	355	219	173	156	456	845
7 D04	6	Gammaproteobacteria	Uncultured gamma proteobacterium clone JTB254	91	AB015253	32	125	226	180	163	463	128
8 A08c	1	Gammaproteobacteria	Uncultured gamma proteobacterium clone MBMPE4	92	AJ567535	34	367	297	345	168	468	857
3 D12	3	Gammaproteobacteria	Sulfur-oxidizing bacterium NDII1.2	91	AF181991	33	340	204	770	218	41	399
7 H04	1	Gammaproteobacteria	Acinetobacter radioresistens strain M 17694T	99	Z93445	31	348	159	114	226	450	709
2 C11	1	Gammaproteobacteria	Sulfur-oxidizing bacterium NDII1.1	94	AF170424	32	351	21	329	229	452	841
3 C06	3	Gammaproteobacteria	Uncultured bacterium clone P13-69	98	EU287162	32	70	150	330	230	102	842
7 F03	1	Gammaproteobacteria	Uncultured bacterium clone B78-41	94	EU287005	32	70	150	72	230	102	607
7 B01	4	Gammaproteobacteria	Uncultured Ectothiorhodospiraceae bacterium clone MBAE54	90	AJ567603	33	354	152	529	232	455	797
7 B06	4	Gammaproteobacteria	Uncultured bacterium clone E77	92	AJ966605	34	26	165	26	232	455	842
8 G02c	1	Gammaproteobacteria	uncultured gamma proteobacterium Sva0071	92	AJ240986	33	354	165	529	232	455	843
3 D05	4	Gammaproteobacteria	Uncultured bacterium clone P13-33	90	EU287126	168	74	220	408	234	106	612
2 E06	1	Gammaproteobacteria	Coxiella burnetii RSA 331	88	CP000890	34	74	288	533	236	459	613
3 B08	8	Gammaproteobacteria	Uncultured gamma proteobacterium clone Belgica2005/10-140-3	96	DQ351776	210	365	28	343	243	467	855
2 F08	1	Gammaproteobacteria	Uncultured proteobacterium clone Bol37	90	AY193142	213	86	179	186	246	163	859
3 A01	1	Gemmatimonadales	Uncultured bacterium clone P13-87	93	EU287180	31	203	24	338	155	26	454

Appendix 6.1.2. 549X3 (cont'd).

Clone	# seqs	Closest match in BLAST	Classification	ACCESSION	%	AluI	BstUI	HaeIII	HhaI	MboI	MspI	RsaI
7_G12	1	Uncultured bacterium clone NO27FW100501SAB69	Nitrospirae	DQ230952	88	32	379	209	197	34	121	24
7_C06	3	Uncultured Nitrospira sp.	Nitrospirae	AY225654	91	164	125	226	331	130	640	128
2_F04	1	Uncultured Nitrospira sp.	Nitrospirae	AY225654	87	116	365	140	166	152	609	448
2_E08	1	Uncultured bacterium clone B78-107	Nitrospirae	EU287071	95	110	355	192	324	257	129	172
3_C09	1	Uncultured bacterium clone Biofilm_94d_c2	Nitrospirae	DQ058678	93	178	105	164	54	268	407	451
8_D07	1	Uncultured bacterium clone NO27FW100501SAB69	Nitrospirae	DQ230952	96	179	379	216	348	281	121	419
8_H06	1	Uncultured bacterium clone Biofilm_94d_c2	Nitrospirae	DQ058678	84	150	375	172	56	997	125	31
8_B11_c	1	uncultured bacterium clone TopBa6	Nitrospirae	EF999345	93	35	77	195	334	1258	110	405
3_E02	1	Uncultured bacterium clone Biofilm_94d_c2	Nitrospirae	DQ058678	85	183	371	235	56	1331	125	457
2_A10	1	Uncultured organism clone MAT-CR-H5-H07	OD1	EU245317	84	192	347	211	1430	980	89	872
7_B05	1	Unidentified bacterium clone BD7-1	OD1	AB015577	82	182	337	167	1029	1405	251	24
7_D05	2	Uncultured bacterium clone FS275-24B-03	Planctomycetes	DQ513105	91	199	354	191	526	83	117	842
3_A10	3	Uncultured planctomycete clone AT-s2-38	Planctomycetes	AY225652	95	96	169	26	313	84	88	39
3_H11	1	Uncultured bacterium clone 101-74	Planctomycetes	EF157236	88	163	352	428	330	128	85	81
3_D11	2	Uncultured planctomycete clone VHS-B5-11	Planctomycetes	DQ395030	92	25	70	203	232	138	92	224
2_H11	1	Uncultured planctomycete clone CI35cm.2.15a	Planctomycetes	EF208657	85	211	366	274	541	165	134	788
3_C01	1	Uncultured Pirellula sp. clone 9NBGBact_17	Planctomycetes	DQ070794	93	114	84	104	69	167	137	493
3_G02	1	Uncultured bacterium clone 35-49	Planctomycetes	DQ833489	86	208	363	227	112	265	88	41
3_G09	1	Uncultured planctomycete 6FN	Planctomycetes	EF591887	96	195	350	254	806	409	150	95
7_A10	1	Planctomyces maris (strain DSM 8797T)	Planctomycetes	AJ231184	91	718	354	258	332	1424	91	80
8_E10c	1	Leptospira illini	Spirochaetes	M88719	86	115	124	244	322	255	132	127
7_E03	1	Uncultured bacterium clone B55	TM6	AM162488	89	26	345	149	183	570	233	43
7_D08	2	uncultured bacterium clone BotBa30	Unclassified	EF999397	84	211	66	230	51	128	46	450
3_F09	1	Uncultured bacterium clone B78-35	Unclassified	EU286999	88	180	69	260	116	247	257	27
3_B05	1	Uncultured bacterium clone PK019	Unclassified	EF076072	94	178	137	164	137	1323	254	45
2_E07	1	Uncultured organism clone ctg_CGOCA85	Unclassified	DQ395545	90	27	357	112	223	1467	245	442
2_H06	1	Uncultured candidate division OP3 clone pItb-vmat-13	Unclassified	AB294931	89	177	491	163	426	1476	467	450
7_G07	1	Unclassified bacterial species koll11	Verrucomicrobia	AJ224540	88	242	231	208	1103	60	609	481
3_G08	1	Waddlia sp. G817	Verrucomicrobia	AY184804	87	32	543	381	344	167	467	136
3_C08	2	Uncultured Cytophaga sp. Clone JT75-104	Verrucomicrobia	AB189358	97	31	69	367	328	250	123	189
3_E06	1	Cytophaga sp. Dex80-64	Verrucomicrobia	AJ431235	88	198	67	858	329	255	394	414
3_B09	1	Unclassified bacterial species clone koll11	Verrucomicrobia	AJ224540	89	130	99	211	71	303	1351	163
3_F04	4	Unclassified bacterial species clone koll11	Verrucomicrobia	AJ224540	90	130	230	162	71	418	39	482
7_H12	2	Mariprofundus ferrooxydans strain JV-1	zeta	EF493244	88	114	67	180	52	228	101	27

Appendix 6.2. In-silico restriction digests of isolates

This appendix takes isolates from Templeton et al. (2005) and performs an in-silico digest with all 8 restriction enzymes used in this study. The resultant fragment lengths can then be compared to the data to determine abundances of species within the bacterial communities.

Subset Templeton isolate in-silico TRFs	In silica Trfs								
	Alu I	BstU I	Hae III	Hha I	Hinf I	Mbo I	Msp I	Rsa I	
Marinobacter (LOB-4 M17)	33	352	216	170	78 A	153	104	841	Oligotrophic MnOB from M17
Pseudoalteromonas (LCB-1)	199	354	165	332	289 C	232	455	530	MnOB/Siderophore producers, Pele's pit
Pseudoalteromonas (MnOB M17)	34	356	167	334	291 C	180	457	532	MnOB/Siderophore producers, M17
Sulfitobacter (SPB-4)	209	56	152	299	257 C	146	398	381	MnOB
Halomonas (LOB-5)	29	342	357	517	74 A	244	410	831	Oligotrophic MnOB/FeOB
Pseudomonas tolassii (2r1-7)	31	348	159	166	74 A	250	449	837	Lithotrophic FeOB
Pseudomonas stutzeri (LCB-20)	114	164	841	166	74 A	149	41	837	Heterotrophic MnOB, FeOB and Siderophore producer
Meiothermus (3N)	186	175	22	180	301 A	69	116	399	"moderate thermophile from 48 fluids"
Geobacillus (3N-J)	33	197	168	202	298 C	1321	95	448	thermophile from M48 fluids and M26 mat
Idiomarina loihiensis (1s1-3)	34	354	165	423	289 C	232	455	530	MnOB from Pele's pit mats
Methylarcula (9C4-1)	353	56	186	300	257 C	146	89	67	MnOB
Microbulbifer (6x1-1)	190	20	397	20	71 A	146	97	600	MnOB from Kbay
Alteromonas (8x2-1)	191	346	176	166	281 C	224	161	835	MnOB from M4 rocks
Exiguobacterium (1s1-1)	28	373	202	20	308 C	275	183	428	Heterotroph from Pele's pit
Paracoccus (3N)	31	349	160	167	74 A	227	450	1195	Mesophile heterotroph from M48 fluids
Rhodococcus (4s9)	98	182	28	626	283 C	73	120	39	Heterotroph from Pele's pit
Acinetobacter (8R2)	31	474	159	166	74 A	226	450	709	Mesophile from M26 and M17 rocks
Rubrobacter (8R2)	164	20	170	328	294 C	1314	99	126	Thermophile from M26 mats
Pseudoxanthamonas (8R2)	193	164	212	166	283 C	149	41	432	Clone from M26 mat
Cytophaga (8R2)	34	74	805	59	290 C	257	451	93	Clone from M26 mat
Microbacterium (8R2)	31	184	187	102	87 C	42	122	414	Clone from M26 mat
Arthrobacter (4/s9)	30	185	188	139	85 C	22	108	415	Mesophile from M48 Mat
Rhodobacter/Roseobacter (3s6-1)	208	56	151	866	256 C	21	89	380	Heterotroph from M18 scoop, MnOB?
Shewanella (601R-1)	35	356	286	334	291 C	157	457	185	Fe Reducing Heterotroph from M36

Chapter 7

Conclusions and Future Work

This chapter is devoted to the discussion of how the overall dissertation fits into the current body of scientific literature and where the next steps in the field of geobiology should take us.

7.1 Overview of the Thesis

The work completed in this dissertation contributed to the field of geobiology by using laboratory techniques along with in-situ environmental work to explore the interactions between microorganisms and basaltic glass. Our main goals were to qualitatively and quantitatively characterize microbial diversity found on basaltic glass surfaces and to try and elucidate the effect that the microbial communities had on the basalt surface and, in turn, how the basaltic glass chemistry had an effect on the microbial populace.

Accomplishing these goals proved to be difficult for a variety of reasons. First, microbial biomass on basalt surfaces was fairly low (confirmed via fluorescent microscopy and scanning electron microscopy), making DNA extraction difficult. Second, current phylogenetic diversity analyses are centered on clone library generation, a time- and cost-consuming process, which is not feasible when screening several samples for a study. Third, this work requires model organisms to study the interactions between microbe and basaltic glass, and culturing/isolation techniques are tedious and

time-consuming, not to mention the difficulty in isolating a good candidate microorganism.

Chapter 2 described a new laboratory protocol for DNA extraction from metal-rich, low biomass samples. An efficient and robust method for DNA extraction is extremely important for these studies as these environments host an assortment of bacterial types from which we need to extract DNA: gram-negative and gram-positive bacteria, spore-formers, cells encased in minerals and extracellular polysaccharides, epilithic cells attached to the surface, endo-lithic cells buried within the silicate matrix, etc, and in order to get a complete picture of the bacteria represented, it is vital to retrieve as much DNA as possible from these surfaces without introducing any bias to the system. Our new method used a combination of chemical and mechanical cell disruption for DNA extraction, which ultimately outperformed two commercially available extraction kits by 70% to >700% in terms of total DNA yield. This new method allowed us to more efficiently (and cheaply!) retrieve clean, PCR-ready DNA from basalt surfaces as well as iron-rich microbial mats for our work in Chapter 6.

Chapter 3 was primarily a technology demonstration to show how Mössbauer spectroscopy could be used to help characterize iron-bearing minerals before and after reaction with biota. We created basalts of various oxidation states in the laboratory by firing powdered basalts at sub-solidus temperatures to oxidize the iron and then remelted the basalts. Mössbauer was used to characterize these basalt glasses for experiments (Chapter 4) and experimental deployments (Appendix 1). Results showed that unaltered natural basalt glass (NB) is approximately 92% $Fe(II)/Fe_{Total}$, while our oxidation procedure produced oxidized basalt (OB) at 70% $Fe(III)/Fe_{Total}$. These samples were then

deployed on Loihi Seamount and allowed to react for 2 years. Reaction products were analyzed and ultimately were oxidized with respect to the parent material. Mössbauer spectroscopy proved to be a valuable tool in the characterization of iron oxidation states in the designer glasses we modified in the lab and used in Chapter 4 and for deployment samples on Loihi. These experiments demonstrated that Mössbauer spectroscopy can be used to characterize Mars mineral formations which may indicate what type of energy sources are available for a subsurface Martian biosphere.

Chapter 4 explored the abilities of *Shewanella* and *Pseudomonas* isolates to obtain energy sources and/or nutrients directly from the basaltic glass silicate matrix. Three basalts were altered in the laboratory to either change the iron speciation (Fe(II) $\rightarrow$ Fe(III)) or enhance the phosphate concentration present in the glass. We used *Pseudomonas* sp. LOB-7, an Fe(II)-oxidizing bacterium, to detect its ability to grow using basaltic glass as its sole source of reduced iron and/or phosphate. We also used *Shewanella* sp. isolate 601R-1 to determine its ability to grow on lactate and the oxidized iron in the oxidized glass. Major results from this research indicate that microbial life is able to obtain electron donors/acceptors and/or nutrients (at least phosphate) directly from the basaltic glass, which allows us to conclude that basalt substrates can play an important role in the biological acquisition of energy and/or metabolites in the oligotrophic deep oceanic biosphere. LOB-7 additionally played an important role in Chapter 6.

Chapter 5 compared the efficiency and accuracy with which terminal restriction fragment length polymorphism (t-RFLP) and clone libraries were able to accurately predict phylogenetic diversity. We characterized microbial communities from two

different rock samples on Loihi Seamount using each method and compared the results. Major findings from this study showed that t-RFLP generally underestimates the biodiversity in high diversity samples, but does moderately well in low to medium diversity samples. Correlation of the data between the two datasets indicated that both methods predicted the same dominant peaks within each basalt glass, but T-RFLP should be the preferred method of determining relative abundance of a species within a bacterial community as it can more easily track presence/absence/abundance over a given time series of data given its high-throughput, low-cost method. We used both t-RFLP and clone library generation in Chapter 6.

Chapter 6 used clone libraries and comparative t-RFLP to characterize and compare the microbial communities across several different hydrothermally and non-hydrothermally influenced basaltic glasses in and around Loihi Seamount and Kealakekua Bay. Results showed that non-hydrothermally influenced basalts host dramatically more diverse bacterial communities than the hydrothermal basalts. Additionally, basaltic glass substrates are home to a much less diverse community than microbial mats exposed to similar hydrothermal input. The peaks we identified as being the most dominant members of the microbial communities associated with all of these basalts and mats belong to the g- and a-Proteobacteria subclass. Additionally, we were able to identify one of our isolates, the Fe(II)-oxidizing *Pseudomonas* sp. LOB-7 used in Chapter 4, as being either the primary, secondary or tertiary peak in several samples, indicating that this isolate is dominant within the microbial communities.

7.2 Relevance and Contribution to Geobiology at Large

A large portion of this dissertation, Chapters 2, 3, and 5, were needed to lay the ground work for exploration in the other chapters. Only a handful of previously existing studies have looked at microbial communities associated with environmental basalt surfaces (Thorseth et al., 2001; Fisk et al., 2003; Lysnes et al., 2004a, 2004b; Santelli et al., 2008) primarily due to the difficulty of working with these samples as has been alluded to already. Our work on DNA extractions from basaltic substrates (Chapter 2) coupled to the sample comparison and analysis techniques used in t-RFLP and clone libraries (Chapters 5 and 6) could lay the ground work for methodologies which would allow a much broader spectrum of basalt-hosted community analysis studies to be completed.

Several additional studies have sequenced the prokaryotic community structure of basalt enrichment cultures where they inoculated cultures with basalt fragments and characterized those enrichments (e.g. Einen et al., 2006, Mason et al. 2007); however, it has been predicted that only ~5% of environmental organisms are culturable, leaving a majority of the natural basalt communities unaccounted for. Only Mason et al. (2007) (who did a literature search and compiled data from preexisting studies) and Santelli et al. (2008) have completed a large scale comparison of microbial diversity across several distinctly different research sites. However, upon closer inspection, from both studies combined, there are only five geographical locations from which full, natural basalt communities were profiled (Cobb Seamount, Loihi Seamount/Hawaii, East Pacific Rise, Arctic spreading ridges, SE Indian Ridge). Even our own work (Chapter 6), while contributing to the growing database on basalt-hosted microorganisms, remains as a

relatively isolated geographic study. From previous studies combined with our own, it is possible that diversity on basalts is highly diverse when the basalts are buffered by open ocean seawater and a severe decrease in basalt diversity when located near hydrothermal activity, which could render geographical location irrelevant and only dependant upon the seawater/substrate chemistry. In order to get an overall picture of basaltic glass as a niche for microbial habitation, many more basalts from geographically and chemically distinct locations need to be profiled and combined into a single database from which we can begin to determine which microbes are the major players in the global basalt dissolution/alteration.

From our research on basalts from Loihi Seamount, it appears as though microbial diversity is not the same everywhere. Santelli et al. (2008) report that basalts are nearly as diverse as farm soils. However, our research suggests that diversity is a product of location and surrounding environment/input. Orcutt et al. (2008, paper in review, Chapter 5) show that a basalt from Pisces Peak on Loihi has a clone library rarefaction curve that predicts a total of ~400 unique species, while another basalt from the deep south rift of Loihi only indicates ~100 unique species of bacteria. Our data (Chapter 6) corroborates these findings and show several significant peaks (along with abundant minor peaks) on the Pisces Peak sample but only a single dominant peak with a few minor peaks on the Loihi south rift sample indicating both high and low diversity respectively. Additionally, our data show another phylogenetically diverse sample from a non-hydrothermal basalt (1877 submarine flow, Kealakekua Bay), and also another low diversity sample from a hydrothermal system near the crater rim on Loihi. Thus, seafloor basalts host wildly variable microbial communities that are likely significantly influenced

by seawater chemistry. From this data, it is possible to speculate that initial basaltic glass-colonizing bacteria are suitably adapted to the hydrothermal environment in which the basalt was extruded, resulting in a low diversity bacterial community structure. But when the basalt is moved away from the hydrothermal environment (e.g. through tectonic movement), other bacteria may move in and build up into a fully developed mature microbial community with (relatively) high diversity.

Building further upon this idea, chemolithoautotrophic growth may be the primary metabolic pathway for initial basalt colonizing bacteria. The Fe(II)-oxidizing *Pseudomonas* sp. LOB-7, which was isolated from a basalt surface, (Templeton, unpublished data) was found in several t-RFLP electropherograms (Chapter 6) in both high diversity and low diversity samples. The presence of the LOB-7 peak in the low diversity sample from the crater rim of Loihi indicates that LOB-7 is well adapted to a low-flow hydrothermally influenced basaltic surface. LOB-7's ability to obtain both Fe(II) and phosphate from a basaltic glass substrate (Chapter 4) and its apparent ubiquity within the Loihi environment make it a good model organism for future studies into the interaction between mineral (glass) and microbe.

Our work in the laboratory on microbial ability to obtain energy and/or nutrients from basaltic glass (Chapter 4) corroborate other field studies which show microbial colonization of minerals/substrates that contain quantities of elements otherwise limited in the environment (e.g. Rogers et al., 1998; Stillings et al. 1996; Welch et al., 2002; Rogers and Bennet, 2004) Rogers et al (1998) showed in a one-year exposure experiment that microcline ($KAlSi_3O_8$) with 0.24% P_2O_5 that after exposure was heavily colonized and weathered by microbes whereas a microcline with no detectable

phosphorus was unaffected. The ramifications of this finding suggest that in addition to seawater chemistry, substrate composition plays a role in determining the diversity of the colonizing microbial consortia. The ability for a microbe to obtain nutrients from the basalt suggests that as authigenic minerals start to fill in the oceanic crust and prevent fluid circulation (and therefore fresh nutrients being transported to the biota), select missing nutrients may be gleaned from the host basaltic glass, allowing biological alteration of the basaltic glass to continue well into the overall lifetime of the oceanic crust.

7.3 Open-ended Questions and Future Directions

As this field of study is still relatively young, there are several gaps in our knowledge base which must be filled before we can begin understanding and linking the biogeochemical processes which control the chemical fluxes into and out of the deep oceanic biosphere. Perhaps the largest question which must be answered first is, "Which microbes are responsible for basaltic glass alteration?" It appears from our research that a combination of phylogenetic analysis methods should produce the most information about the given system. As suggested before, in order to begin elucidating the primary contributors to basaltic glass dissolution and alteration, a phylogenetic database should be instated which collects and catalogs 16S rRNA sequences of known microorganisms associated with basalt surfaces. Additionally, as new basalts are being categorized, t-RFLP patterns should be generated which allows for rapid screening and comparing of different basalt samples. Therefore, if a sample contains unidentified major t-RFLP

peaks from the pre-existing database, obtaining a few clone sequences (~20-30) should identify the missing major peaks and fill in the database.

Another major question revolves around the mechanism by which the microbes are able to obtain elements from the basaltic glass. Current hypotheses center around microenvironments around the microbial cell creating a pH gradient and dissolving the silicate thereby liberating the necessary nutrient. Obtaining a model microorganism(s) which is able to perform this dissolution is essential.

Using fully oxidized and reduced glasses (with respect to iron(II)/iron(III)) would really allow us to determine a microbe's ability to obtain various nutrients/energy sources from basaltic glass irrespective of Fe oxidation state. A paper by Hasaan (2002) reports on a method for creating completely reduced basaltic glass by making additions of between 5-10 wt% sulfur. Gustav Arrhenius (pers. Comm.) suggested that firing crushed basalt powder in a pure oxygen environment may produce a >99% oxidized basalt for remelting. These new methods for basaltic glass modifications, would have allowed our work from Chapter 4 to more accurately determine microbial basalt substrate specificity and further work using these new basaltic glasses along with a suite of other microorganisms/metabolisms will help to constrain the range of microbes responsible for basalt glass alteration.

Additionally, most of the work done thus far on phylogenetic characterization of basalt-hosted microbial communities has been done on surface basalts. This does not address the problem of reactions happening well into the basaltic basement. The upper 300 m of ocean crust hosts a much more narrowly defined environment which could lead to relatively low diversity in an upwelling (hydrothermal) or effectively sealed (by

authigenic minerals in ancient crusts) type of environment. Down-welling environments may boast higher diversity by being flushed with background seawater. More robust methods for obtaining uncontaminated basalt samples from drill holes need to be developed in order to determine the phylogenetic diversity within the interior of the basaltic ocean crust.

7.4 References

Bennett, P.C., J.R. Rogers and W.J. Choi. (2001) Silicates, Silicate Weathering and Microbial Ecology. *Geomicrobiology Journal*. **18**:3-19

Daughney, C.J., J-P. Rioux, D. Fortin and T. Pichler. (2004) Laboratory Investigation of the Role of Bacteria in the Weathering of Basalt near Deep Sea Hydrothermal Vents. *Geomicrobiology Journal*. **21**:21-31

Einen, J., C. Kruber, L. Øvreas, I.H. Thorseth, and T. Torsvik. (2006) Microbial colonization and alteration of basaltic glass. *Biogeosciences Discuss* **3**:273–307

Fisk, M.R., M.C. Storrie-Lombardi, S. Douglas, R. Popa, G. McDonald, and C.A. Di Meo-Savoie. (2003) Evidence of biological activity in Hawaiian subsurface basalts. *Geochemistry Geophysics Geosystems*. **4**:10.1029/2002GC000387

Hasaan, M.Y. (2002) An easy and economic method for preparing completely reduced basalt glass. Journal of Non-Crystalline Solids. **306**:200-203

Lysnes, K., I.H. Thorseth, B.O. Steinsbu, L. Øvreas, T. Torsvik, and R.B. Pedersen. (2004a) Microbial community diversity in seafloor basalt from the Arctic spreading ridges. *FEMS Microbiol Ecol* **50:**213–230

Lysnes, K., T. Torsvik, I.H. Thorseth and R.B. Pedersen. (2004b) Microbial populations in ocean floor basalt: results from ODP Leg 187. *Proc ODP, Sci Res* **187:**1–27 [http://www-odp.tamu.edu/publications/187_SR/VOLUME/CHAPTERS/203.PDF]

Mason, O.U., U. Stingl, L.J. Wilhelm, M.M. Moeseneder, C.A. Di Meo-Savoie, M.R. Fisk and S.J. Giovannoni. (2007) The phylogeny of endolithic microbes associated with marine basalts. *Environmental Microbiology*. **9**:2539-2550

Maurice, P.A., M.A. Vierkorn, L.E. Hersman, J.E. Fulghum and A. Ferryman. (2001a) Enhancement of kaolinite dissolution by an aerobic Pseudomonas mendocina bacterium. *Geomicrobiology Journal*. **18**:21-35.

Rogers, J.R., P.C. Bennett, W.J. Choi. (1998) Feldspars as a source of nutrients for microorganisms. American Mineralogy **83**:1532–1540.

Rogers, J.R. and P.C. Bennett. (2004) Mineral stimulation of subsurface microorganisms: release of limiting nutrients from silicates. *Chemical Geology*. **203**: 91-108

Santelli, C., B. Orcutt, E. Banning, C. Moyer, W. Bach, H. Staudigel, K. Edwards. (2008) Abundance and diversity of microbial life in the ocean crust. *Nature.* **453**: 653-656.

Stillings, L.L., J.I. Drever, S.L. Brantley, Y. Sun and R. Oxburg. (1996) Rates of feldspar dissolution at pH 3-7 with 0-8 mM oxalic acid. *Chemical Geology*. **132**(1-4):79-89

Thorseth, I., T. Torsvik, V. Torsvik, F. Daae, R. Pedersen, and K.-S. Party. (2001) Diversity of life in ocean floor basalt. *Earth Planet. Sci. Lett.* **194:**31–37.

Welch S. A. and J.F. Banfield. (2002) Modification of olivine surface morphology and reactivity by microbial activity during chemical weathering. *Geochimica et Cosmochimica Acta.* **66**:213–221.